AD-A033 766   IRT CORP   SAN DIEGO CALIF   F/G 20/3
LARGE-AREA ELECTRON-BEAM EXPERIMENTS.(U)
OCT 76   D C OSBORN, R H STAHL, T N DELMER   DNA001-75-C-0071
UNCLASSIFIED   INTEL-RT-8101-011   HDL-CR-76-006-1   NL

| OF |
AD
A033766

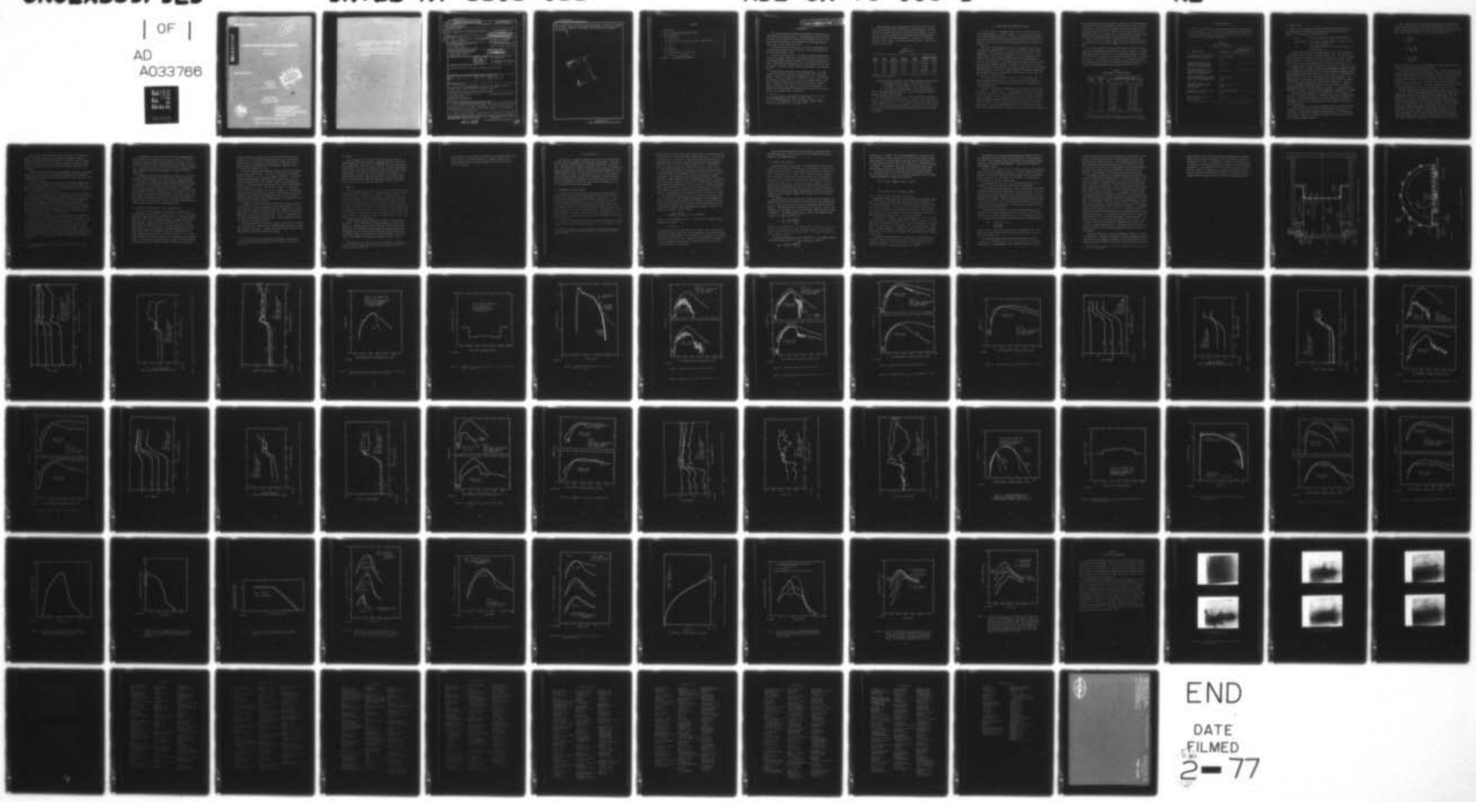

END
DATE
FILMED
2-77

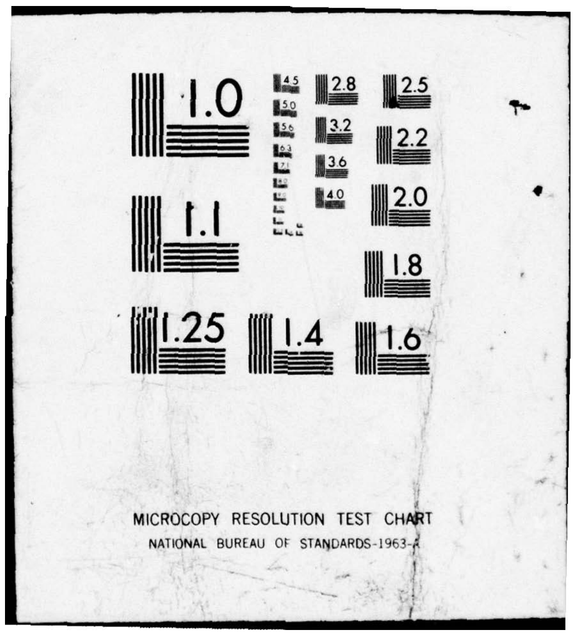
1.0
1.1
1.25
1.4
1.6
1.8
2.0
2.2
2.5
2.8
3.2
3.6
4.0
MICROCOPY RESOLUTION TEST CHART
NATIONAL BUREAU OF STANDARDS-1963-A

HDL-CR-76-006-1

LARGE-AREA ELECTRON-BEAM EXPERIMENTS

Final Report

October 1976

Prepared by

IRT Corporation
P.O. Box 80817
San Diego, California 20305

Under Contract

DAAG39-74-C-0006
DNA001-75-C-0071

U.S. Army Material Development
and Readiness Command
HARRY DIAMOND LABORATORIES
Adelphi, Maryland 20783

This work was sponsored in part by the Defense Nuclear Agency
under task R99QAXEB089, Work Unit 41, EMP; DNA MIPR: 73664.

APPROVED FOR PUBLIC RELEASE: DISTRIBUTION UNLIMITED

Experiments—Final Report by D.C. Osborn, R.H. Stahl and T.N. Delmer

UNCLASSIFIED

SECURITY CLASSIFICATION OF THIS PAGE (When Data Entered)

(19) REPORT DOCUMENTATION PAGE		READ INSTRUCTIONS BEFORE COMPLETING FORM
(18) 1. REPORT NUMBER HDL-CR-76-006-1	2. GOVT ACCESSION NO.	3. RECIPIENT'S CATALOG NUMBER (9) Rept. Sep 73-Jul 75
(6) 4. TITLE (and Subtitle) LARGE-AREA ELECTRON-BEAM EXPERIMENTS.		5. TYPE OF REPORT & PERIOD COVERED Final. September 1973 to July 1975
		(14) 6. PERFORMING ORG. REPORT NUMBER INTEL-RT-8101-011
(10) 7. AUTHOR(s) Daniel C. Osborn, Ralph H. Stahl and Thomas N. Delmer		(15) 8. CONTRACT OR GRANT NUMBER(s) DNA001-75-C-0071, new DAAG39-74-C-0006
9. PERFORMING ORGANIZATION NAME AND ADDRESS IRT Corporation P. O. Box 80817 San Diego, California 92138		10. PROGRAM ELEMENT, PROJECT, TASK AREA & WORK UNIT NUMBERS Prog. element: 6.27.04H (16)
11. CONTROLLING OFFICE NAME AND ADDRESS Harry Diamond Laboratories 2800 Powder Mill Road Adelphi, MD 20783		(11) 12. REPORT DATE October 1976
		13. NUMBER OF PAGES 77
14. MONITORING AGENCY NAME & ADDRESS(if different from Controlling Office) (12) 68p.		15. SECURITY CLASS. (of this report) Unclassified
		15a. DECLASSIFICATION/DOWNGRADING SCHEDULE

16. DISTRIBUTION STATEMENT (of this Report)

Approved for public release; distribution unlimited.

17. DISTRIBUTION STATEMENT (of the abstract entered in Block 20, if different from Report)

(9) Final rept. Sep 73 - Jul 75,

18. SUPPLEMENTARY NOTES

This work was sponsored in part by the Defense Nuclear Agency under task R99QAXEB089, work unit 41, EMP. DRCMS Code: 691000.22.10794; DNA MIPR: 73664.

19. KEY WORDS (Continue on reverse side if necessary and identify by block number)

Internal electromagnetic pulse
Electron beams
Space-charge-limiting
Numerical simulation
Experimental measurement

20. ABSTRACT (Continue on reverse side if necessary and identify by block number)

This report contains experimental and analytical descriptions of IEMP produced with electron beams. The basic objective of the work reported was to obtain experimental data on space-charge neutralization in cavities, to test the adequacy of the existing theoretical model. → next page

The Simulation Physics, Inc., SPI-5000 electron-beam machine was used on this program. Included in this report are a description of the experimental hardware and a discussion of the data.

DD FORM 1 JAN 73 1473 EDITION OF 1 NOV 65 IS OBSOLETE

UNCLASSIFIED

SECURITY CLASSIFICATION OF THIS PAGE (When Data Entered)

409 388

JB

UNCLASSIFIED

SECURITY CLASSIFICATION OF THIS PAGE(When Data Entered)

A portion of the analysis of experimental results is included. The general trends in the transmitted current, such as variation of the pulse shape with pressure, are described by computer simulation.

CONTENTS

1. INTRODUCTION

This report contains experimental and analytical descriptions of IEMP produced with electron beams. The experimental work was done for the Harry Diamond Laboratories under contract DAAG39-74-C-0006. The data reduction and analysis were performed for the Defense Nuclear Agency under contract DNA001-75-C-0071.

The basic objective of the work was to obtain experimental data on space-charge neutralization in cavities, to test the adequacy of the existing theoretical model.

The Simulation Physics, Inc., SPI-5000 electron-beam machine was used on this program, modified by SPI personnel with the addition of a 30-cm-diameter field emission diode and a vacuum-tight transmission anode. The design and construction of the test chamber and the internal sensors, including a simple magnetic spectrometer, were performed at IRT.

Two preliminary experiments were conducted using 4- to 6-inch diameter electron beams from the Simulation Physics SPI Pulse 5000 machine. Results are summarized in References 1 and 2. Rosado (Ref. 1) measured transmitted beams as a function of chamber depth. Stahl (Ref. 2) measured transmitted electrons as a function of chamber depth, gas pressure, gas composition, and collector impedance. An attempt was made to compare the measured pulse shapes with analytical results; this comparison was inconclusive.

---

1. J. A. Rosado, "Space-Charge-Limited Currents in Cavities," DNA IEMP Symposium (U), DNA 3098P, June 1973 (SRD).
2. R. H. Stahl et al., "Pressure Effects on Space-Charge-Limited Current Transmitted Across a Cylindrical Cavity," IEEE Trans. Nucl. Sci. NS-20, No. 6, December 1973.

The experimental effort has amassed 15 data sets, involving some 185 shots, and approximately 1000 oscilloscope photographs. From this group, four selected sets (cases) of data have been reduced. In each data set, the cavity geometry and parameters of the injected current are held constant; the varied parameter is the cavity air pressure, from 10^{-4} torr or lower to at least as high as 0.3 torr. Table 1 summarizes the four cases.

Table 1

SUMMARY OF DATA

Case Number	Shot Dates	Shot Numbers	Cavity Diameter	Cavity Depth	Emitted Current*	
					FWHM	Peak
13	8/74	5178-96	30 cm	14 cm	30 nsec	4 kA
6	8/74	5235-42	30 cm	30 cm	30 nsec	4 kA
4	8/74	5214-25	45 cm	30 cm	30 nsec	4 kA
15	8/74	5138-64	30 cm	14 cm	100 nsec	10 kA

*Measured with I_T monitor.

The cases above were chosen so that three comparisons could be made:

1. The effect of cavity depth - case 13 versus case 6,
2. The effect of cavity diameter - case 6 versus case 4,
3. The effect of emitted current - case 13 versus case 15.

The SPI field emission diode gap was 1.5 cm and the machine charging voltage was 250 kV for all cases.

The experimental results are now in a form suitable for theoretical analysis, and a portion of the analysis is included. The general trends in the transmitted current, such as variation of the pulse shape with pressure, are described by computer simulation. However, some of the details of the spatial distribution of the transmitted current are not presently understood.

2. VACUUM CHAMBER AND EXPERIMENTAL CAVITY

The IEMP cavity is an adaptable affair that is contained within a larger vacuum chamber, as shown in Figure 1. The vacuum chamber attaches to the electron-beam machine via an insulating ring such that the Mylar/mesh anode of the machine diode becomes the emitting end of the cavity. A removable liner and a rear collector assembly form the walls and rear end of the cavity.

The liner is an aluminum cylinder that is supported and electrically connected to the chamber walls via a collar containing rf fingers under compression. The rear collector assembly consists of a central circular aluminum plate, two concentric aluminum rings, and a supporting sleeve. Adjacent collectors are supported and electrically interconnected by a circular ring of resistors. The support sleeve maintains electrical contact with the liner through rf fingers. The depth of the IEMP cavity can be changed simply by sliding the rear collector assembly. The liner is removed and replaced with a short liner, which is moved to the rear to create the larger diameter cavity. For these four cases, the edge of the liner was positioned 1 cm from the anode.

The vacuum system (not shown) consists of a 4-inch-diameter oil diffusion pump and roughing pump. The cavity pressure was monitored by discharge gages and a thermistor gage, which have been calibrated against a McLeod pressure gage.

A sketch of the magnetic spectrometer used to measure electron energy distributions is shown in Figure 2. The spectrometer consisted of two steel pole pieces, each with a 2.5-inch radius and 0.5-inch thickness, separated by a 0.5-inch gap. A static magnetic field in the gap was obtained from several permanent magnets attached to the pole pieces across the gap at the outer radius. The field strength in the gap depended on the number of magnets used. The ten aluminum collectors, 0.13 inch wide and 0.38 inch high, were positioned as shown in the figure. Each collector was connected

to a miniature 50-ohm coaxial cable that terminated in a BNC feedthrough connector at the wall of the chamber, where the oscilloscope connection could be made. The spectrometer assembly was attached behind the rear collector assembly, with its 0.12-inch by 0.5-inch rear entrance slit positioned on the cavity centerline. All measurements were made at high vacuum, with the rear collector 1 cm away from the Mylar window.

Table 2 gives the acceptance range of electron energy at each collector for the two static field strengths used, and estimated uncertainties.

It was found necessary during the experiments to use a relatively large 0.75-inch-diameter front aperture (as shown in Figure 2) to obtain reasonable signal-to-noise ratios. This degrades the energy resolution (ΔE) at collector #10 to about ±10%, and at the smaller radii, proportionately less.* At collector #1, the effects of the fringing field and space charge limiting produce an estimated ±10% energy resolution. The results of the measurements are discussed in Sections 3.1 and 3.4.

Table 2

SPECTROMETER ELECTRON ENERGIES

Collector Number	Collector Radius (cm)	Electron Energy (keV) B_{gap} = 233 ±3 gauss	B_{gap} = 296 ±5 gauss
1	1.4	7.9-10.0 ±10%	12.7- 15.9 ±10%
2	2.0	16.5-19.3	17.8- 30.8
3	2.4	25.1-28.6	40.0- 45.4
4	2.8	33.7-37.6	53.4- 59.6
5	3.1	42.7-47.0	67.3- 74.0
6	3.4	51.3-56.1	80.7- 87.9
7	3.7	60.0-65.2	93.9-102.0
8	4.0	68.7-74.2	107.0-115.0
9	4.3	77.8-83.6	121.0-130.0
10	4.5	86.8-92.7 ±10%	134.0-143.0 ±10%

*The ±10% energy resolution is obtained even with the relatively wide 0.75-inch aperture, due to 180° focusing inherent in the design.

3. DATA ORGANIZATION

Table 3 is an index of the eight figures relating to each data case. Note that Figures 6, 7, and 8 describe the emitted current parameters for all three short-pulse cases. The measured quantities are defined in the discussion of the case 13 data, Section 3.1.

Table 3
INDEX OF THE FIGURES

Figure Titles	Parameters	Figure Numbers: Case 13	6	4	15
Peak currents in rear and wall collectors versus pressure	I_T, I_{FC1}, I_{FC2}, I_{FC3}	3	10	14	18
Time of occurrence of peak currents in rear and wall collectors versus pressure	I_T, I_{FC1}	4	11	15	19
Peak current density averaged within each ring of rear collector versus pressure	J_1, J_2, J_3	5	12	16	20
Current collected at 1 cm depth (I_{FC1}) and total current (I_T)	I_T, I_{FC1} at 1 cm depth	6	6	6	21
Estimation of peak current uniformity through transmission anode	J_1, J_2, J_3 at 1 cm depth	7	7	7	22
Estimation of average electron energies versus time	V_D, IRT Spectrometer data	8	8	8	23
Comparison of I_{FC1} and I_T time histories	I_{FC1}, I_T	9	13	17	24

3.1 CASE 13 DATA

Figure 3 shows the peak currents collected on the rear and the wall of the test cavity, as measured in the four shunt resistor rings shown in Figure 1. The currents are defined as follows.

I_{FC1}:	the total current collected on the rear plate.
I_{FC2} and I_{FC3}:	the currents collected within a radius of 10.2 cm and 5.1 cm, respectively.
I_T:	the current collected on the liner plus the rear plate current.

The shunt resistances are each approximately 10 mΩ; thus, the maximum voltage drop across each shunt is several hundred volts. The voltage drop across the inductance formed by the liner collar and the I_T shunt is approximately 600 volts. The shunts were calibrated against the machine current monitor using a resistive load between the cathode and the center of the rear collector, and passing the machine current through all shunts in series.

In August 1974, a series of open-shutter photographs (reproduced in Appendix A) was made of the beam and the rear collector through a chamber window. Some photographs show bright spots at the steel screws in the collector rings and, in several cases, also at the gap in front of the I_{FC3} shunt. The largest spots are observed at the 100-nsec pulse width. There was speculation that the I_{FC3} measurement was disturbed by this effect. A review of the I_{FC3} waveforms recorded during this series do not show any unusual effects when the local optical emission is observed. It is possible that the optical emission is associated with recombination occurring at late times.

For case 13, the pressures were varied from 5 x 10^{-5} to 20 torr, in 18 steps. A majority of shots was confined to the pressures between 20 and 150 mtorr. Note the large increase in currents between 20 and 60 mtorr. See Figures 9a-9d for the time histories of those currents indicated by a circled data point.

Figure 4 shows the time of peak currents in the rear collector versus pressure. Note that the I_T and I_{FC1} current peaks do not occur at the same relative time within the pulse except near the 40- to 150-mtorr pressure region. The times to peak are referenced to the initial rise of the diode voltage waveform (Figure 8).

Figure 5 shows the peak current density within each ring of the rear collector versus pressure. To calculate current density in a ring, the current from the inner rings must be subtracted before dividing by the ring area. The current densities J_1, J_2, and J_3 are defined below.

$$J_3 = \frac{I_{FC3}}{80\ cm^2}$$

$$J_2 = \frac{I_{FC2} - I_{FC3}}{240\ cm^2}$$

$$J_1 = \frac{I_{FC1} - I_{FC2}}{400\ cm^2}$$

Note that as pressure is increased beyond 45 mtorr, the current densities J_2 and J_3 increase significantly more than J_1.

At pressures near 10 torr and above, there is evidence to suggest that the Mylar/mesh anode may have bowed slightly, changing the emitted current profile. Both the diode voltage and current waveforms and the transmitted current waveforms suggest that the field emission diode gap decreases, particularly on the axis, due to the forces on the experiment side of the window (22 pounds at 10 torr). This would account for the observed decrease in the diode impedance and increase in the current density on axis.

The next three figures describe the emitted current for the short-pulse cases. Figure 6 is an approximation to the emitted current as all measurements are necessarily collected current measurements. The time histories of I_T and I_{FC1} are compared in this figure, when the rear collector was moved to 1 cm from the anode, flush with the edge of the liner. A cavity depth of 1 cm is sufficiently small to have eliminated longitudinal space-charge effects at the peak of the pulse. Similar measurements made at 2 cm and 5 cm cavity depths produced nearly the same I_T and I_{FC1} peak values, indicating little limiting at the peak. Following the peak, limiting seems to occur rapidly, as discussed further below. The FWHM's of I_{FC1} and I_T are 25 and 32 nsec, respectively.

Figure 7 shows the uniformity of currents through the transmission anode. The current density is given here as a function of radius, as measured at the rear collector positioned 1 cm from the anode. Although the radial resolution is coarse, there are higher collections near the edge of the beam, while the collections at the center and middle rings are lower.*

This data was recorded after a new cathode was installed. The current densities in the center of the beam observed using the old cathode were significantly lower, and have been recorded both on the rear collector and in an array of CaF TLD's.

Note that, although this data was taken with a 20-nsec FWHM emitted pulse, the profile is believed to be similar to the 30-nsec FWHM cases. However, the magnitudes in Figure 7 must be multiplied by 1.4 to correspond to the peak magnitude shown in Figure 6.

Figure 8 is an estimation of electron energies in the emitted pulse. A plot of the diode voltage waveform is given, recalibrated using the latest SPI calibration of 9.8 kV/V and corrected for a 22-nH diode inductance. This curve corresponds to electrons impinging on the Mylar window. A second curve, corresponding to electrons leaving the window and entering the test cavity, was obtained by subtracting the electron energy losses in the 0.25-mil Mylar window. The methods used to calculate energy loss and energy spread (ΔE) are discussed in Section 4.

Also plotted on Figure 8 are data from our magnetic spectrometer, showing the time of occurrence of the peak signal versus the width of the spectrometer energy bin. The good agreement obtained in two of the three bins may be somewhat fortuitous, considering the poor signal-to-noise ratios of the short-pulse spectrometer oscilloscope records. However, since much better agreement between spectrometer and modified diode waveforms was obtained in the case of the long pulse using good-quality records (see Section 3.4), we tend to have faith in the modified diode waveform shown here.

---

*Later measurements by SPI personnel confirmed this radial distribution measurement.

A comparison of Figures 6 and 8 shows that the average electron energy at 50 nsec, the peak of the I_T and I_{FC1} pulses, is $\sim$30 keV, a value high enough to produce little limiting at 1 cm depth. However, between 50 and 60 nsec, the average energy decreases rapidly to several keV. I_{FC1} decreases rapidly, while the wall current I_T decreases more slowly, implying a shift from longitudinal to transverse electron trajectories.

In Figures 9a-9d, the time histories of current I_{FC1} and I_T are plotted for seven pressures. The oscillations on the I_{FC1} waveform are most likely a consequence of a small resonant network between the I_{FC1} shunt resistor ring and the RF finger contacts and can be ignored. The values of L and C calculated from the geometry of the network yield a resonant frequency of 280 mHz, very close to the observed ringing at 290 mHz. Note that a small prepulse is observed at 7 to 8 nsec, very likely associated with the initial peak of the diode voltage. The Mylar anode is positively charged, and is the source of displacement current through the Faraday cup resistors. The main current pulse rises $\sim$10 nsec after the initial rise of the diode voltage.

3.2 THE EFFECT OF CAVITY DEPTH: CASE 6 VERSUS CASE 13

The case 6 initial conditions are the same as those of case 13, except that the cavity depth is increased from 14 to 30 cm. The larger volume thus formed might be expected to give rise to a greater negative potential on axis, and an increased electron divergence due to space-charge buildup. Comparing Figure 10 to Figure 3, we see at vacuum approximately the same total current (I_T) but significantly less rear plate current (I_{FC1}), as expected. As pressure increases to 20 to 80 mtorr, self-neutralization increases for both cylinder depths and a larger percentage of the charge is collected at the rear. It is interesting to note that the total current I_T also increases in this pressure range. It seems plausible that low-energy electrons, able to penetrate farther into the cavity, produce additional fields which cause more

ionization electrons near the wall to accelerate to the walls and be counted in I_T. At the higher pressures near 0.3 torr, I_T decreases and the currents I_T and I_{FC1} are very similar in both cases; that is, increasing the cavity depth has not significantly reduced the total rear collector current at 0.3 torr.

The current density plots (Figures 12 and 5) are useful in examining the beam current profile. Note that in both cases the collected beams are hollow ($J_1 > J_2 > J_3$) from vacuum to $\sim$50 mtorr. As pressure increases above 50 mtorr, both plots show an increase in J_2 and J_3 (the central beam density) and a lesser change in J_1 (the beam edge density). At higher pressure, the beam in case 6 (30 cm depth) appears to be focused ($J_3 > J_2 > J_1$). The profile in case 13 (14 cm depth) to 5 to 6 torr is an annulus ($J_2 > J_3 > J_1$), however. It has been suggested that the rate of pinch is such that, in the short (14 cm) cavity, the beam has not had time (or distance) to pinch to less than the FC2 collector radius, while in the 30-cm-deep cavity, it has pinch at least to the radius of the FC3 collector.

A comparison of the time to peak current data of Figures 11 and 4 reveals that the currents I_T and I_{FC1} peak at the same time, only near those pressures where the currents are maximum. Otherwise, I_{FC1} always peaks before I_T reaches its maximum value*. We also see that the I_{FC1} peak occurs much earlier in the 30-cm case. This is a consequence of the onset of space-charge-limiting earlier in time; compare the vacuum time histories of Figure 9a and 13a.

The high-pressure time histories of Figure 13b are similar to those of Figures 9b and 9c, except that I_T waveforms show significantly longer decay times at late times. It may be that these "tails" are due to magnetic effects in the high-conductivity plasma.

*At low pressures (pre-breakdown), this effect is due to space-charge-limiting. At high pressures (post-breakdown), the mechanism has not been identified, but magnetic field (inductive) effects are suspected.

3.3 CASE 4

Case 4 (Figures 14-17) is the same as case 6 except that the cavity diameter has been increased to approximately 45 cm. This feat was accomplished by removing the 30-cm-diameter liner and substituting a short liner on the collar to support the rear collector (see Figure 1). The rim of the short liner was positioned flush with the surface of the rear collector, and the collar slid to the rear of the chamber to increase the cavity depth. Note that the radii of the emitter and the rear collector remain the same; the significant change is the removal of the conducting cylinder boundary conditions at the 15-cm radius.

3.4 CASE 15

Case 15 (Figures 18-24) is the same as case 13 except for the parameters of the emitted current pulse. Figures 21 and 22 characterize the emitted current by the collected current in a 1-cm-deep cavity. This pulse is significantly wider (100-nsec FWHM) and more intense than the short pulse. However, the I_T waveform in Figure 21 exhibits the same long tail observed in Figure 6 for the short pulse, implying that some low-energy electrons are "squirted" to the sides of this 1-cm-deep cavity. The current density versus radius plot of Figure 22 is interesting, showing a distinctly different beam profile from the short-pulse cases. Compared to Figure 7, the long pulse exhibits a higher density in the center and an improved overall uniformity.

Figure 23 shows electron energies as a function of time for the long pulse. The two continuous curves are obtained, as described in Section 3.1, from the diode voltage waveform of a typical shot. The data points are obtained from the magnetic spectrometer measurements representing the time of occurrence of the peak signal placed at the bin midpoint energy. The agreement is very good except at very early times.* The uncertainty in the timing accuracy is about ±2 nsec.

---

*The reason for the modest early-time discrepancy is uncertain; the spectrometer suffers from low signal-to-noise ratios at early times, whereas the voltage probe does exhibit some overshoot according to recent information from SPI.

The uncertainty in the midpoint bin energies are estimated to be on the order of ±10%, as discussed in Section 2. Measured values of ΔE (FWHM) obtained from the experiment range from ±7.5 keV at 45 keV to ±12.5 keV at 100 keV.

4. DATA ANALYSIS

The results of a computer simulation of one of the sets of data are presented here and compared to the experimental measurement. Some agreement is obtained for the current at the outer radius of the collecting wall. Time histories are similar and trends in the decay of the persisting currents are duplicated. However, we note significant differences in the vacuum response, as well as in the spatial distribution of peak currents on the collecting surface. Whereas the differences in vacuum response may be attributable to inaccuracies in the electron spectra or zoning used in the calculation, it does not appear that the difference in spatial distribution can be easily explained.

4.1 APPROXIMATIONS IN THE ANALYSIS

The data of case 13 were analyzed to determine to what extent the effects of the presence of the background gas can be simulated. The calculations were performed using the DYNACYL code (Ref. 3). In light of the fact that the method used to treat the secondary electrons is strictly applicable only when the concept of an electron drift velocity is meaningful, and the fact that the high fields encountered here cause runaway so that the concept of a drift velocity is not applicable, a minor modification had to be made to the code to allow a meaningful analysis of the experiments. To put this in perspective, a brief summary of the treatment is given here.

In these calculations, the secondary electrons are treated as a fluid. Primary electrons cause ionization of the gas at a rate determined by the

3. E. P. dePlomb et al., "Two-Dimensional Time-Dependent Computer Code Development and Applications to Problems in IEMP (U)," DNA 3503F, August 1974 (SRD).

Bethe approximation for slowing down, and the conversion of primary energy to ionization is at the rate of three Rydbergs per ion pair. This has the limitation that the secondaries dissipate their initial high energy in producing further ionization, possibly not the case for extremely high ratios of electric field to gas number density (E/N). In the latter case, this ionization rate may be high by as much as a factor of two.

The fluid of secondaries is followed in an Eulerian grid with drift velocity determined by experimental values of the velocity of electrons in nitrogen. This assumes that the collision frequency for momentum exchange is large compared with other frequencies of interest. As to further ionization by secondaries (the cause of avalanche), the treatment is again based on experimental data. What is more, this empirical treatment shows a phenomenon which is the basis for the method used to extend the calculations to the regime covered by the present experiments. This phenomenon is the decrease of ionization rate above a certain value of E/N.

The secondary ionization rate shows an increase with E/N up to 10^{17} V-m^2. At that point, the rate begins to decrease with increasing field. This is at a point where the drift velocity begins to exceed 10^6 m/sec. To maintain the simplicity of the method, an *ad hoc* value for the drift velocity was chosen for fields causing higher secondary velocities. In particular, we choose a drift velocity

$$v_d = \left(\frac{v_e + 0.5c\ x}{1 + x}\right) \quad \text{for} \quad v_e \geq 10^6 \text{ m/sec} ,$$

where v_e is the tabulated velocity, c is the velocity of light, and the dimensionless quantity x is

$$x = 10^{17}\ E/N .$$

The direction of drift is parallel to the electric field. Although this ignores the inertial properties of the secondaries, it maintains an essential physical characteristic of the problem: the secondaries travel rapidly in the direction of the fields. However, since the effects of magnetic forces are ignored, the assumption of motion parallel to the electric field introduces a source of error.

There are other assumptions and simplifications incorporated into the calculation (Ref. 3), but the use of a drift velocity is the most suspect in the present analysis.

4.2 RESULTS OF THE ANALYSIS

Seven experiments were analyzed. The experimental results are presented in Figures 9a-9d. Calculations were performed for a tank 15 cm in length and 15 cm in radius. The problem was represented by a grid of five zones in length and five in radius. This limited zoning was imposed by the restriction of maintaining a tractable quantity of output and the reluctance of the analyst to permit particles representing electrons to traverse more than a zone in a particle time step. However, the coarse zoning may cause substantial error in the vacuum and 20-mtorr cases, and at higher pressures for early times (prior to the peak of the pulse). Emission took place from 45 equally spaced radial points on the emission surface for the two lowest pressures and 15 points for the five higher-pressure cases.

For emission from zones within 10.5 cm of the axis, the current was reduced by a factor of 0.3 relative to the emission at radii greater than 10.5 cm. This was motivated by the curve of measured currents shown in Figure 7. The peak emission current density was 7 amp/cm^2. Current time history was as in Figure 6 (I_{FC1}), and the digital representation is shown in Figure 25. The energy time history was taken as the corrected diode voltage V_D of Figure 8, modified by

$$E = V_D \left[1 - \left(\frac{20 \text{ keV}}{V_D} \right)^2 \right] \text{eV} ,$$

where 20 keV was assumed to be the cutoff of the Mylar window. This formulation is based on the fact that electron energy loss is approximately inversely proportional to the electron energy. The digitized representation is shown in Figure 26.

The electron emission was taken to be uniform in solid angle confined to the polar angle interval 0 to Θ_{max}, where Θ_{max} is given by

$$\Theta_{max} = \min \left[1.0, \frac{20 \text{ keV}}{E} \right] ,$$

where Θ_{max} is in radians. This is an approximation to a function indicated by SPI and is shown in Figure 27; we note that the spread in polar angle appears to be substantially broader than what one would expect to see from electrons incident normal to the Mylar being scattered off normal by the Mylar. Furthermore, some studies were made using random energy distributions; these will be discussed after the main body of results.

The results for the seven pressures are seen in Figures 28a-28c. The calculated results are at 13.5 cm and were extended to 15 cm by using linear extrapolation in radius by the formula

$$I(r = 15 \text{ cm}) = \frac{15}{13.5} 2\pi \, 15 \, H(r = 13.5 \text{ cm})$$

or

$$I(r \pm 15 \text{ cm}) \simeq H(r = 13.5 \text{ cm}) \times 1 \text{ meter} ,$$

where I is the current collected on the rear plate.

Immediately evident from Figure 28a is the fact that predicted results for the vacuum case are higher than experiment by up to a factor of two. This could be explained if the true electron energy were lower than that used in the calculations. There is also the possibility that the zoning is too crude to describe the two lowest-pressure cases. In the vacuum and 20-mtorr cases, the current oscillated over the range indicated in the figure and has been averaged over 4 nsec for presentation.

At a pressure of 20 mtorr, the calculated response is still too large, which could be due to spectral differences, to the coarse zoning, or to the treatment of the primary ionization rate. The last possibility is examined later. The late-time tail is represented well by the calculation, a fact which is probably fortuitous. However, the shape of this tail is probably valid since, after collapse of the fields, the drift approximations should not be so bad.

At 45 mtorr, the peaks agree well, a fact which is probably not too significant since nearly all of the current is getting through in both experiment and theory. The tail falls off a bit too rapidly in the calculation, but still the shapes of the curves are similar.

The 90-mtorr case is interesting because the decrease at 60 nsec in the experiment, due to the drop in driving voltage, is not predicted by the theory. This difference can be explained by the approximate primary ionization rate being high (See page 14). Except for this difference, the agreement is good.

Looking at the 150-mtorr results, it can be seen that the experimental results also lose the decrease at 60 nsec, a further indication that the phenomena are being described accurately but begin occurring at somewhat too low a pressure (i.e., 90 mtorr) in the analysis. The theoretical falloff in the tail has the correct slope.

At higher pressure (3.5 torr), the rate of decay of the tail has increased, a fact which appears in both theory and experiment.

At the highest pressure examined, 15 torr, the agreement deteriorates although both theory and experiment show a slower decay rate. This divergence is not considered too serious since the high pressure on the anode may deform the diode and change the spatial distribution of the electrons incident on the chamber. Since the calculated tail disappears for totally hollow emission, one is led to believe that the falloff would be slower in the case of more uniform emission, a fact which is consistent with the assumed distortion in the anode.

In the calcuations discussed so far, we considered monoenergetic electrons, with electron energy varying during the pulse. To calculate the effect of an energy distribution in place of the monoenergetic electrons, we performed calculations assuming a distribution approximated by

$$\frac{\Delta E}{E} = \frac{0.9}{1 + \left(\frac{E}{10\ \mathrm{keV}}\right)^2} + 0.01\ .$$

This is shown in Figure 29 along with the data supplied by SPI. The energy was taken as random about the central energy given in Figure 26 with a full width of ΔE.

For the vacuum case, the oscillations and response were both decreased by approximately 20% by the use of an energy distribution; see Figure 28a. The agreement is not substantially better. For the

20-mtorr case, the ionization rate by primaries was reduced by a factor of two to examine the possibility that the secondaries do not immediately slow by further ionization. This modification and the use of the random energy distribution produced the results shown in Figure 30, which may be construed as an improvement but could be explained by the use of an electron spectrum substantially harder than the real spectrum. Again, effects of the coarse zoning may be significant.

The comparison between the calculated and measured current on the outside of the collector (Figures 28a-c) is not too discouraging. However, the situation deteriorates when one examines the spatial distribution of current. In general, the current calculated theoretically shows a definite pinching effect. The calculated peak current enclosed with a radius of 4.5 cm is more than that experimentally measured for the 5.2-cm collector (see Figure 3). As an example, Figure 31 shows the calculated spatial distribution of currents for the 150-mtorr case, where the predicted total-current time history agreed well with experiment. The theoretical values lie above the experimental curve for the peak interior currents. The peak currents occur at successively later times for decreasing radii which may be due to pinching. Since magnetic forces are not allowed to act on secondaries,* there was interest in studying the effect on the calculations of ignoring these forces on the primary particles also. To investigate this possibility, the same problem (Figure 31) was run ignoring the magnetic forces altogether. As seen from Figure 32, the currents maintain their hollow shape. Thus, it appears that ignoring the effect of magnetic force on the secondaries is somewhat compensated for by the neglect of this force on the primaries; but there is no longer agreement with the rate of decay of the currents.

The above comparison of theory and experiment leads to the following conclusions. The method used here of treating secondaries as moving at a drift velocity outside the regime of strict applicability of the concept produces satisfactory results for total transmitted currents at

*This would have made the conductivity a nondiagonal tensor, which the code could not handle.

pressures above 45 mtorr for the experiments examined here. Detailed results such as spatial distribution of the transmitted current are substantially in error. In particular, a substantial pinching effect is noticed in the calculation which is not present in the experimental measurements. This treatment, which was initially intended to complement the treatment of secondaries as inertial particles and thereby eliminate stability problems caused by plasma oscillations, does not appear adequate to describe the full effects of the background gas.

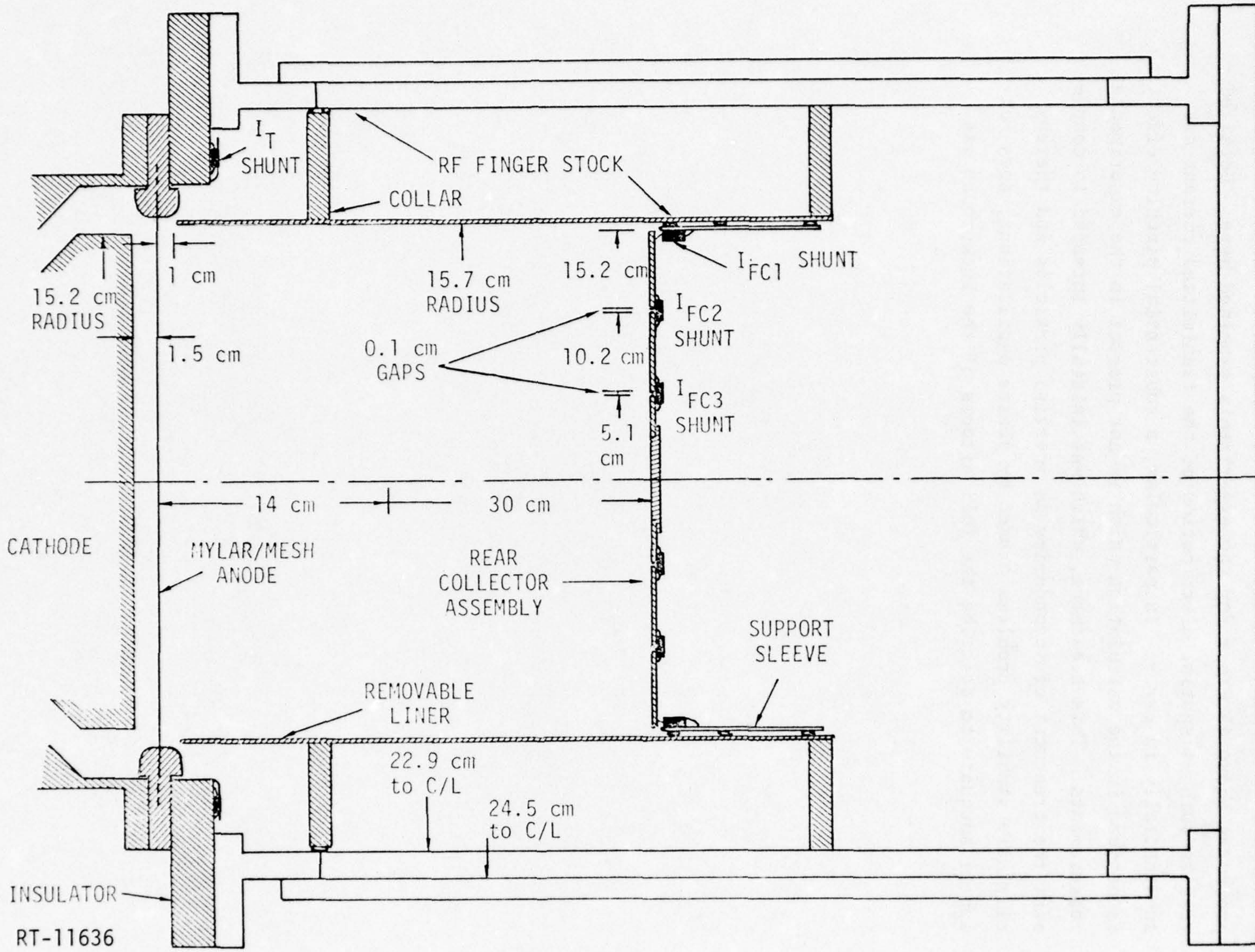

Figure 1. Vacuum chamber and experimental cavity

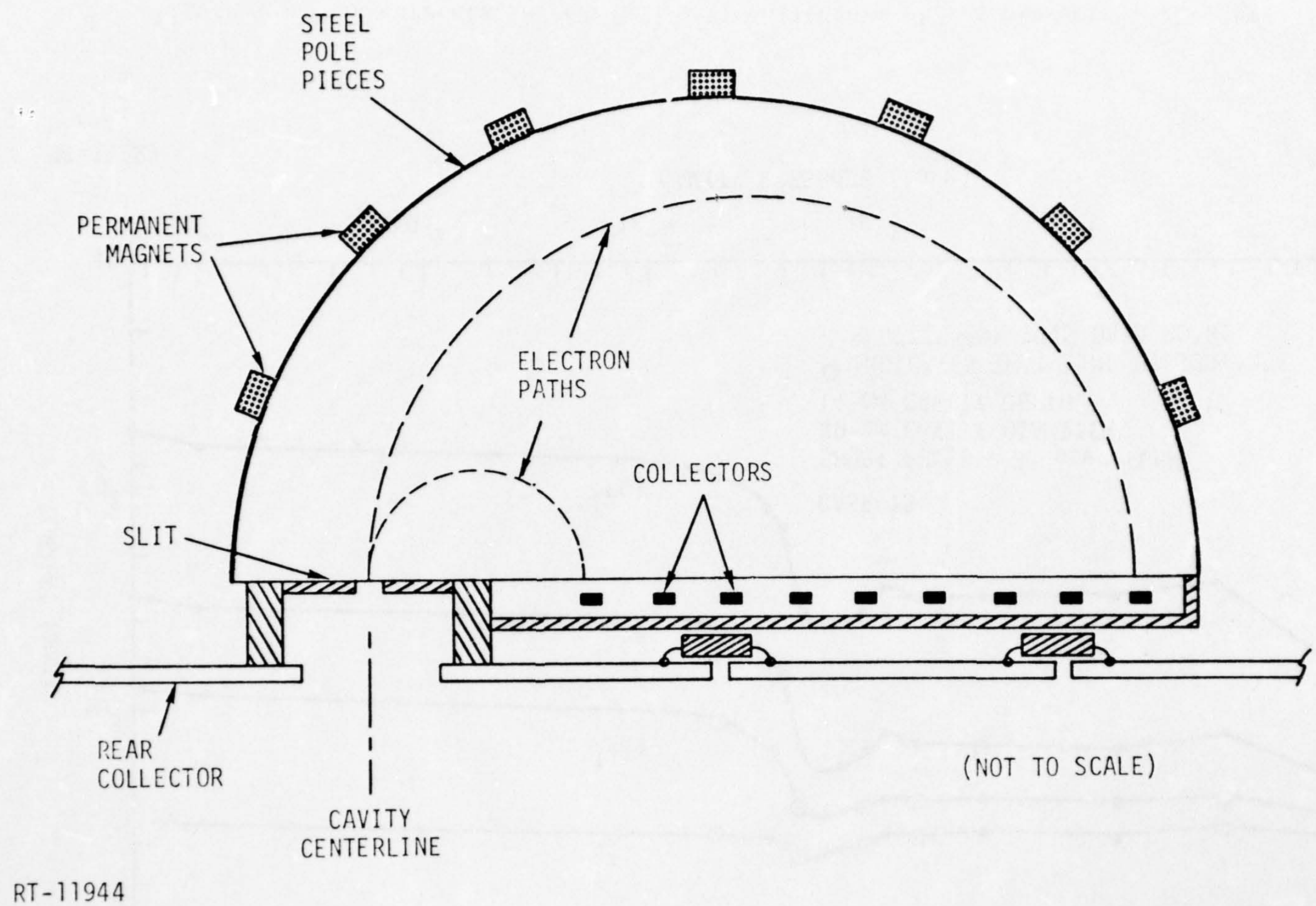

Figure 2. IRT magnetic spectrometer

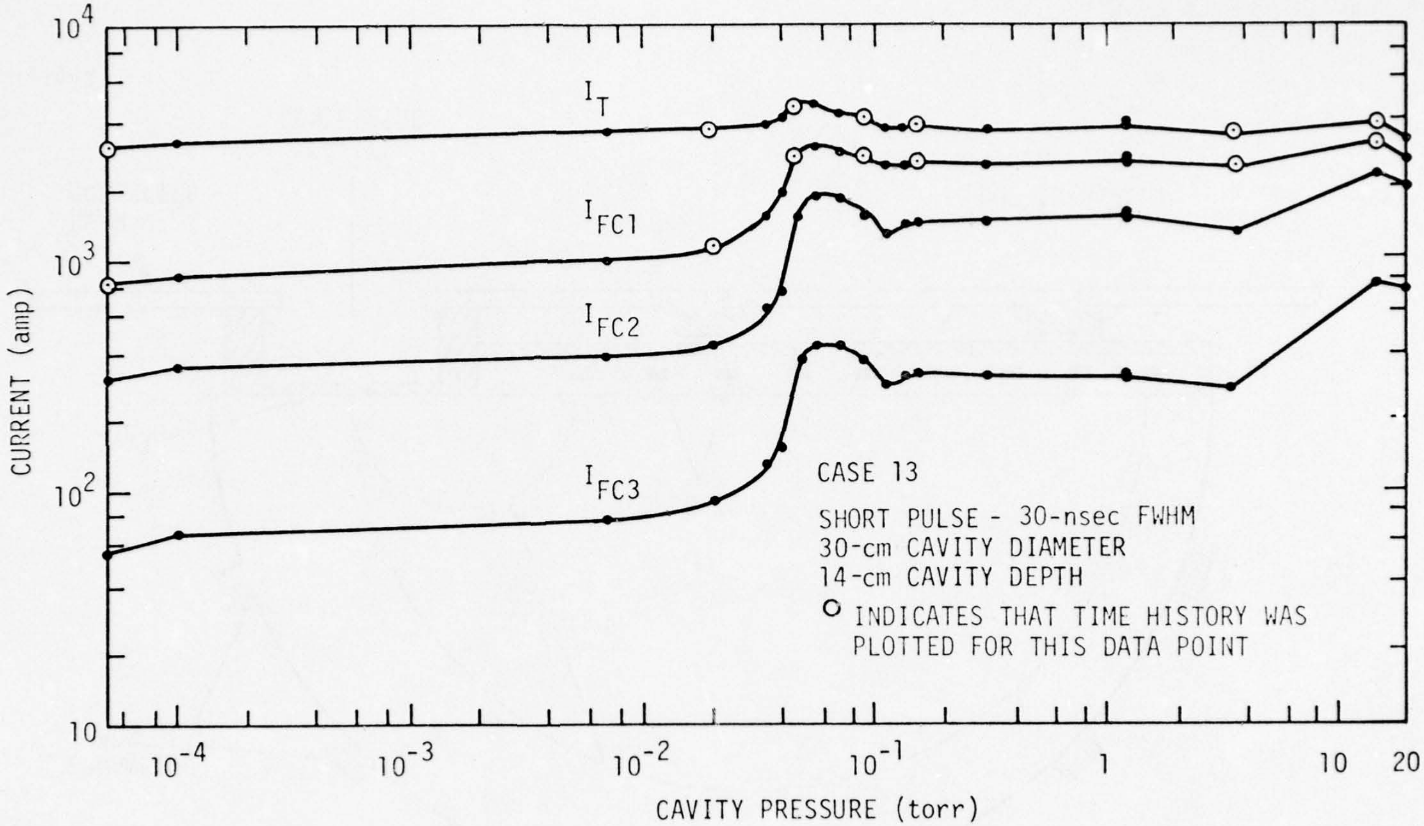

RT-11627

Figure 3. Peak currents in rear and wall collectors versus pressure - case 13

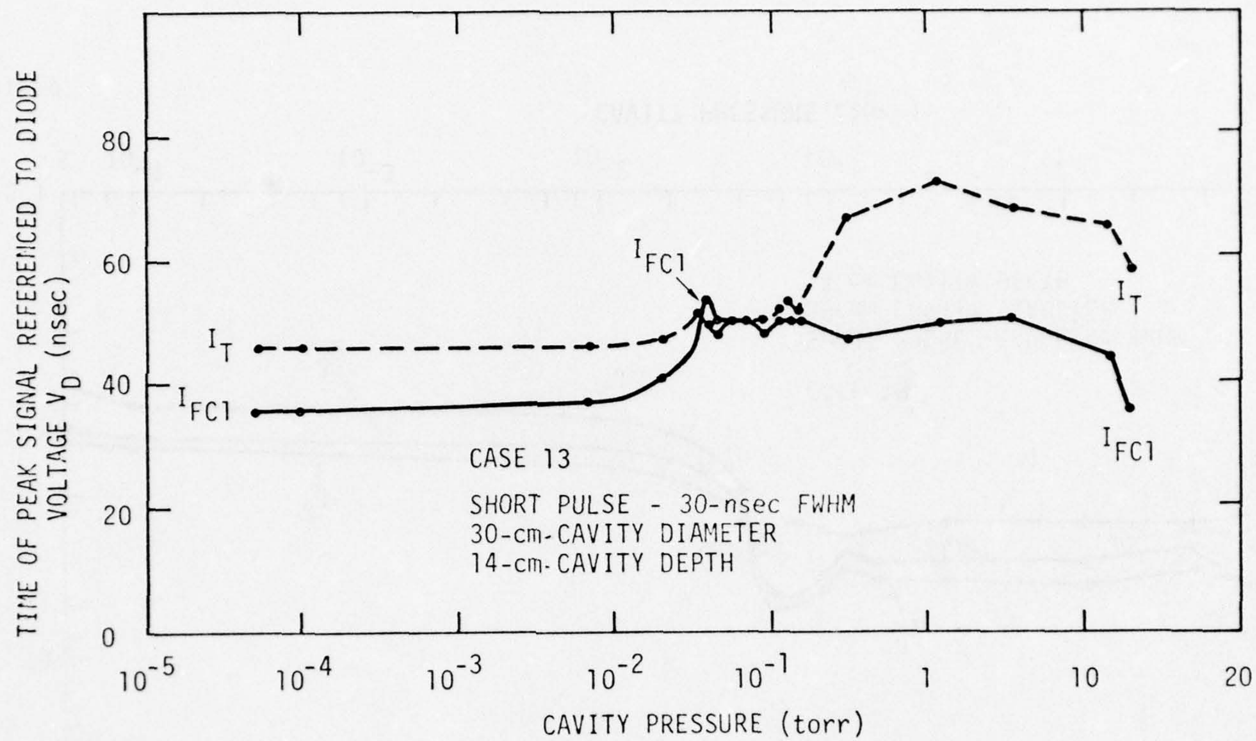

RT-11628

Figure 4. Time of occurrence of peak currents in rear and wall collectors versus pressure - case 13

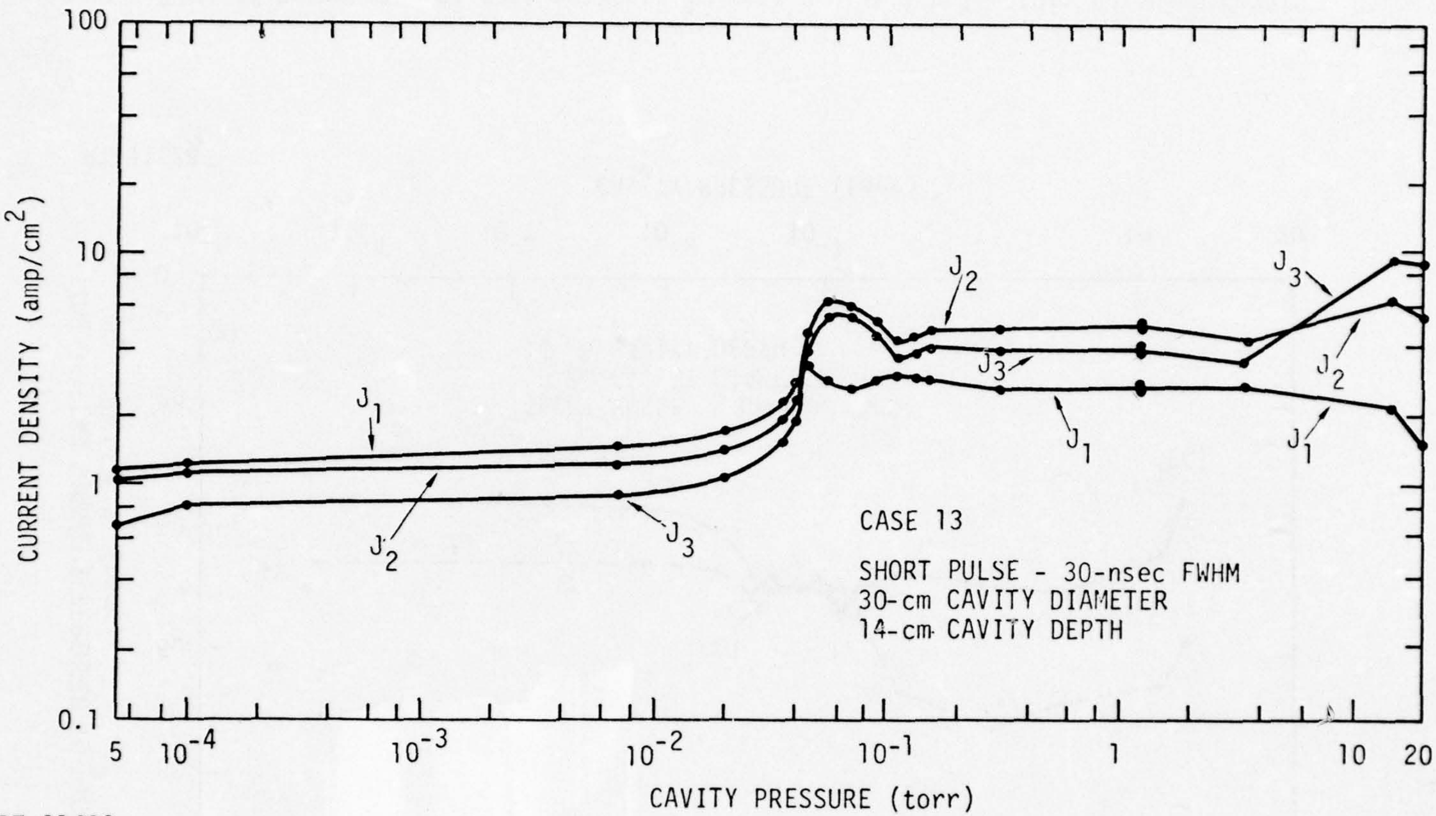

RT-11629

Figure 5. Peak current density averaged within each ring of rear collector versus pressure - case 13

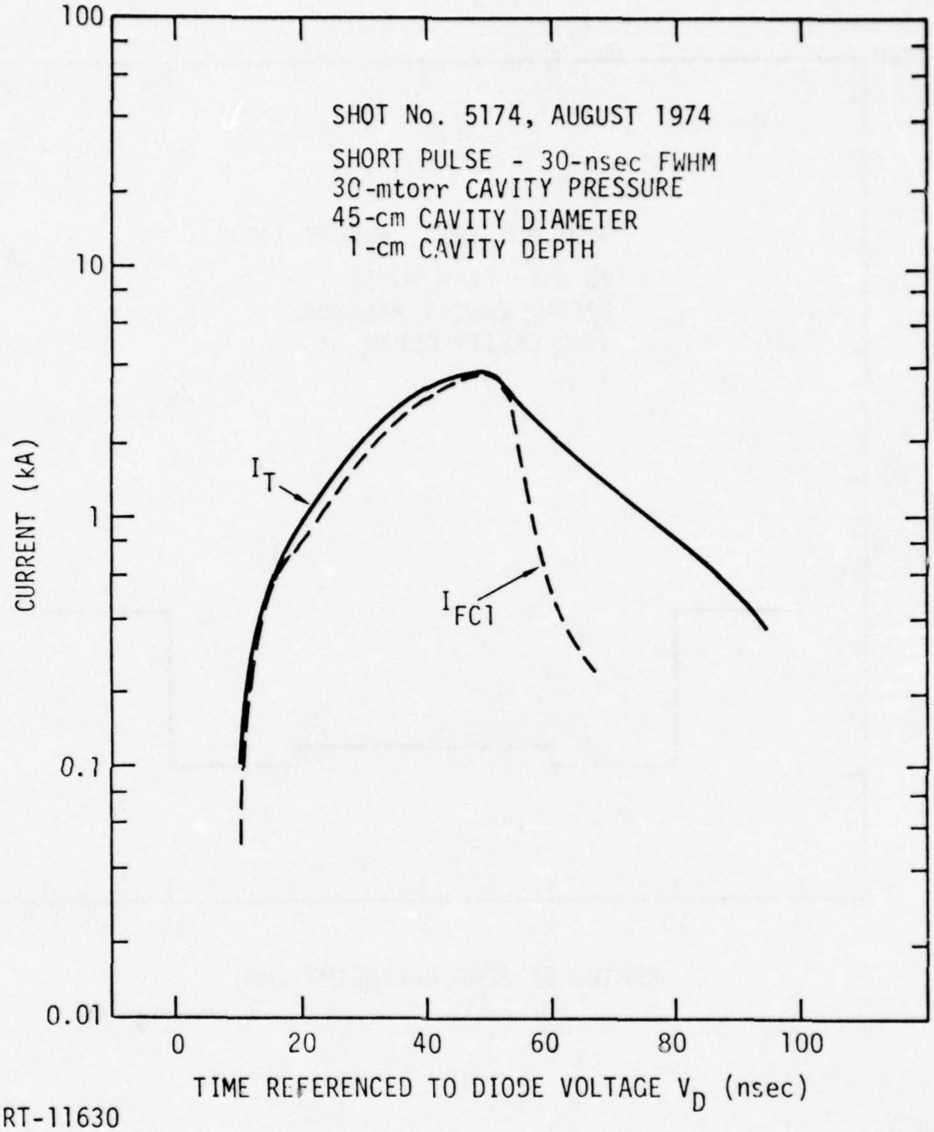

Figure 6. Current collected at 1 cm depth (I_{FC1}) and total current (I_T); approximation to emitted current - short pulse

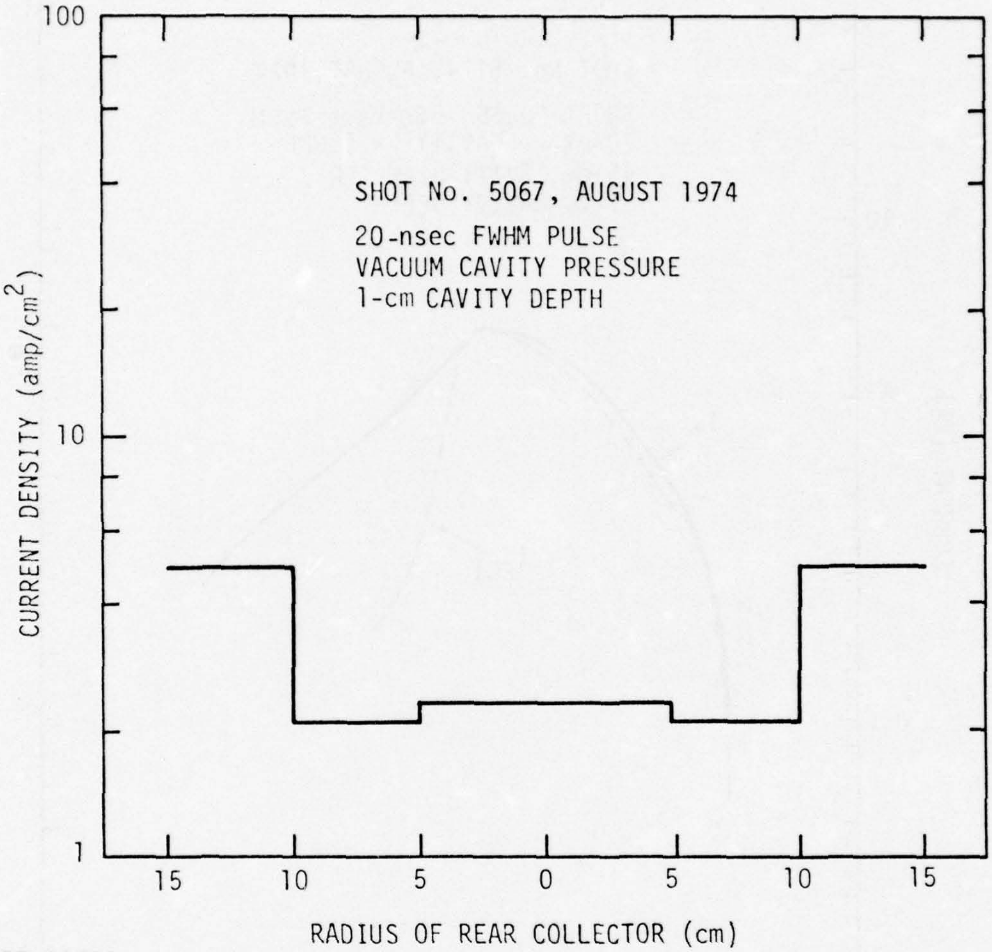

RT-11631

Figure 7. Estimation of peak current uniformity through transmission anode - short pulse

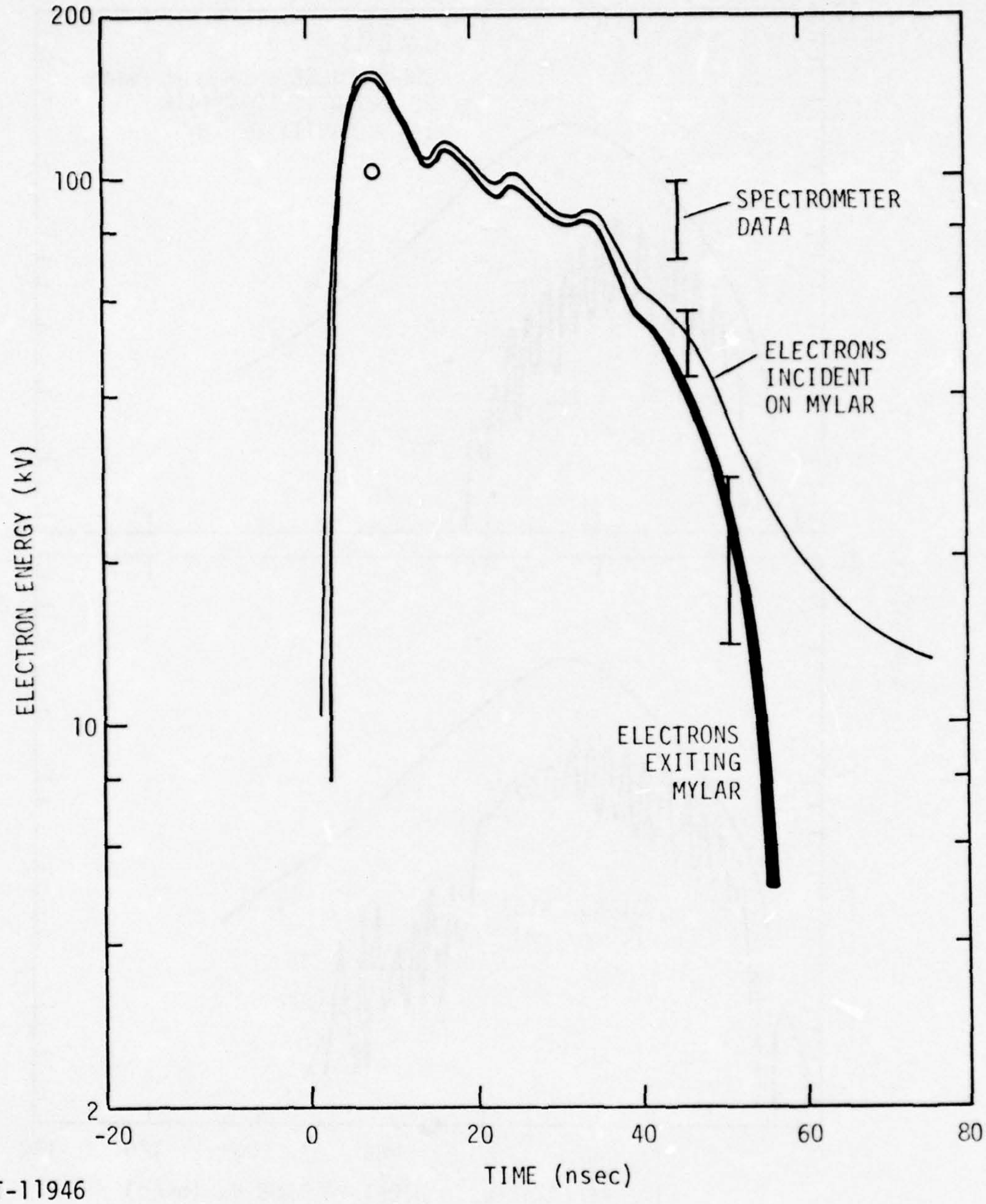

Figure 8. Estimation of average electron energies versus time - short pulse

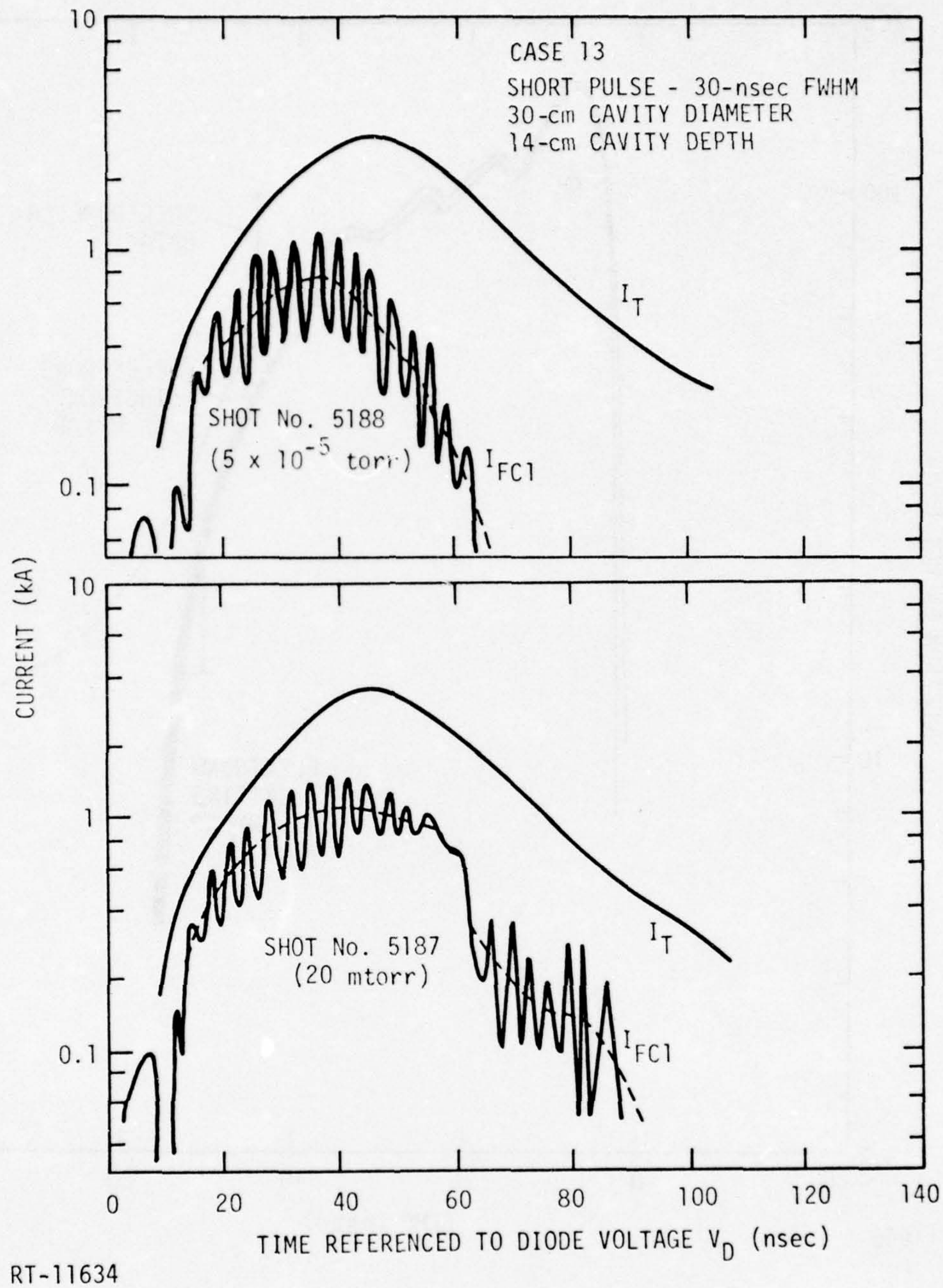

Figure 8a. Comparison of I_{FC1} and I_T time histories

Figure 9a. Comparison of I_{FC1} and I_T time histories - case 13

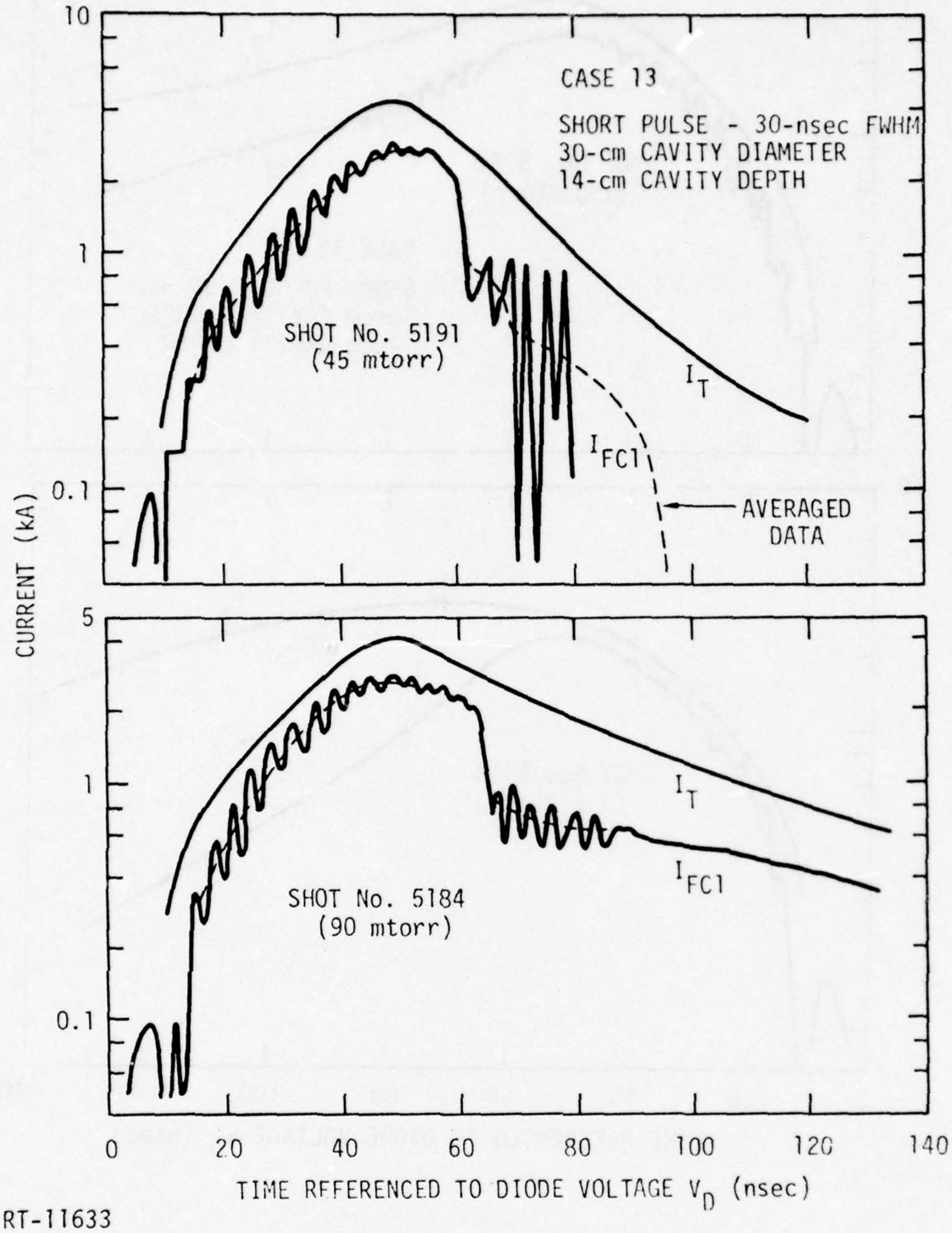

Figure 8b. Comparison of I_{FC1} and I_T time histories

Figure 9b. Comparison of I_{FC1} and I_T time histories - case 13

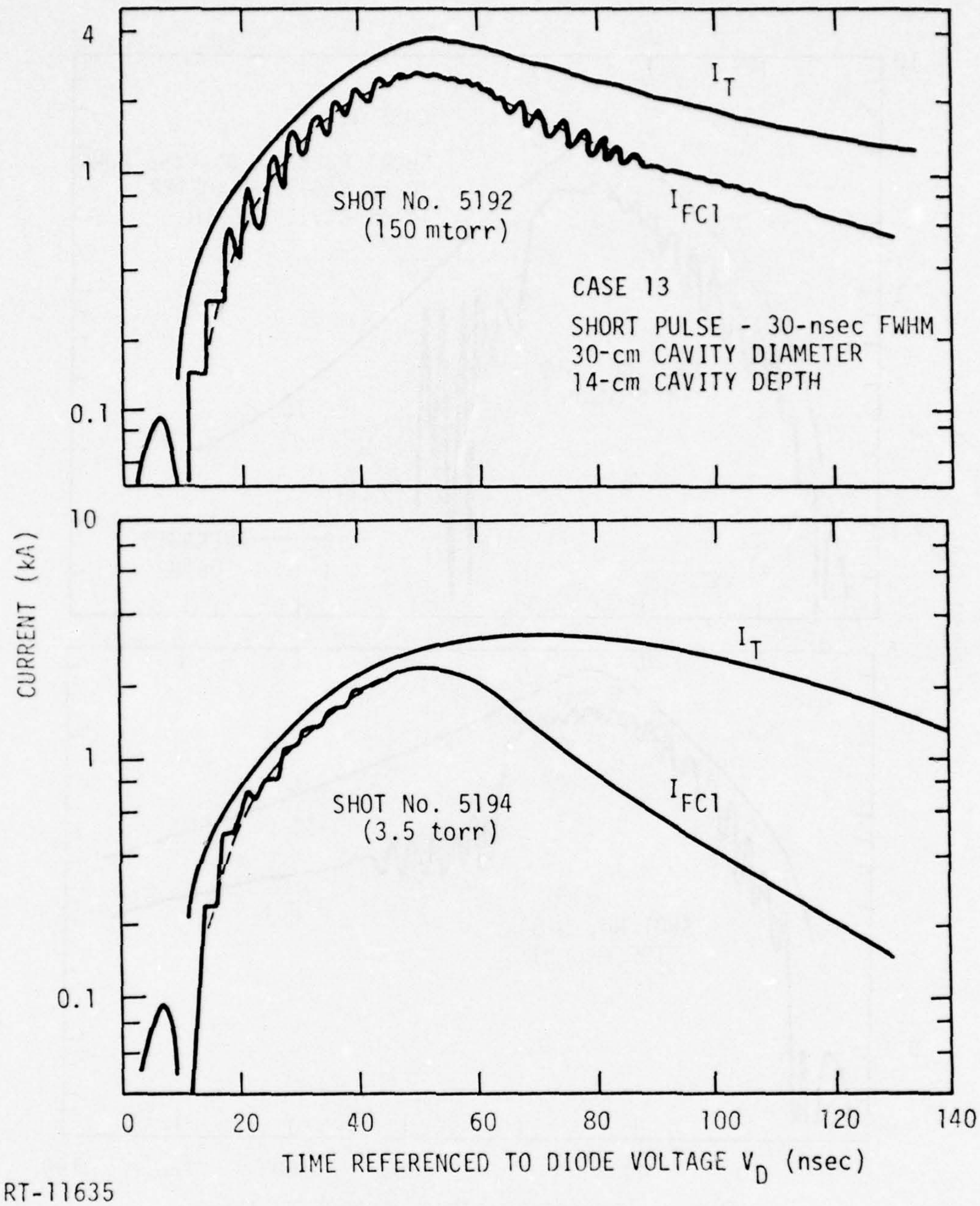

Figure 8c. Comparison of I_{FC1} and I_T time histories

Figure 9c. Comparison of I_{FC1} and I_T time histories - case 13

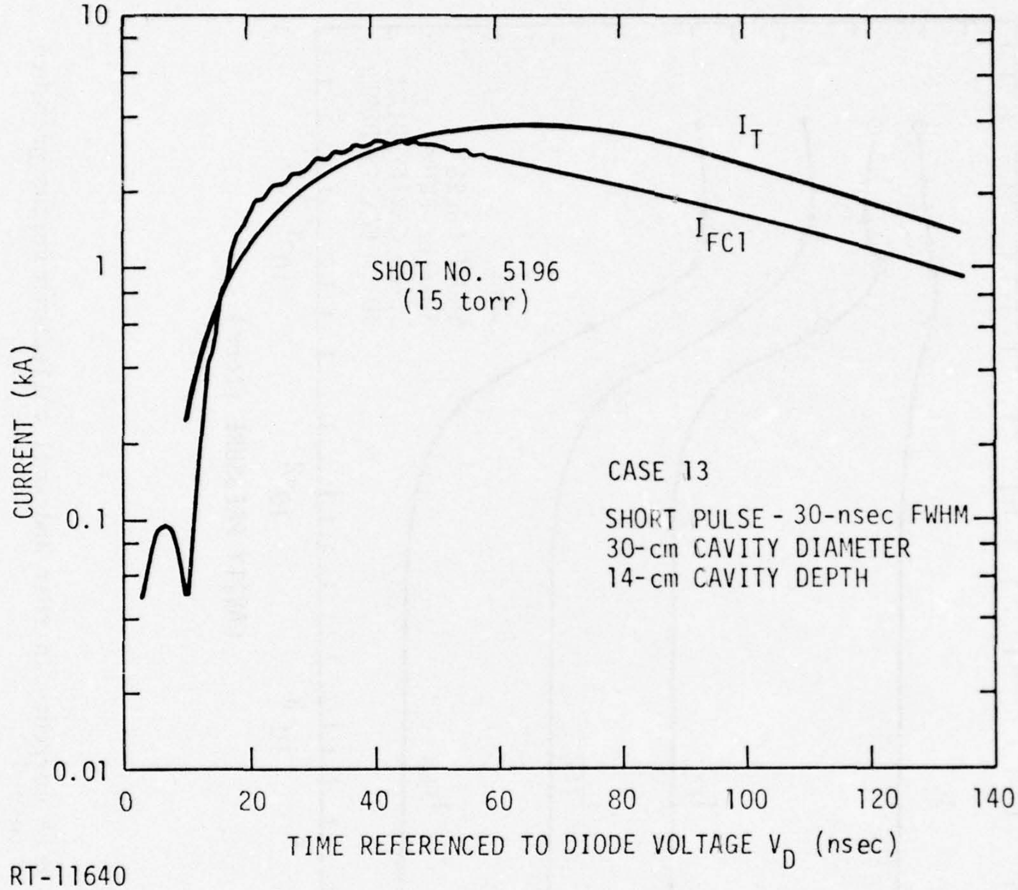

RT-11640

Figure 9d. Comparison of I_{FC1} and I_T time histories - case 13

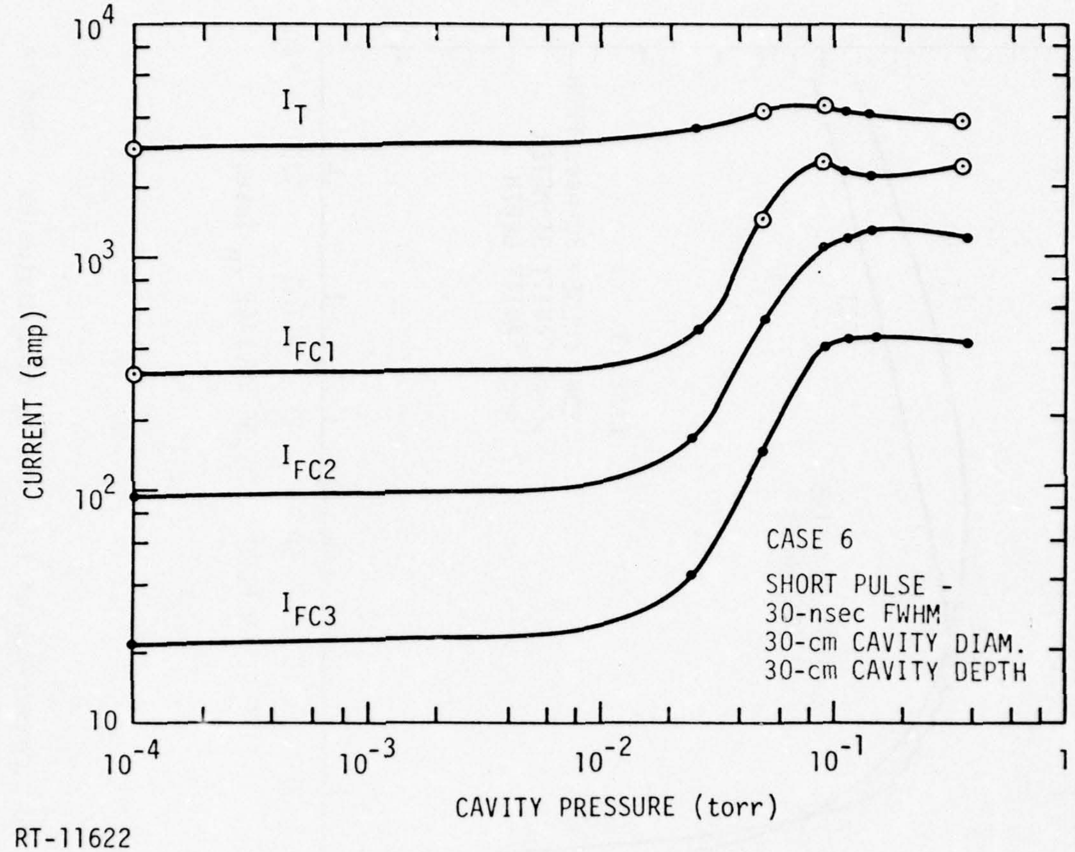

Figure 10. Peak currents in rear and wall collectors versus pressure - case 6

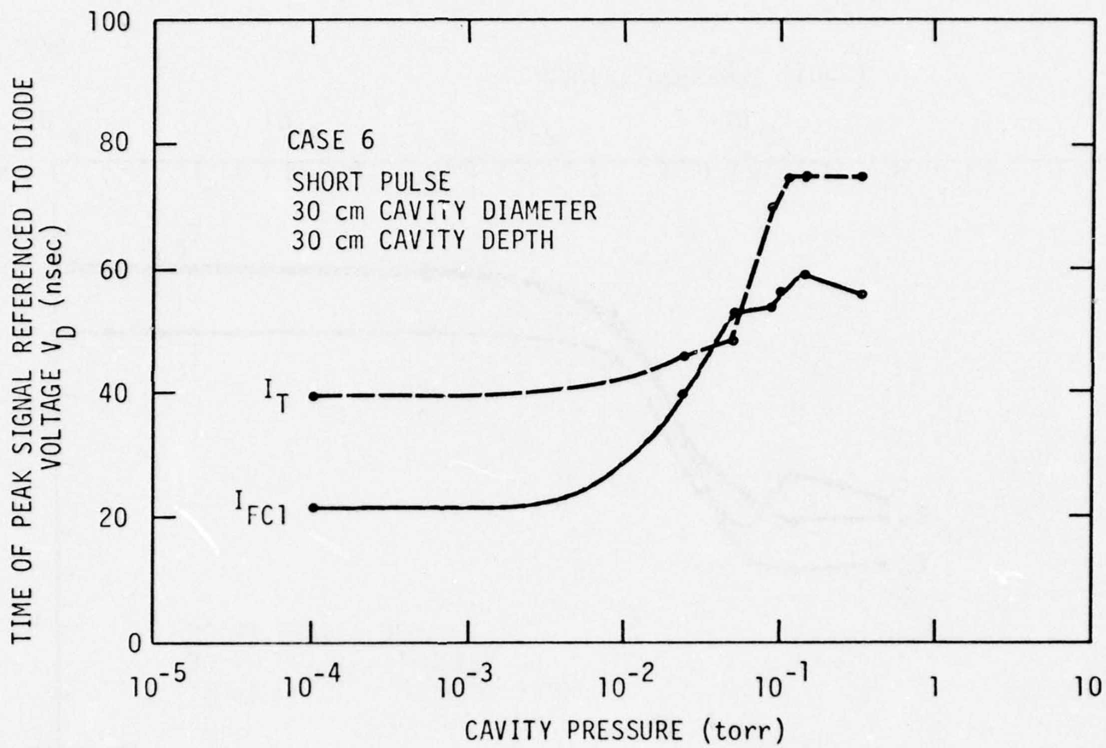

RT-11623

Figure 11. Time of occurrence of peak currents in rear and wall collectors versus pressure - case 6

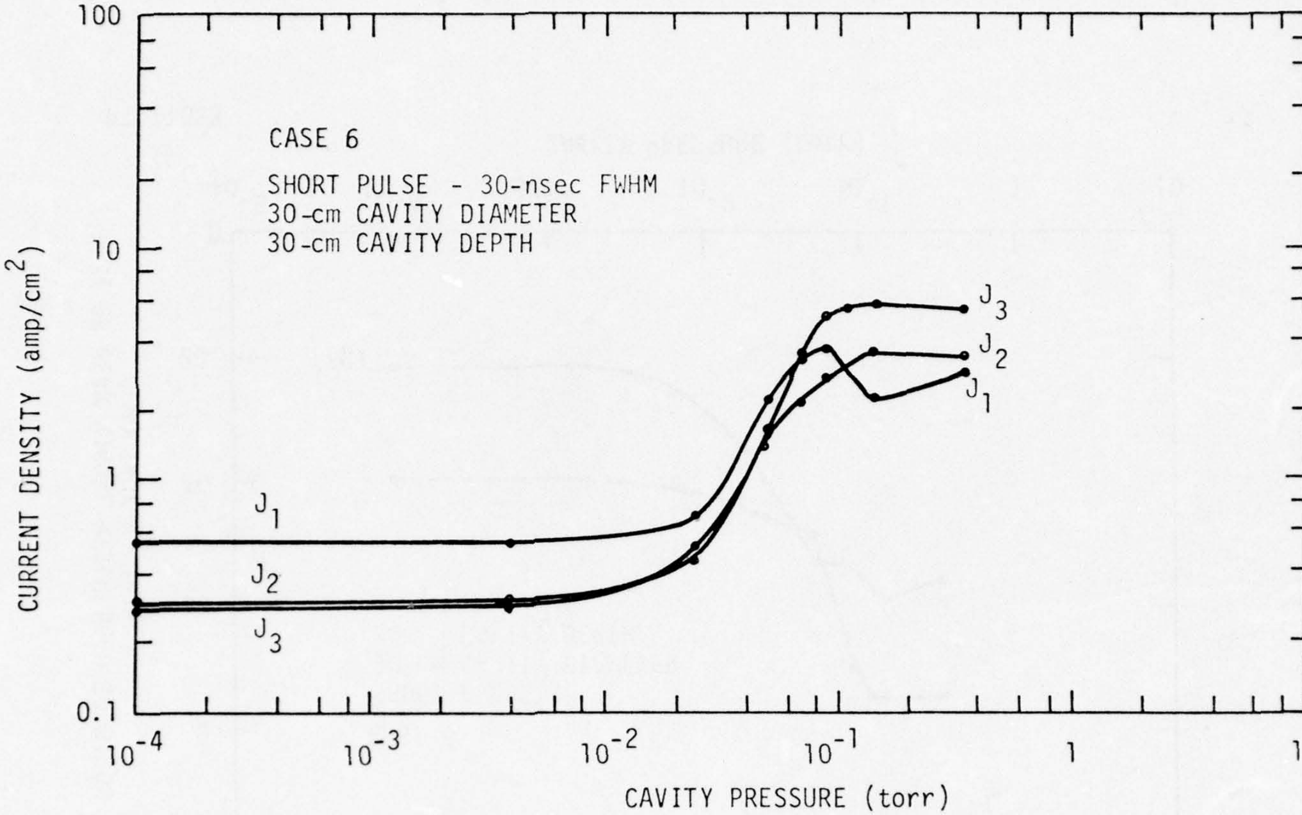

RT-11624

Figure 12. Peak current density averaged within each ring of rear collector versus pressure - case 6

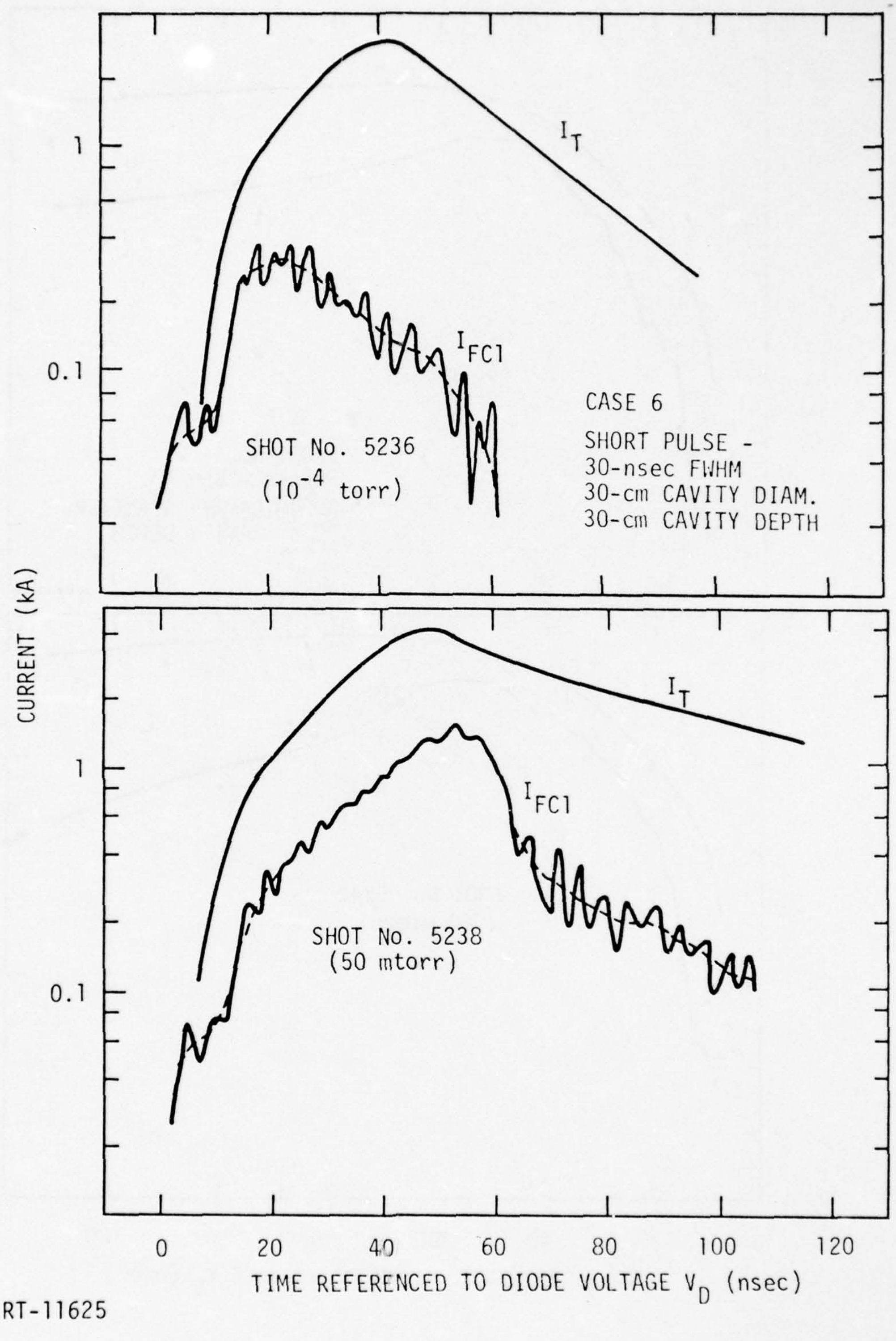

Figure 13a. Comparison of I_{FC1} and I_T time histories - case 6

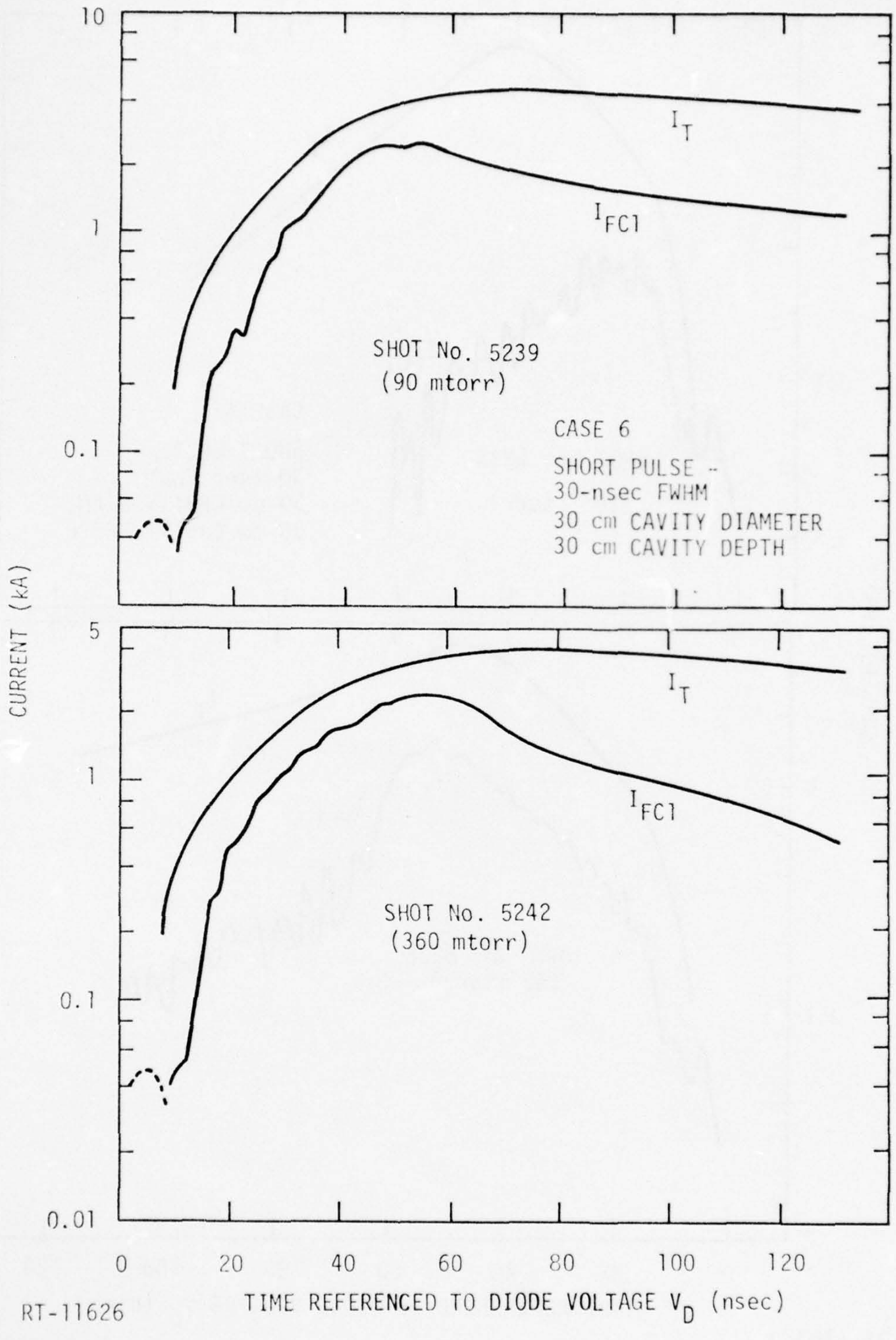

Figure 13b. Comparison of I_{FC1} and I_T time histories - case 6

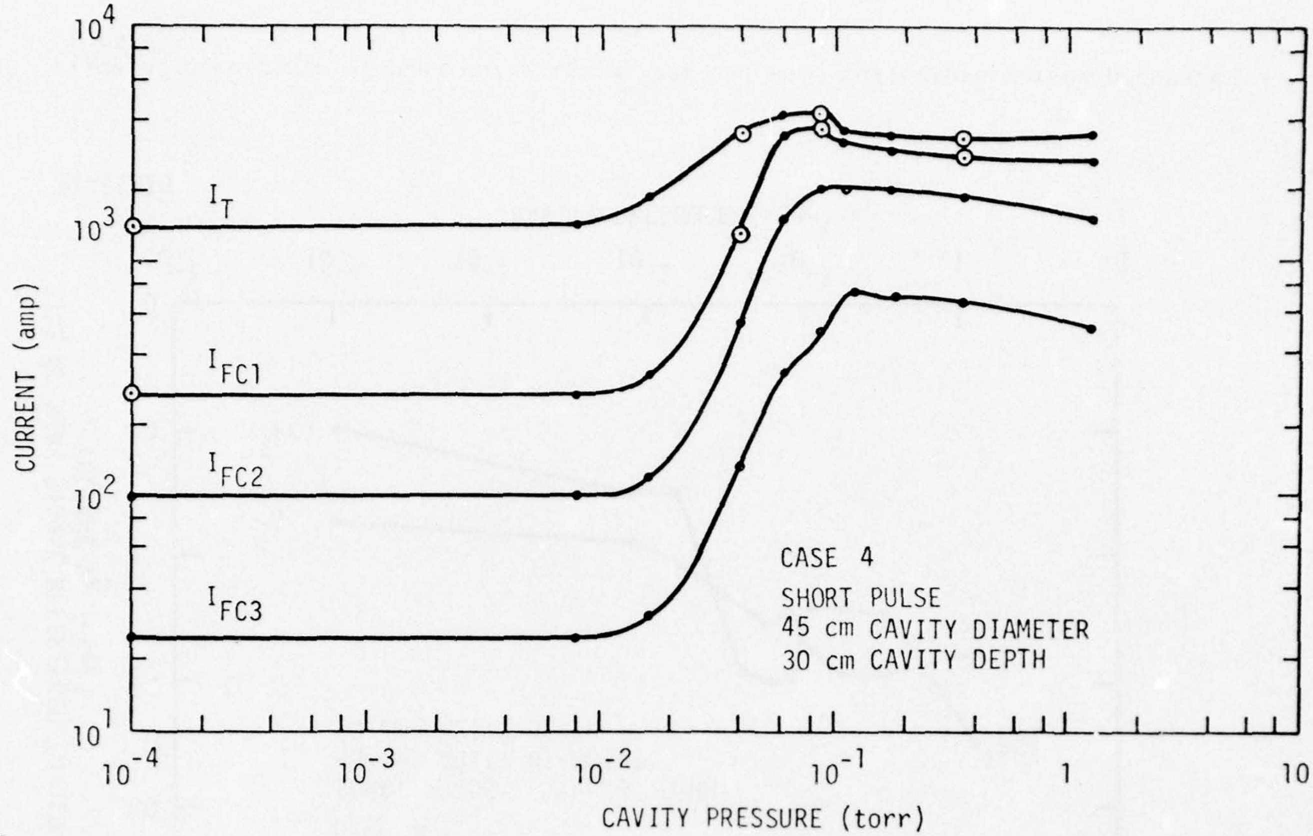

Figure 14. Peak currents in rear and wall collectors versus pressure - case 4

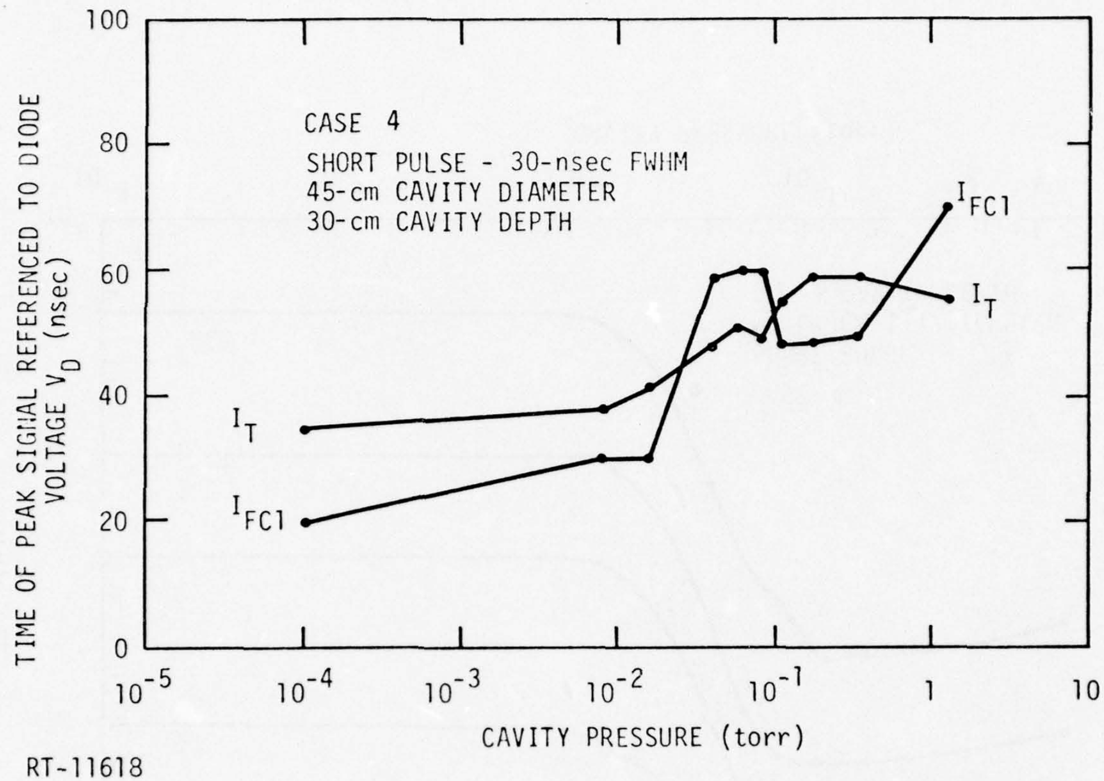

Figure 15. Time of occurrence of peak currents in rear and wall collectors versus pressure - case 4

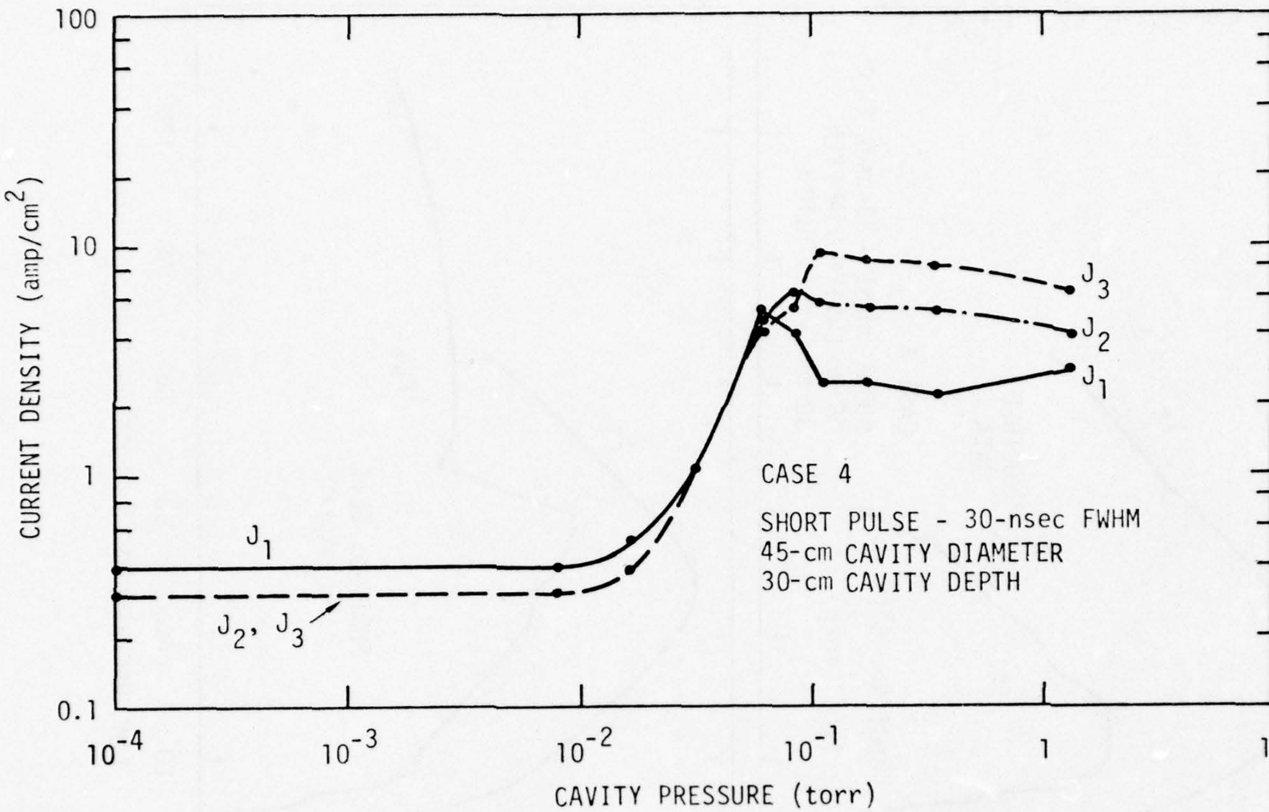

RT-11619

Figure 16. Peak current density averaged within each ring of rear collector versus pressure - case 4

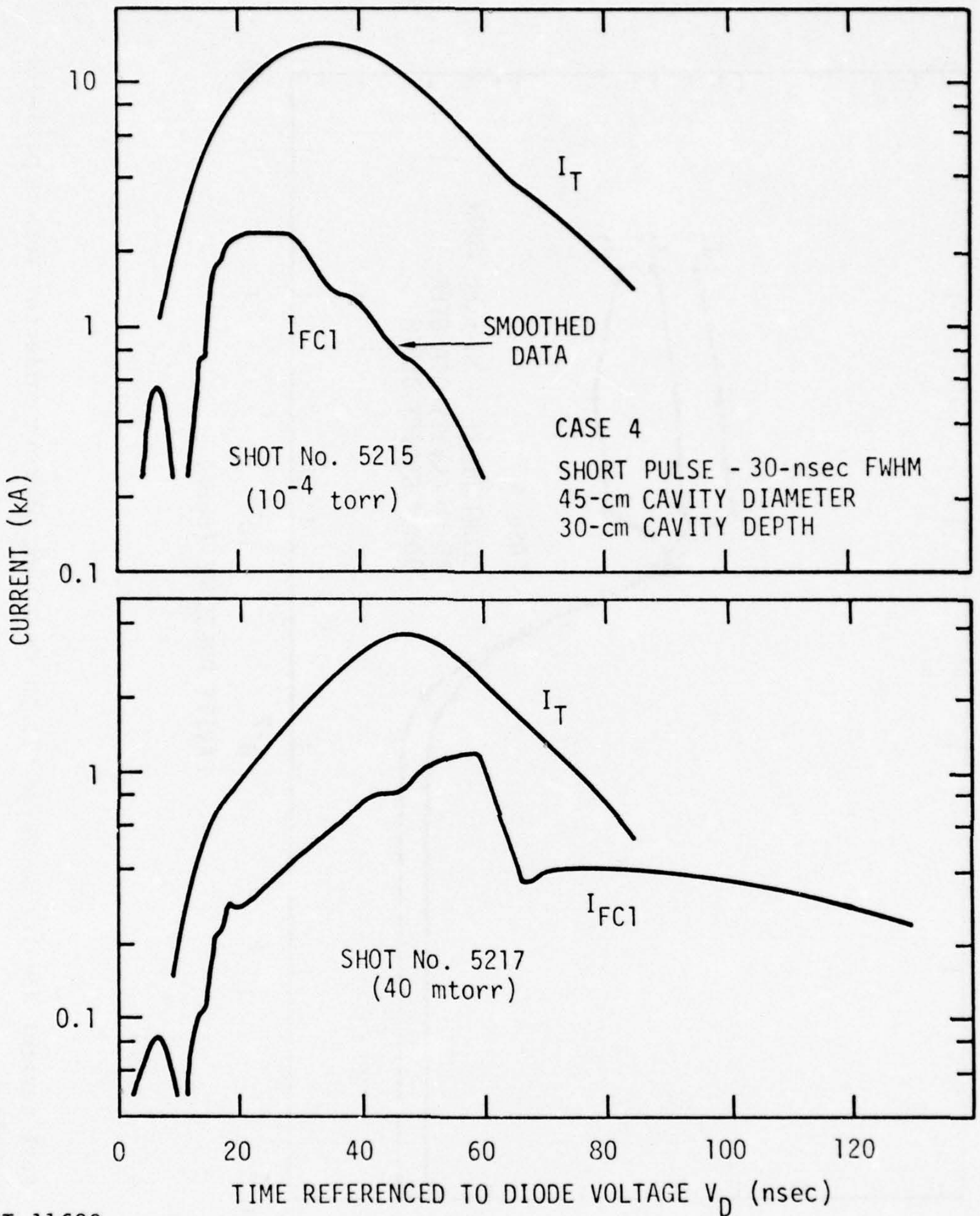

RT-11620

Figure 17a. Comparison of I_{FC1} and I_T time histories - case 4

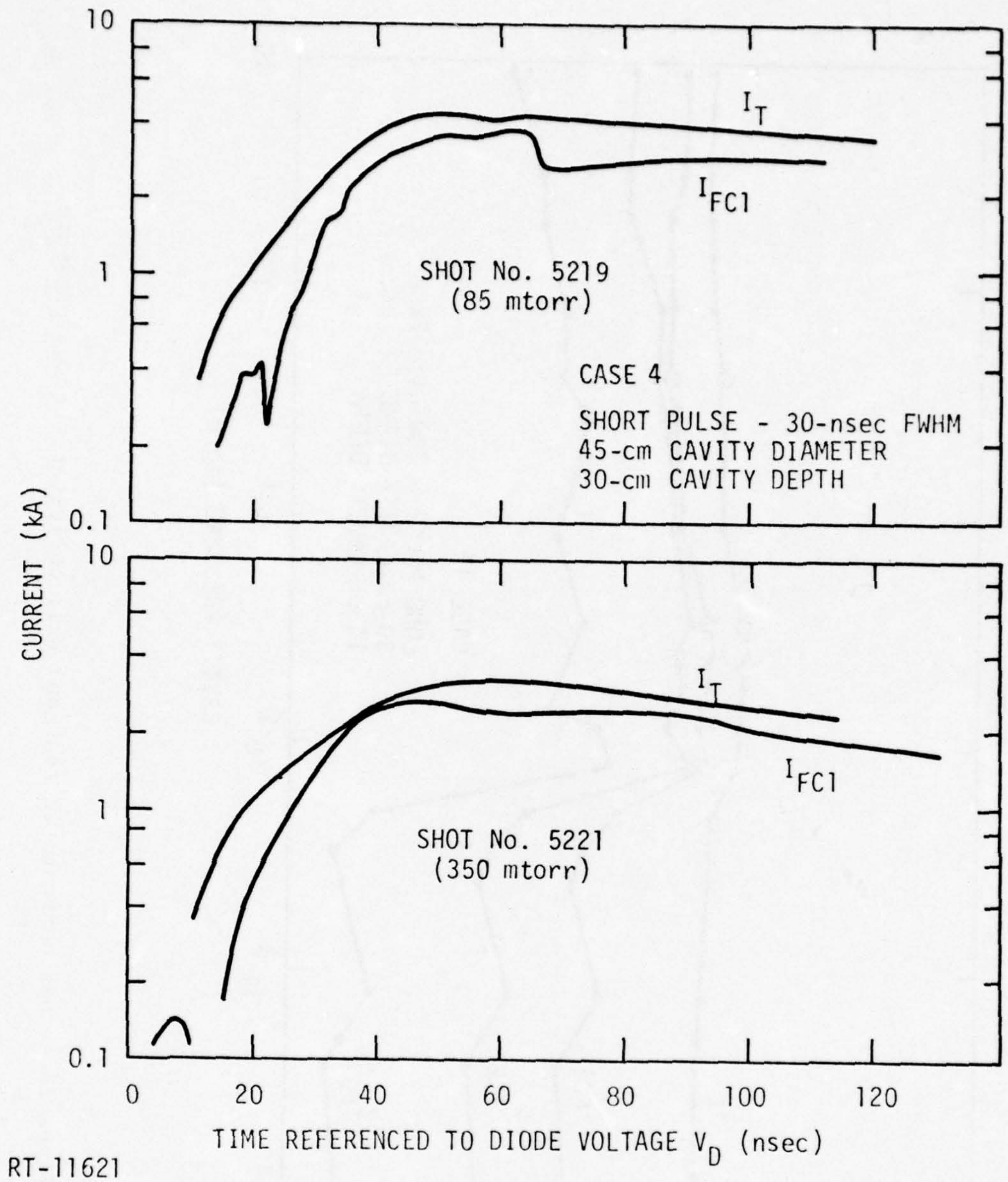

Figure 17b. Comparison of I_{FC1} and I_T time histories - case 4

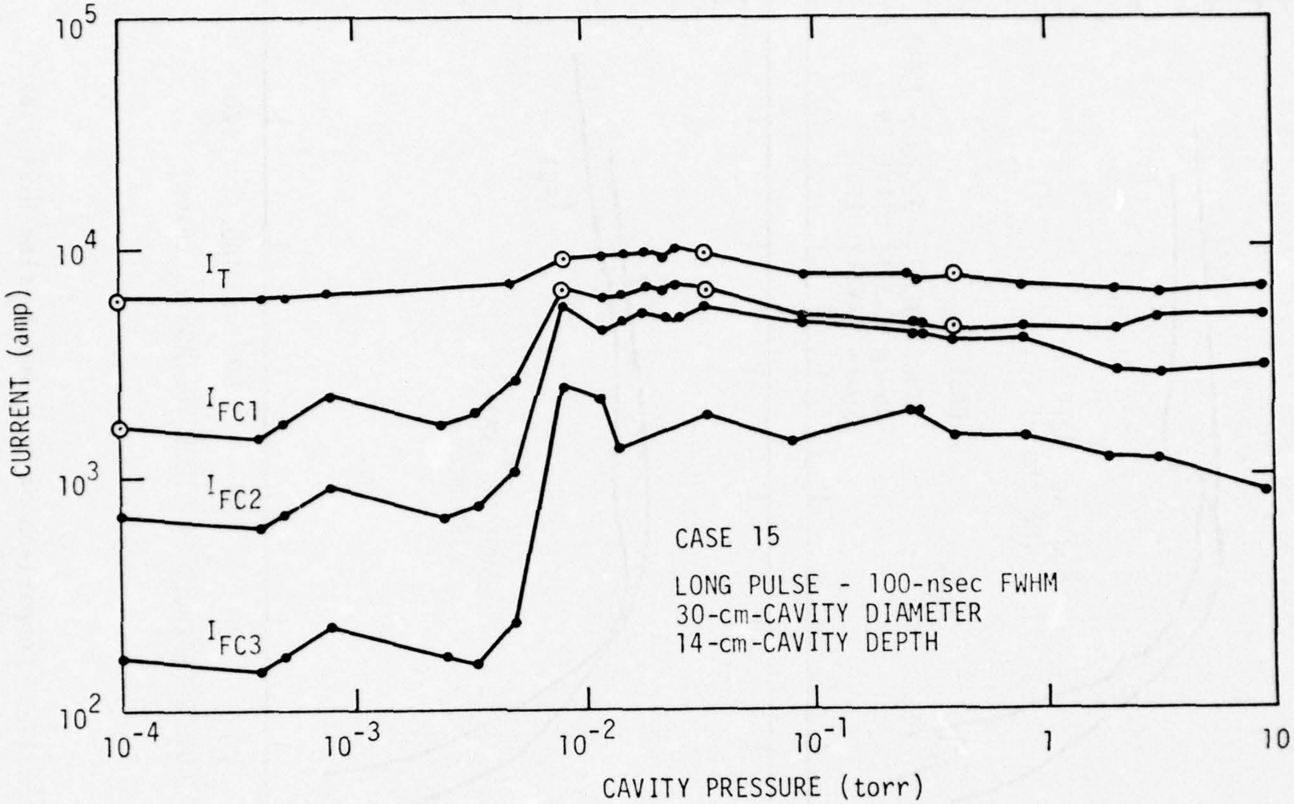

RT-11609

Figure 18. Peak currents in rear and wall collectors versus pressure - case 15

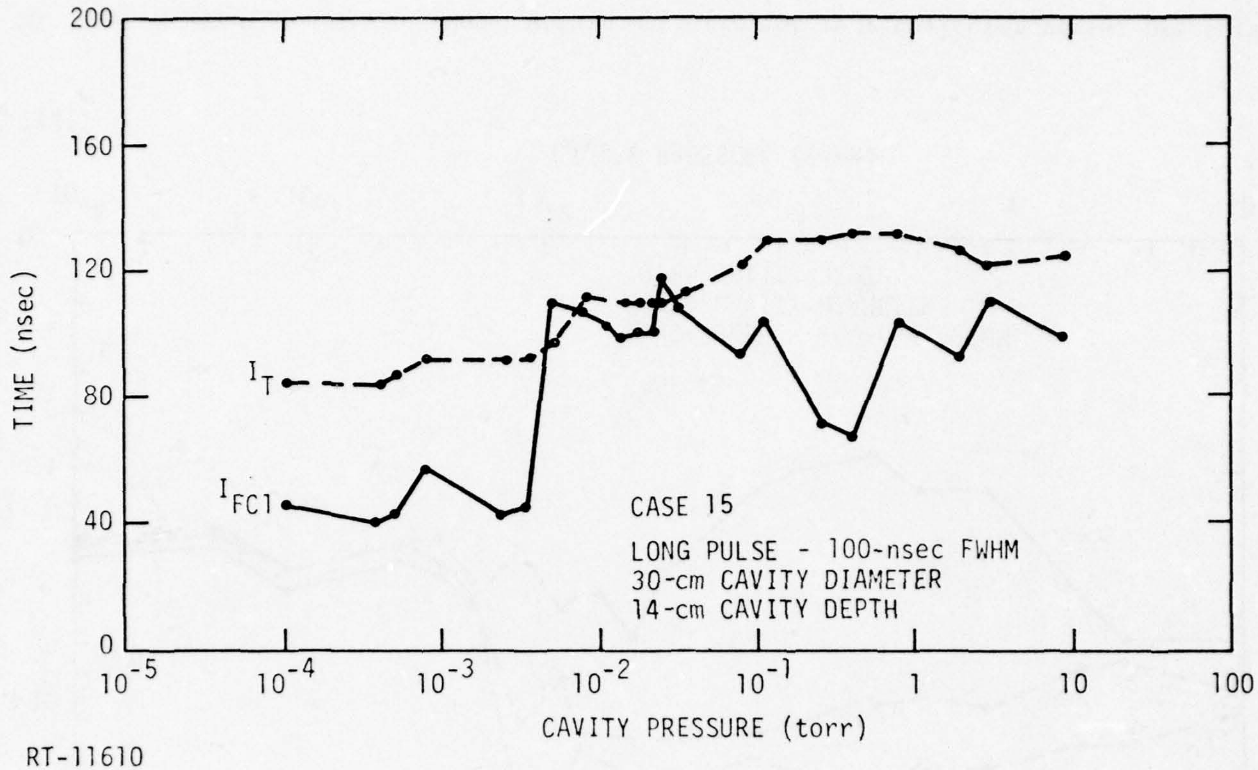

Figure 19. Time of occurrence of peak currents in rear and wall collectors versus pressure - case 15

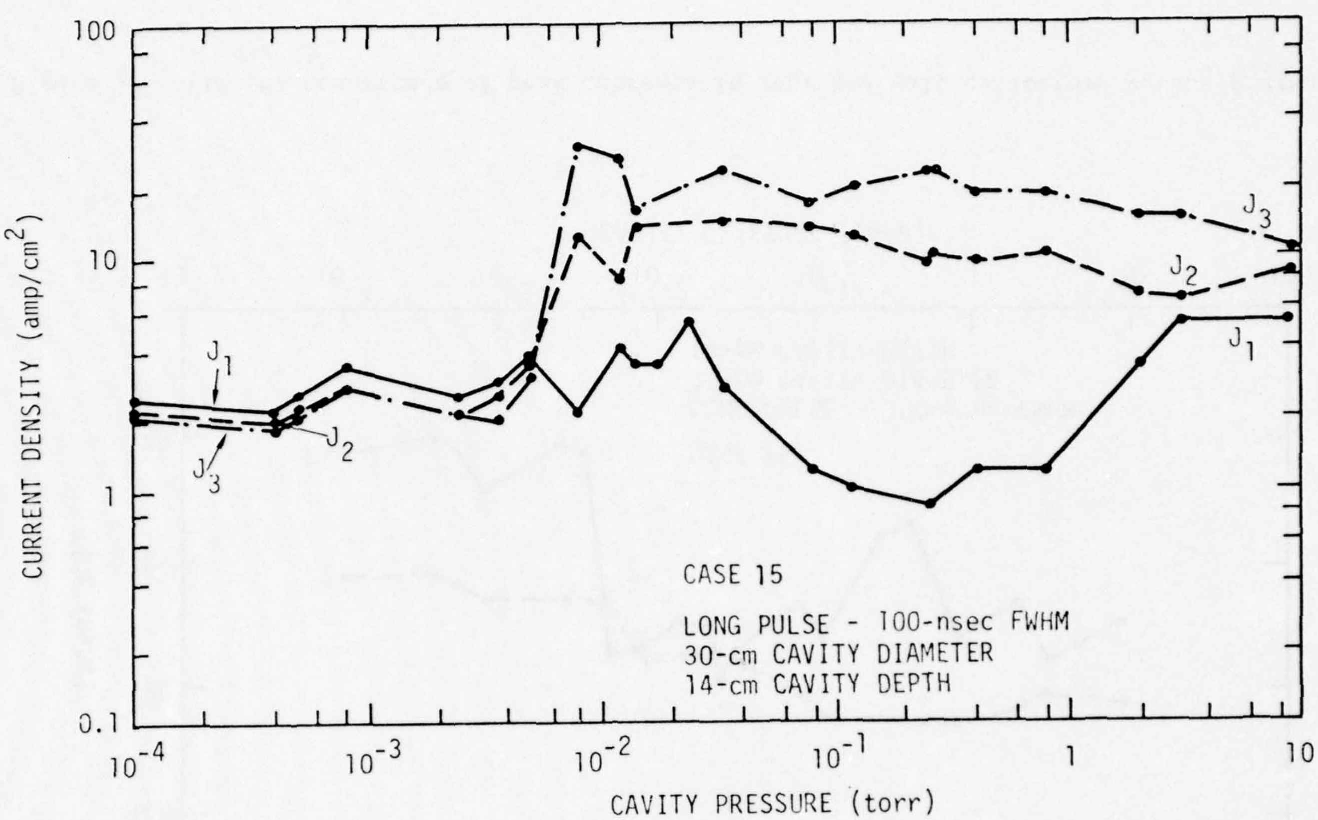

RT-11611

Figure 20. Peak current density averaged within each ring of rear collector versus pressure - case 15

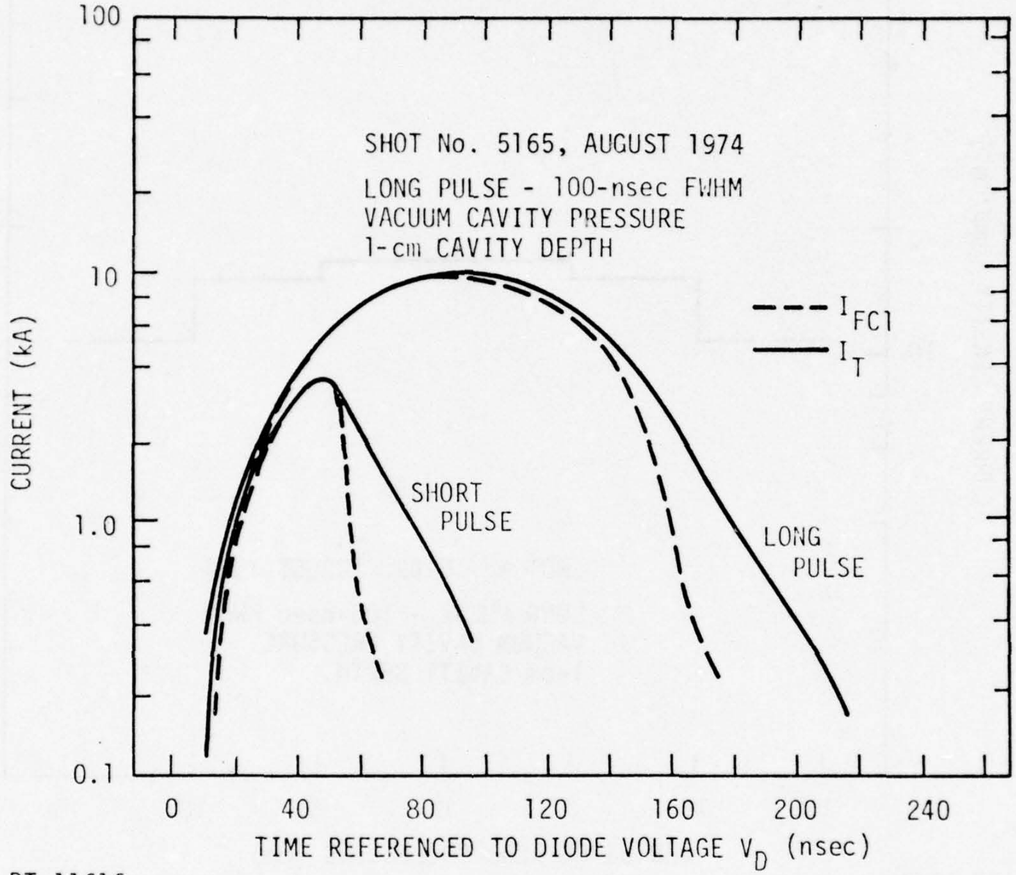

RT-11616

Figure 21. Current collected at 1 cm. depth (I_{FC1}) and total current (I_T); approximation to emitted current-long pulse

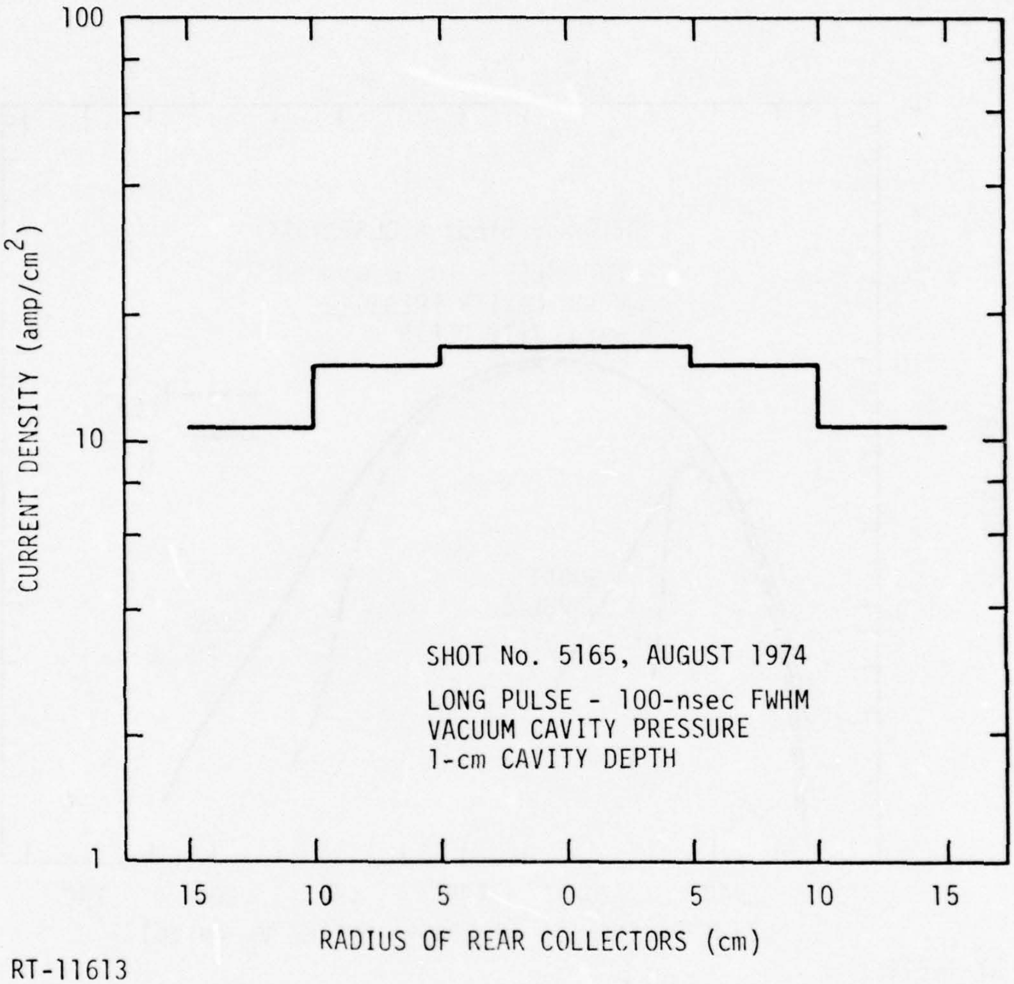

Figure 22. Estimation of peak current uniformity through transmission anode - long pulse

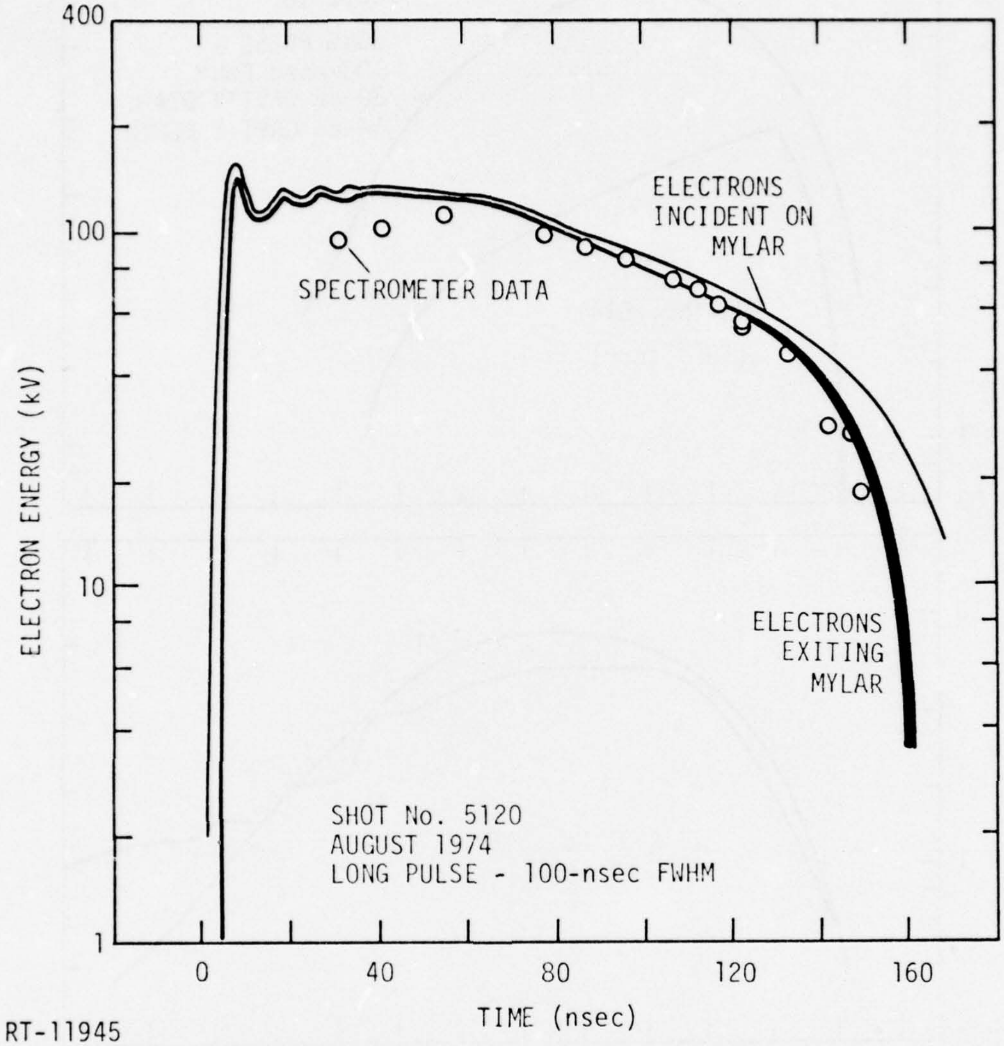

Figure 23. Estimation of average electron energies versus time - long pulse

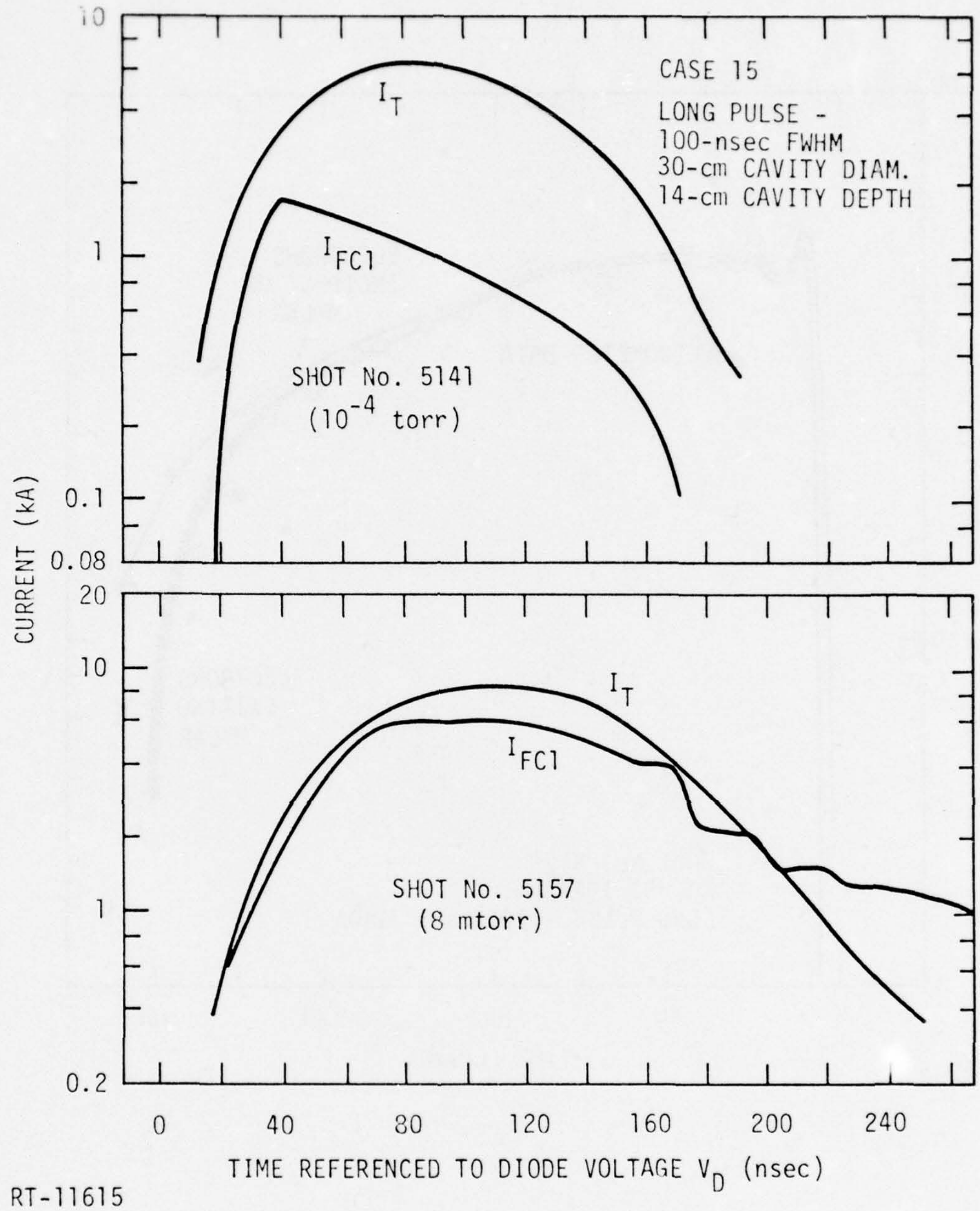

Figure 24a. Comparison of I_{FC1} and I_T time histories - case 15

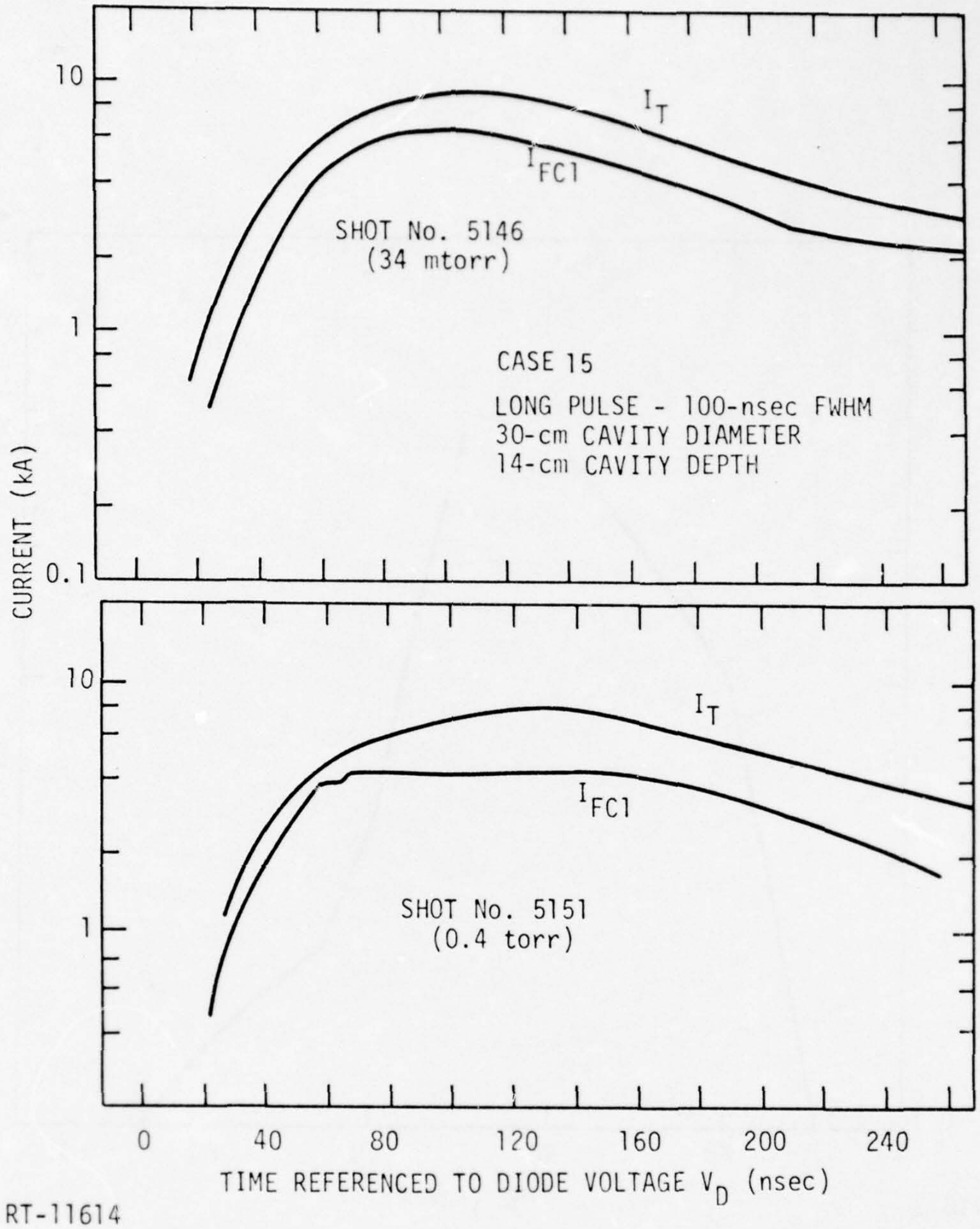

Figure 24b. Comparison of I_{FC1} and I_T time histories - case 15

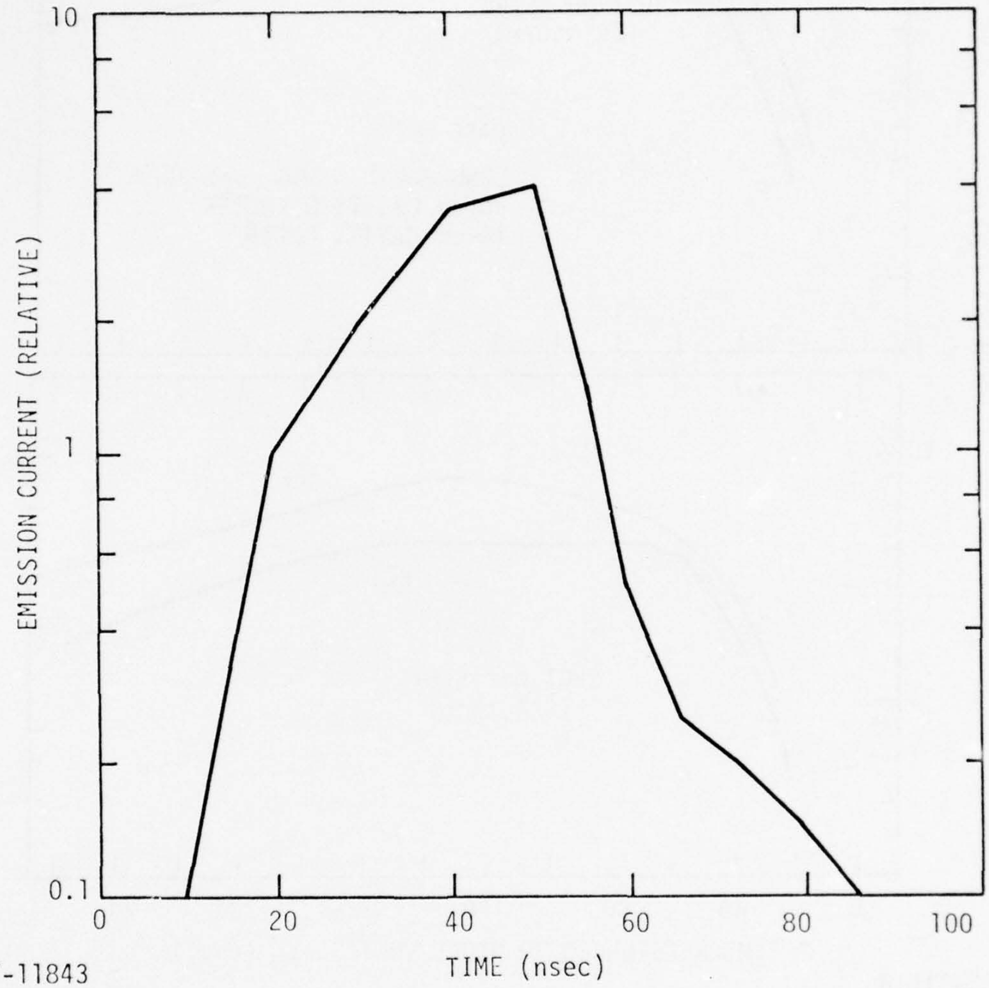

RT-11843

Figure 25. Digitized pulse shape used to describe emission current as a function of time. This is an approximation to the curve I_{FC1} of Figure 6.

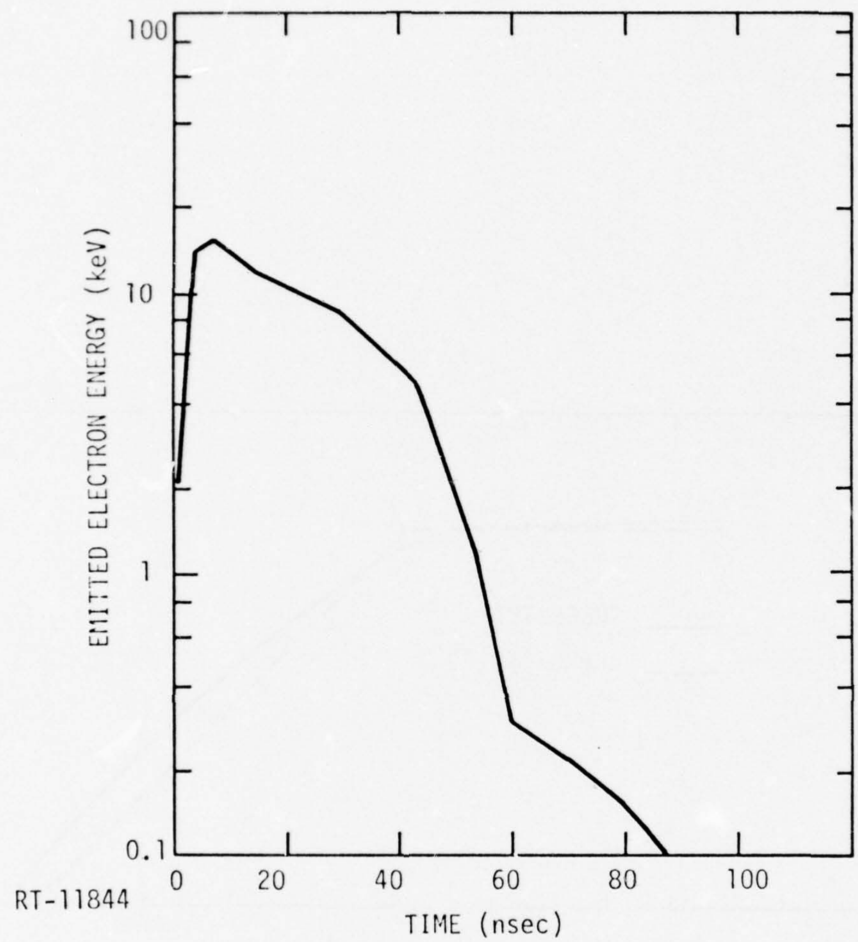

Figure 26. Digitized energy of emitted electrons as a function of time. This is an estimate of the electron energy (Figure 8) as modified after passing through the Mylar anode.

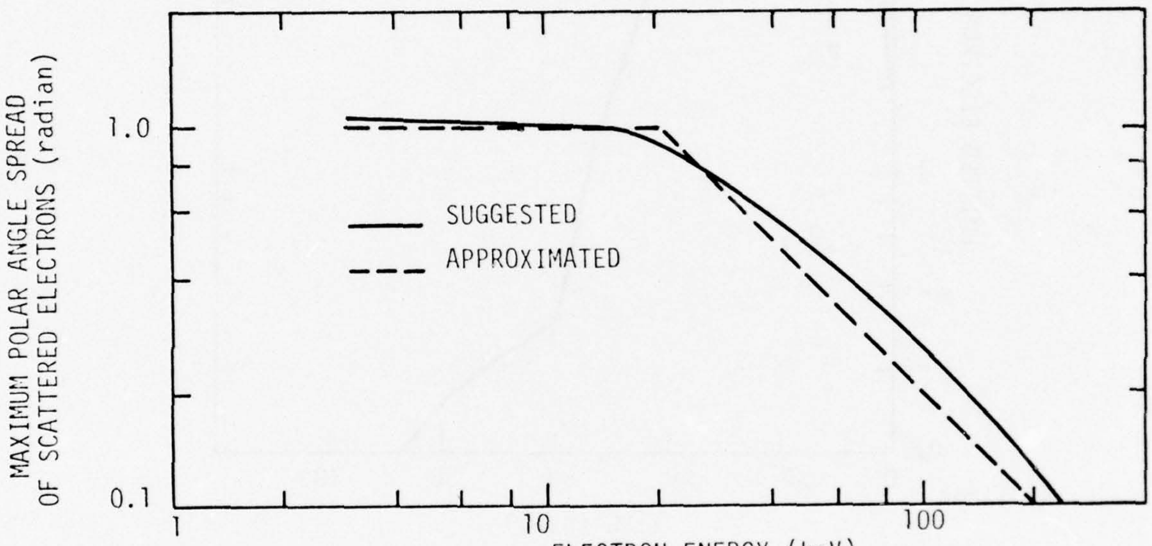

RT-11845

Figure 27. Angular spread of emitted electrons. The approximation used to represent this curve is given in the text.

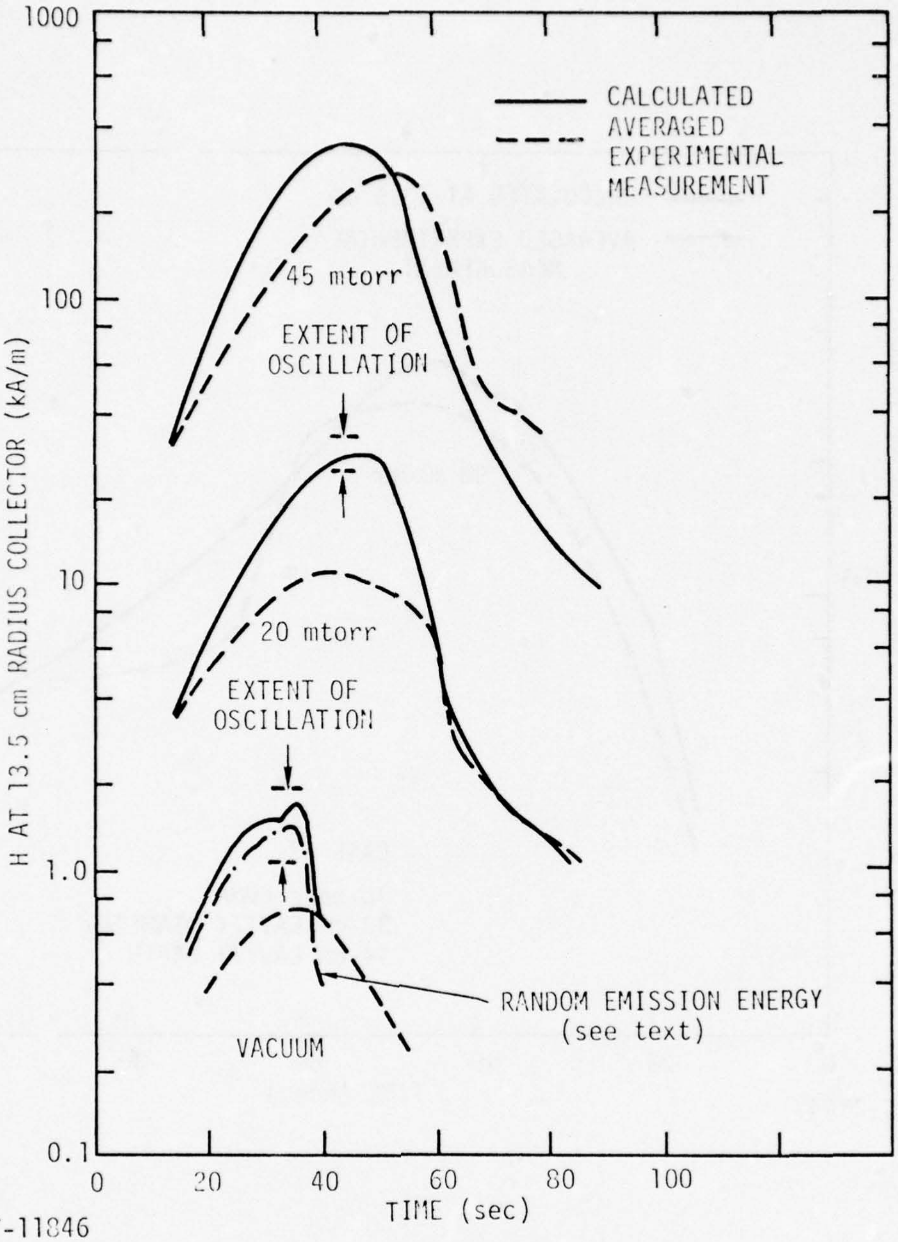

Figure 28a. Total current collected on rear plate for various pressures. Where oscillations are indicated, the presented results represent a 4-nsec average. Note that the vertical scales are displaced.

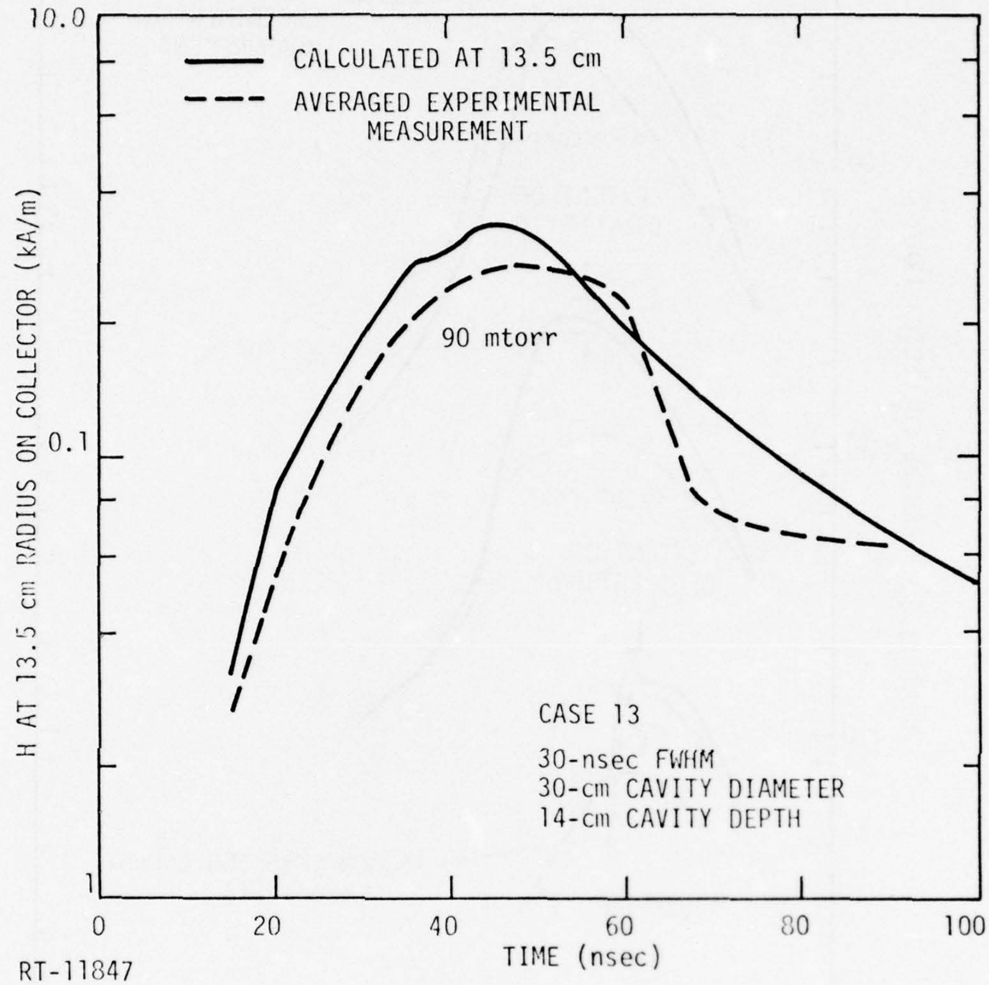

Figure 28b. Total current collected on rear plate for 90 mtorr

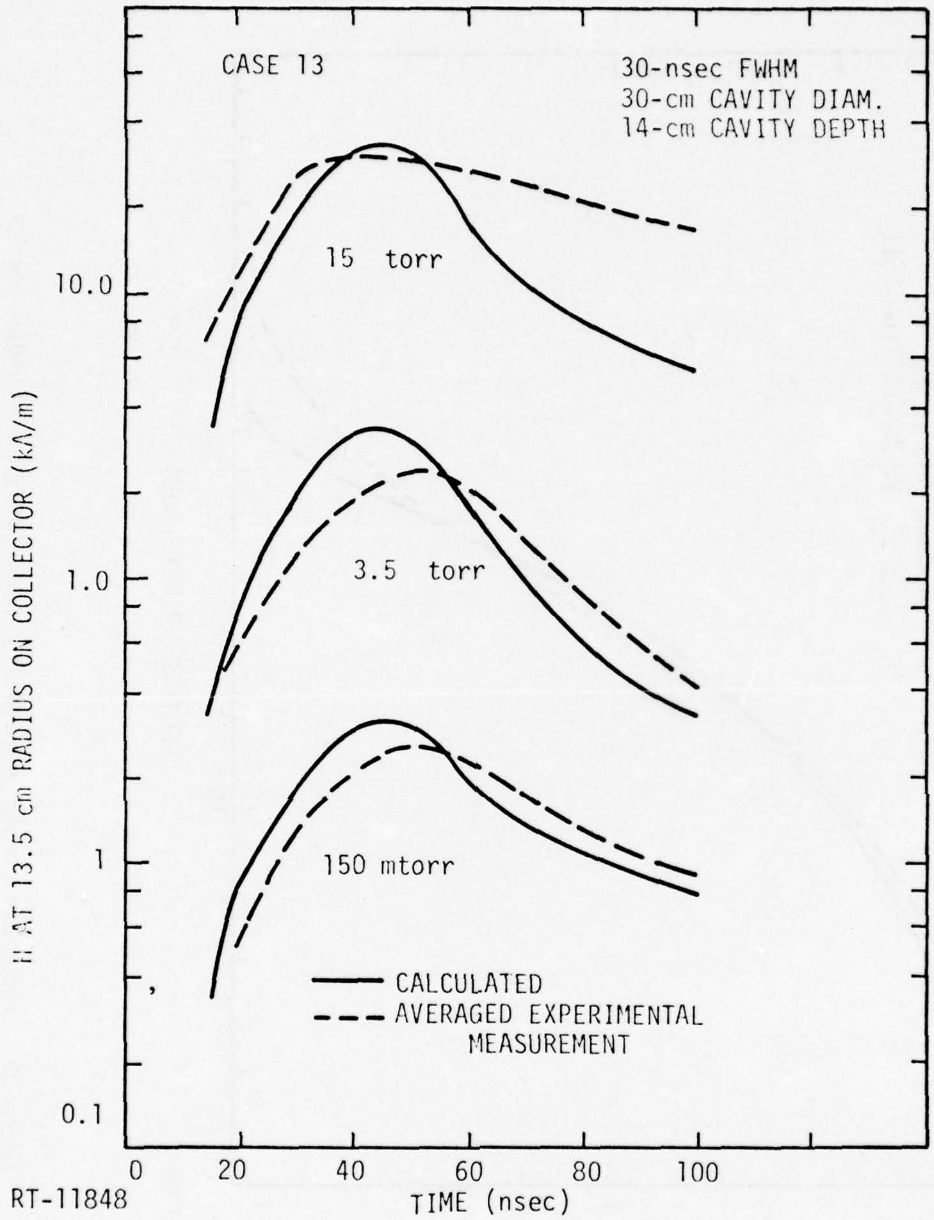

Figure 28c. Total current collected on rear plate for various pressures

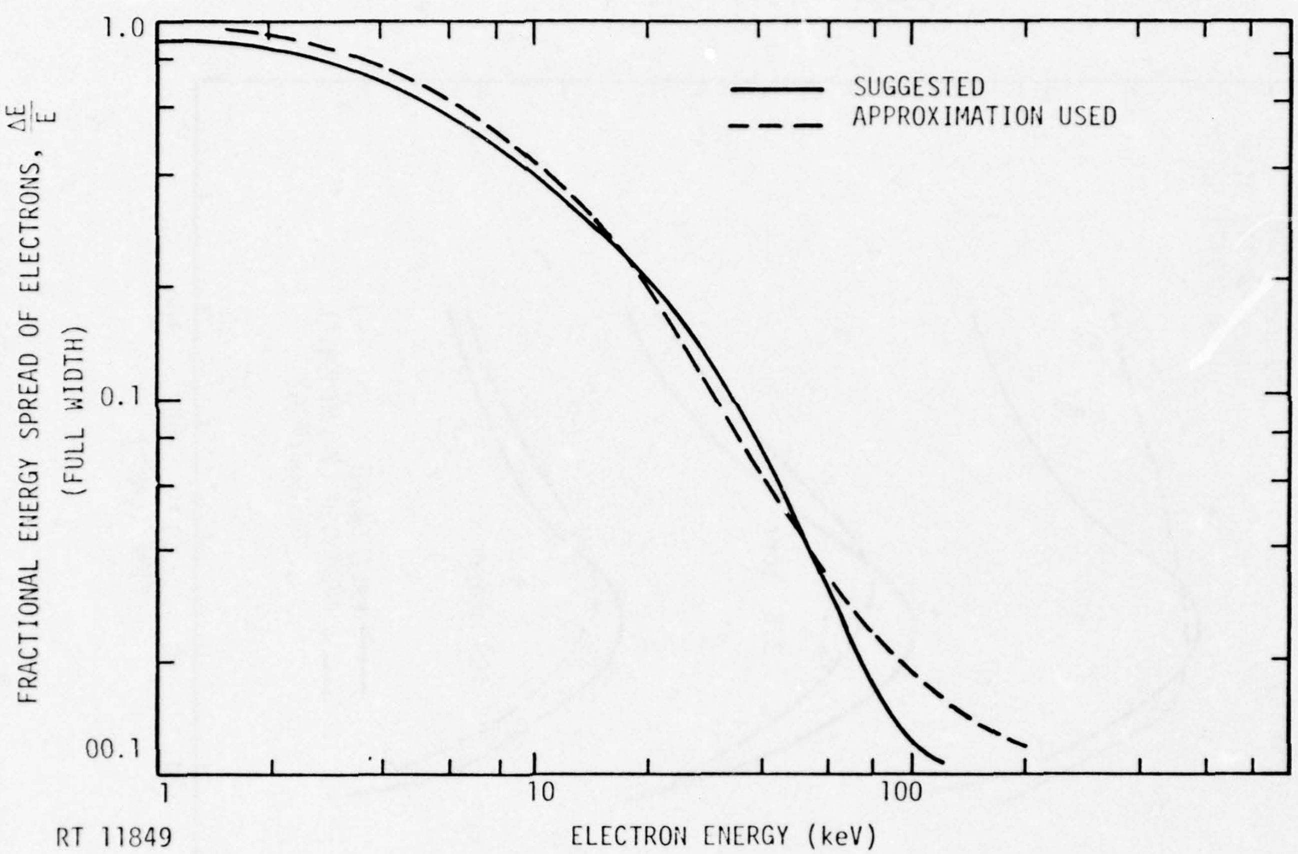

Figure 29. Emission energy spread for calculation of random energy

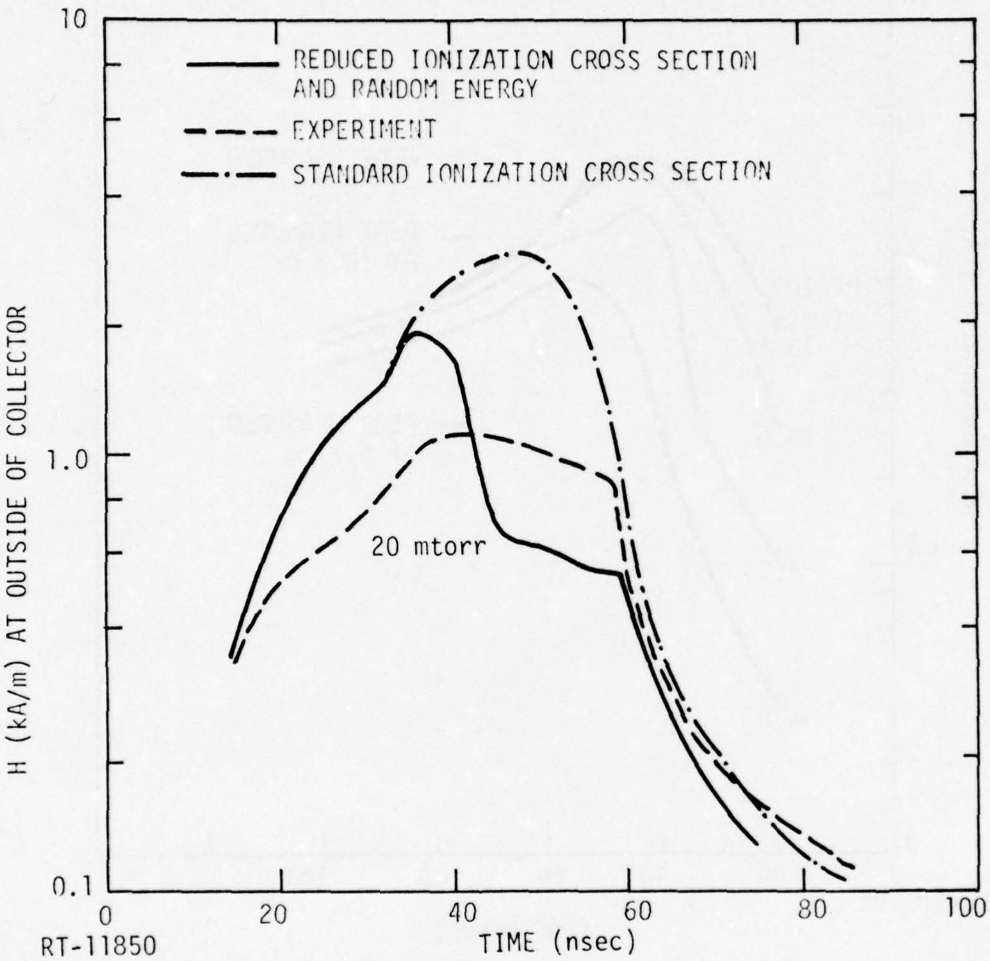

Figure 30. Effect of varying the ionization cross section. Reducing the ionization reduces the transmitted current, but the injected electron energy appears to be too high.

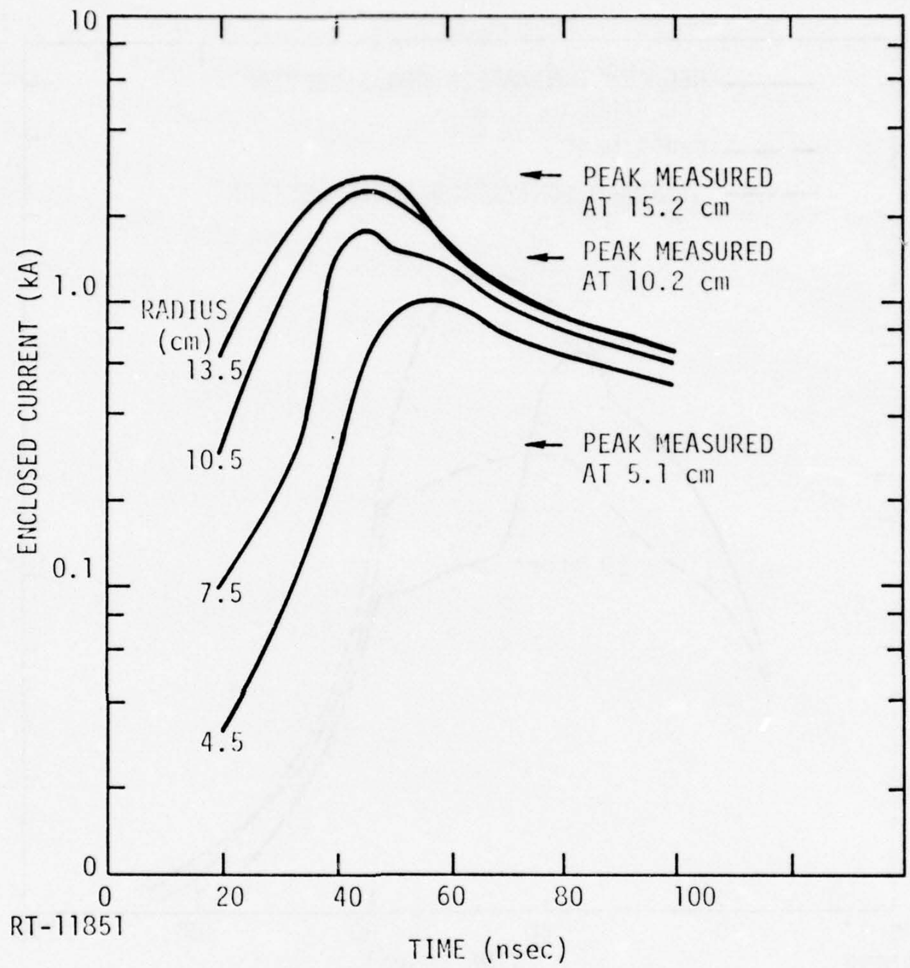

Figure 31. Spatial distribution of collected current at 150 mtorr. This demonstrates that the measured values are much less in the center than the calculated (solid curves) values. Measured values are from Figure 3 at amplitudes designated by the arrows.

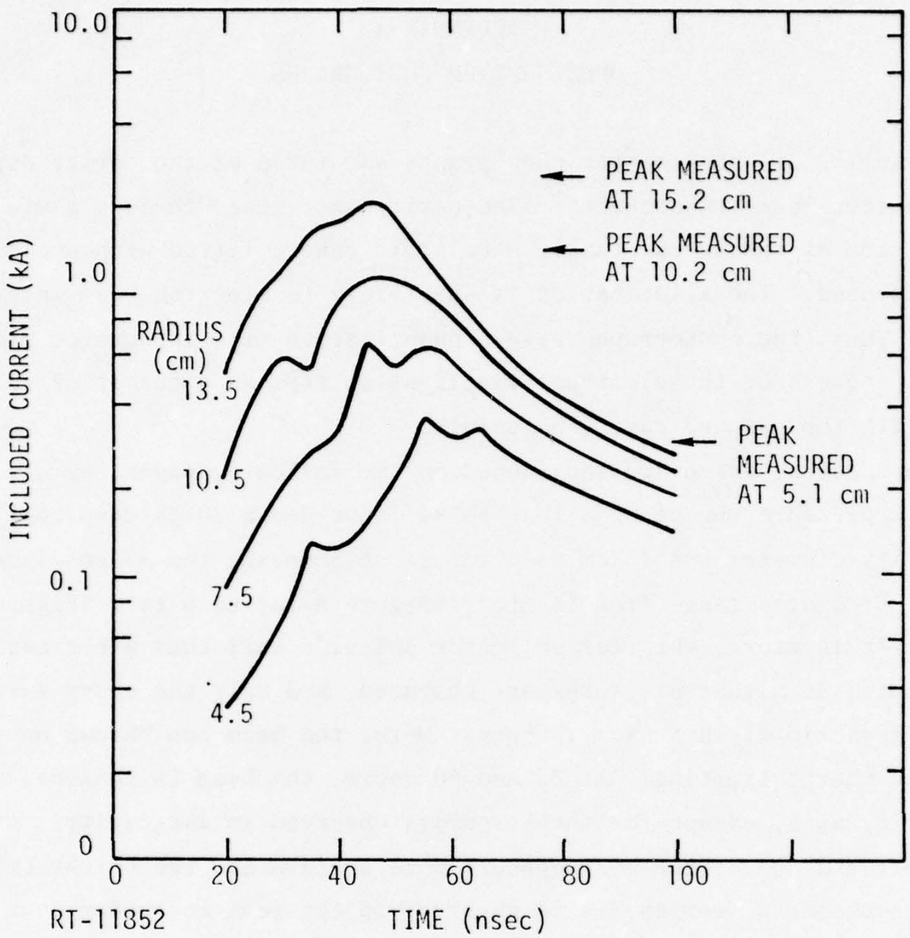

Figure 32. Spatial distribution of collected current at 150 mtorr. Curves are calculated values. The magnetic forces were ignored. This, in comparison with Figure 3, demonstrates the pinching of the magnetic field. The detailed shapes of the curves for radii <13.5 cm are not meaningful since data were available at every 5 nsec and the statistics are worse than in the previous figure due to the reduction in current. Measured values are from Figure 3 at amplitudes designated by the arrows.

APPENDIX A
OPEN-SHUTTER PHOTOGRAPHS

A series of open-shutter photographs was taken of the cavity during the electron-beam measurements. The cavity was viewed through a window in the side of the vacuum tank. A Polaroid camera fitted with a closeup lens was used. The illumination is due solely to electron-beam interactions. Thus, the photographs give a quantitative time-integrated picture of the progress of the electrons via light emitted as a result of collisions with the gas and cavity materials.

The photos, which are reproduced on the following pages, were taken during a pressure run using a long-pulse input and a 30-cm-deep cavity. The cavity diameter was 45 cm as a result of removing the 30-cm-diameter liner. Pressures range from 14 mtorr (Figure A-1a) to 6 torr (Figure A-1f). At 14 mtorr, the rear collector and side wall that are clearly illuminated at higher pressures are obscured, and only the epoxy surface of the magnetic field sensor is seen. Here, the beam has "blown up" due to space-charge-limiting. At 32 and 60 mtorr, the beam is confined to the cavity axis, except for the streamers observed in mid-cavity. At 100 mtorr and above, the beam appears more uniform and the bright emission discussed in Section 3.1 is observed on the rear collector near the screws and the edges of the collector rings.

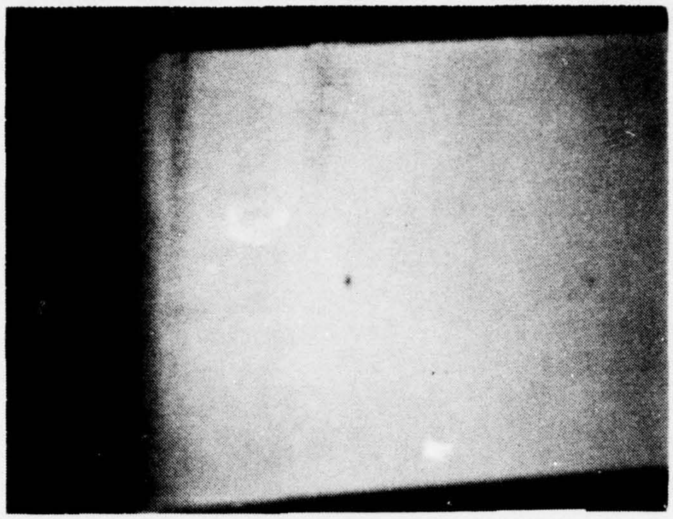

a. Shot 5229, 14 mtorr

b. Shot 5228, 32 mtorr

Figure A-1 Open-shutter photographs for a long-pulse, 30-cm-deep case

c. Shot 5226, 60 mtorr

d. Shot 5230, 100 mtorr

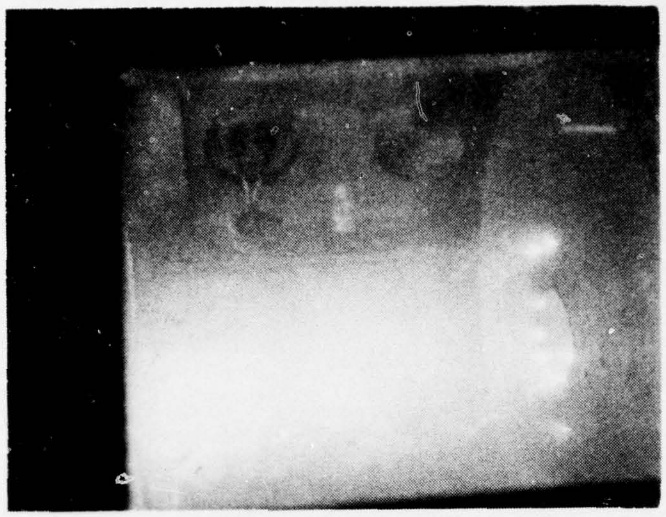

e. Shot 5233, 1.1 torr

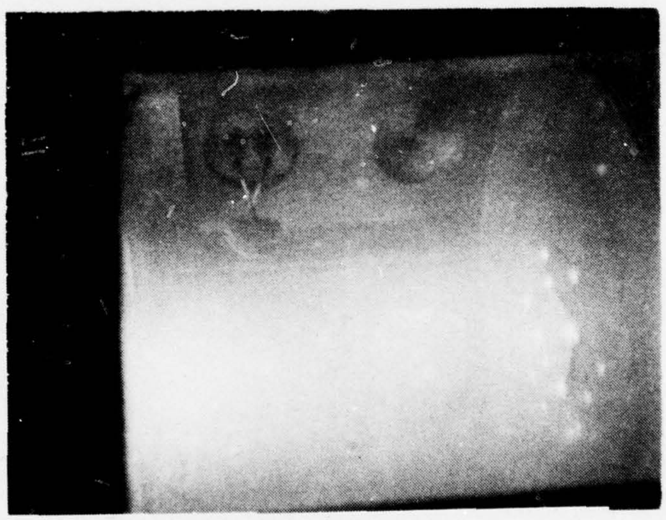

f. Shot 5234, 6 torr

blank
68

DISTRIBUTION

DEFENSE DOCUMENTATION CENTER
CAMERON STATION, BUILDING 5
ALEXANDRIA, VA 22314
ATTN DDC-TCA (12 COPIES)

COMMANDER
US ARMY MATERIEL DEVELOPMENT
& READINESS COMMAND
5001 EISENHOWER AVENUE
ALEXANDRIA, VA 22333
ATTN DRXAM-TL, HQ TECH LIBRARY
ATTN DRCDE-D, LAWRENCE FLYNN
ATTN DRCRD-EM

ASSISTANT TO THE SECRETARY OF DEFENSE
ATOMIC ENERGY
DEPARTMENT OF DEFENSE
WASHINGTON, DC 20301
ATTN DOCUMENT CONTROL

DIRECTOR
DEFENSE ADVANCED RSCH PROJ AGENCY
ARCHITECT BUILDING
1400 WILSON BLVD.
ARLINGTON, VA 22209
ATTN TECHNICAL LIBRARY
ATTN AD/E&PS GEORGE H. HALMEIER
ATTN NMR

DIRECTOR
DEFENSE CIVIL PREPAREDNESS AGENCY
ASSISTANT DIRECTOR FOR RESEARCH
WASHINGTON, DC 20301
ATTN TS(AED), ROOM 1C 535
ATTN RE(EO)
ATTN ADMIN OFFICER

DEFENSE COMMUNICATION ENGINEER CENTER
1860 WIEHLE AVENUE
RESTON, VA 22090
ATTN CODE 1035, NICHOLAS A. SICA
ATTN ROBERT ROSTRON
ATTN CODE R103P
ATTN CODE R720, C. STANSBERRY
ATTN CODE R410, JAMES W. MCLEAN
ATTN CODE R400
ATTN CODE R124C, TECH LIB

DIRECTOR
DEFENSE COMMUNICATIONS AGENCY
WASHINGTON, DC 20305
ATTN CODE 430
ATTN CODE 930, FRANKLIN D. MOORE
ATTN CODE 930, MONTE I. BURGETT, FR
ATTN TECHNICAL LIBRARY
ATTN B205, GEORGE B. ADKINS
ATTN NMR
ATTN CODE 800, FRED BOND

COMMANDER
DEFENSE ELECTRONIC SUPPLY CENTER
1507 WILMINGTON PIKE
DAYTON, OH 45401
ATTN TECH LIB

DIRECTOR
DEFENSE INTELLIGENCE AGENCY
WASHINGTON, DC 20301
ATTN DI-7D, MR. EDWARD OFARRELL
ATTN TECHNICAL LIBRARY

DIRECTOR
DEFENSE NUCLEAR AGENCY
WASHINGTON, DC 20305
ATTN RATN
ATTN DDST
ATTN RAEV
ATTN STTL TECH LIBRARY
ATTN STSI ARCHIVES
ATTN STVL

HEADQUARTERS
EUROPEAN COMMAND
J-5
APO NEW YORK 09128
ATTN TECHNICAL LIBRARY

COMMANDER
FIELD COMMAND
DEFENSE NUCLEAR AGENCY
KIRTLAND AFB, NM 87115
ATTN FCPR
ATTN FCSM-F3/CDR SMITH
ATTN FCLMC

DIRECTOR
INTERSERVICE NUCLEAR WEAPONS SCHOOL
KIRTLAND AFB, NM 87115
ATTN TECH LIB
ATTN DOCUMENT CONTROL

DIRECTOR
JOINT STRATEGIC TARGET
PLANNING STAFF, JCS
OFFUTT AFB
OMAHA, NB 68113
ATTN STINFO LIBRARY
ATTN JLTW-2

CHIEF
LIVERMORE DIVISION, FIELD COMMAND DNA
LAWRENCE LIVERMORE LABORATORY
P.O. BOX 808
LIVERMORE, CA 94550
ATTN FCPRL
ATTN DOCUMENT CONTROL FOR L-395

NATIONAL COMMUNICATIONS SYSTEM
OFFICE OF THE MANAGER
WASHINGTON, DC 20305
ATTN NCS-TS, CHARLES D. BODSON

DIRECTOR
NATIONAL SECURITY AGENCY
FT. GEORGE G. MEADE, MD 20755
ATTN O. O. VAN GUNTEN-R-425
ATTN TECHNICAL LIBRARY

OJCS/J-3
THE PENTAGON
WASHINGTON, DC 20301
ATTN J-3, RDTA BT WWMCCS, PLANS DIV

OJCS/J-5
THE PENTAGON
WASHINGTON, DC 20301
ATTN J-5, PALNS & POLICY R&D DIV

OJCS/J-6
THE PENTAGON
WASHINGTON, DC 20301
ATTN J-6, ESD-2

COMMANDER-IN-CHIEF
US EUROPEAN COMMAND, JCS
APO NEW YORK 09128
ATTN TECHNICAL LIBRARY
ATTN ECJ6-P

PROJECT MANAGER
ARMY TACTICAL DATA SYSTEMS
US ARMY ELECTRONICS COMMAND
FORT MONMOUTH, NJ 07703
ATTN DRCPM-TDS/S, PELOSI
ATTN TECH LIBRARY

COMMANDER
BALLISTIC DEFENSE SYSTEM COMMAND
PO BOX 1500
HUNTSVILLE, AL 35807
ATTN BDMSC-TEN, NOAH J. HURST
ATTN TECHNICAL LIBRARY
ATTN SSC-TEN, L. L. DICKERSON

DIRECTOR
BMD ADVANCED TECH CTR
HUNTSVILLE OFFICE
PO BOX 1500
HUNTSVILLE, AL 35807
ATTN TECH LIB
ATTN RDMH-O, F. M. HOKE

CHIEF C-E SERVICES DIVISION
US ARMY COMMUNICATIONS CMD
PENTAGON, RM 1B269
WASHINGTON, DC 20310
ATTN CEEO-7, WESLEY T. HEATH, JR.

CHIEF OF RES, DEV & ACQUISITION
DEPARTMENT OF THE ARMY
WASHINGTON, DC 20310
ATTN DAMA-CSM-N,
LTC E. V. DEBOESER, JR.
ATTN LTC J. OGDEN

COMMANDING OFFICER
NIGHT VISION LABORATORY
US ARMY ELECTRONICS COMMAND
FORT BELVOIR, VA 22060
ATTN TECHNICAL LIBRARY

COMMANDER
PICATINNY ARSENAL
DOVER, NJ 07801
ATTN SARPA-ND-D-C-2
ATTN SARPA-ND-W
ATTN SARPA-TN
ATTN TECHNICAL LIBRARY
ATTN SARPA-TS-I-E, ABRAHAM GRINOCH
ATTN SARPA-FR-E, LOUIS AVRAMI
ATTN SARPA-ND-N-E
ATTN SARPA-ND-N-D

COMMANDER
REDSTONE SCIENTIFIC INFORMATION CTR
US ARMY MISSILE COMMAND
REDSTONE ARSENAL, AL 35809
ATTN CHIEF, DOCUMENTS

PROJECT MANAGER
SAM-D
US ARMY MISSILE COMMAND
REDSTONE ARSENAL, AL 35809
ATTN DRCPM-NEDI,R. HASE

SECRETARY OF THE ARMY
WASHINGTON, DC 20310
ATTN ODUSA OR DANIEL WILLARD

COMMANDER
TRASANA
WHITE SANDS MISSILE RANGE, NM 88002
ATTN ATAA-EAC, FRANCIS N. WINANS

COMMANDER
US ARMY ARMOR CENTER
FORT KNOX, KY 40121
ATTN TECHNICAL LIBRARY
ATTN ATSAR-CD-MS

DIRECTOR
US ARMY BALLISTIC RESEARCH LABORATORIES
ABERDEEN PROVING GROUND, MD 21005
ATTN TECH LIB, EDWARD BAICY
ATTN DRXBR-AM, DONALD ECCLESHALL

COMMANDER
US ARMY COMMUNICATIONS COMMAND
FT. HUACHUCA, AZ 85613
ATTN TECHNICAL LIBRARY

COMMANDER
US ARMY COMMUNICATIONS COMMAND
COMBAT DEVELOPMENT DIVISION
FT. HUACHUCA, AZ 85613
ATTN ACCM-TD-A, LIBRARY

CHIEF
US ARMY COMMUNICATIONS SYSTEMS AGENCY
FORT MONMOUTH, NJ 07703
ATTN SCCM-AD-SV (LIBRARY)

COMMANDER
US ARMY COMPUTER SYSTEMS COMMAND
FORT BELVOIR, VA 22060
ATTN TECHNICAL LIBRARY

COMMANDER
US ARMY ELECTRONICS COMMAND
FORT MONMOUTH, NJ 07703
ATTN DRSEL-NL-0-4
ATTN DRSEL-GG-TD, W. R. WERK
ATTN DRSEL-PL-ENV, HANS A. BOMKE
ATTN DRSEL-TL-ME, M. W. POMERANTZ
ATTN DRSEL-TL-IR, ROBERT A. FREIBERG
ATTN DRSEL-WL-D
ATTN DRSEL-NL-D
ATTN DRSEL-TL-IR, EDWIN T. HUNTER

DIVISION ENGINEER
US ARMY ENGINEER DISTRICT, MISSOURI RIV
P.O. BOX 103 DOWNTOWN STATION
OMAHA, NB 68101
ATTN MRDED-MC, MR. FLOYD L. HAZLETT

COMMANDER-IN-CHIEF
US ARMY EUROPE AND SEVENTH ARMY
APO NEW YORK 09403
ATTN TECHNICAL LIBRARY
ATTN ODCSE-E AEAGE-PI

COMMANDANT
US ARMY FIELD ARTILLERY SCHOOL
FORT SILL, OK 73503
ATTN ATSFA-CTD-ME, HARLEY MOBERG
ATTN TECH LIBRARY

COMMANDER
US ARMY FOREIGN SCIENCE & TECH CTR
220 7TH STREET, NE
CHARLOTTESVILLE, VA 22901
ATTN DRXST-ISI,
DANIEL W. MCCALLUM, JR.

COMMANDER
US ARMY MATERIALS & MECHANICS
RESEARCH CENTER
WATERTOWN, MA 02172
ATTN TECHNICAL LIBRARY
ATTN DRXMR-HH, JOHN F. DIGNAM

DIRECTOR
US ARMY MATERIAL SYS ANALYSIS AGTY
ABERDEEN PROVING GROUND, MD 21005
ATTN TECHNICAL LIBRARY

COMMANDER
US ARMY MISSILE COMMAND
REDSTONE ARSENAL, AL 35809
ATTN DRSMI-RGP, HUGH GREEN
ATTN DRCPM-PE-EA, WALLACE O. WAGNER
ATTN DRSI-RGP, VICTOR W. RUWE
ATTN DRCPM-MDTI, CPT JOE A. SIMS
ATTN DRCPM-PE-EG,
WILLIAM B. JOHNSON

COMMANDER
US ARMY MOBILITY EQUIPMENT R & D CEN
FORT BELVOIR, VA 22060
ATTN TECHNICAL LIBRARY

COMMANDER
US ARMY NUCLEAR AGENCY
FORT BLISS, TX 79916
ATTN ATCN-W, LTC LEONARD A. SLUGA
ATTN TECH LIB
ATTN COL DEVERILL

COMMANDER
US ARMY SAFEGUARD COMMAND
STANLEY R. MICKELSON SAFEGRD COMP
NEKOMA, ND 58355
ATTN CHIEF ACTIVATION DIVISION

COMMANDER
US ARMY SECURITY AGENCY
ARLINGTON HALL STATION
4000 ARLINGTON BLVD
ARLINGTON, VA 22212
ATTN IARD-T, DR. R. H. BURKHARDT
ATTN TECHNICAL LIBRARY

COMMANDANT
US ARMY SIGNAL SCHOOL
FORT GORDON, VA 30905
ATTN ATSO-CTD-CS,
CPT G. M. ALEXANDER
ATTN TECH LIBRARY

COMMANDER
US ARMY TANK AUTOMOTIVE COMMAND
WARREN, MI 48090
ATTN TECH LIBRARY

COMMANDER
US ARMY TEST AND EVALUATION COMMAND
ABERDEEN PROVING GROUND, MD 21005
ATTN DRSTE-EL, R. I. KOLCHIN
ATTN DRSTE-NB, R. R. GALASSO
ATTN TECHNICAL LIBRARY

COMMANDER
US ARMY TRAINING AND DOCTRINE COMMAND
FORT MONROE, VA 23651
ATTN TECH LIBRARY

COMMANDER
WHITE SANDS MISSILE RANGE
WHITE SANDS MISSILE RANGE, NM 88002
ATTN TECHNICAL LIBRARY
ATTN STEWS-TE-NT,
MR. MARVIN P. SQUIRES
ATTN STEWS-TE-AN, A. DE LA PAZ

CHIEF OF NAVAL OPERATIONS
NAVY DEPARTMENT
WASHINGTON, DC 20350
ATTN CODE 604C3, ROBERT PIACESI
ATTN ROBERT A. BLAISE

CHIEF OF NAVAL RESEARCH
DEPARTMENT OF THE NAVY
ARLINGTON, VA 22217
ATTN TECHNICAL LIBRARY
ATTN CODE 427, HENRY MULLANEY
ATTN CODE 464, THOMAS P. QUINN

OFFICER-IN-CHARGE
CIVIL ENGINEERING LABORATORY
NAVAL CONSTRUCTION BATTALION CENTER
FORT HUENEME, CA 93041
ATTN TECHNICAL LIBRARY

COMMANDER
NAVAL AIR SYSTEMS COMMAND
HEADQUARTERS
WASHINGTON, DC 21360
ATTN TECH LIB
ATTN AIR-5202, MURIEL L. SCARBOUGH

COMMANDER
NAVAL ELECTRONIC SYSTEMS COMMAND
HEADQUARTERS
WASHINGTON, DC 20360
ATTN TECH LIB
ATTN PME 117-T
ATTN CODE 5032, CHARLES W. NEILL
ATTN PME 117-215A, GUNTER BRUNHART
ATTN PME 117-21

COMMANDER
NAVAL ELECTRONICS LABORATORY CENTER
SAN DIEGO, CA 92152
ATTN CODE 2400, S. W. LICHTMAN
ATTN CODE 2200 1, VERNE E. HILDEBRAND
ATTN CODE 3100, E. E. MCCOWN
ATTN TECHNICAL LIBRARY

COMMANDER
NAVAL INTELLIGENCE SUPPORT CENTER
4301 SUITLAND ROAD, BLDG 5
WASHINGTON, DC 20390
ATTN TECHNICAL LIBRARY
ATTN NISC-611

SUPERINTENDENT
NAVAL POSTGRADUATE SCHOOL
MONTEREY, CA 93940
ATTN CODE 2124, TECH RPTS LIBRARIAN

DISTRIBUTION (Cont'd)

DIRECTOR
NAVAL RESEARCH LABORATORY
WASHINGTON, DC 20375
ATTN CODE 6601, E. WOLICKI
ATTN CODE 5216, HAROLD L. HUGHES
ATTN CODE 7706, JAY P. BORIS
ATTN GERALD COOPERSTEIN, CODE 7770
ATTN CODE 6631, JAMES C. RITTER
ATTN CODE 4004, EMANUAL L. BRANCATO
ATTN CODE 2027, TECH LIB
ATTN CODE 2627, DORIS R. FOLEN
ATTN CODE 7701, JACK D. BROWN

COMMANDER
NAVAL SEA SYSTEMS COMMAND
NAVY DEPARTMENT
WASHINGTON, DC 20362
ATTN SEA-9931, RILEY B. LANE
ATTN SEA-9931, SAMUEL A. BARHAM

COMMANDER
NAVAL SHIP ENGINEERING CENTER
CENTER BUILDING
HYATTSVILLE, MD 20782
ATTN TECHNICAL LIBRARY
ATTN CODE 6174D2, EDWARD F. DUFFY

COMMANDER
NAVAL SURFACE WEAPONS CENTER
WHITE OAK, SILVER SPRING, MD 20910
ATTN CODE WX21, TECH LIB
ATTN CODE 431, EDWIN B. DEAN
ATTN CODE WA501, NAVY NUC PRGMS OFF
ATTN CODE 431, EDWIN R. RATHBURN
ATTN CODE WA50, JOHN H. MALLOY
ATTN CODE 223, L. LIBELLO
ATTN CODE WR43

COMMANDER
NAVAL SURFACE WEAPONS CENTER
DAHLGREN LABORATORY
DAHLGREN, VA 22448
ATTN TECHNICAL LIBRARY

COMMANDER
NAVAL TELECOMMUNICATIONS COMMAND
NAV TEL COM HEADQUARTERS
4401 MASSACHUSETTS AVE, NW
WASHINGTON, DC 20390
ATTN TECH LIB
ATTN N-7, LCDR HALL

COMMANDER
NAVAL WEAPONS CENTER
CHINA LAKE, CA 93555
ATTN CODE 533, TECHNICAL LIBRARY

COMMANDING OFFICER
NAVAL WEAPONS EVALUATION FACILITY
KIRTLAND AIR FORCE BASE
ALBUQUERQUE, NM 87117
ATTN LAWRENCE R. OLIVER
ATTN CODE ATG, MR. STANLEY

COMMANDING OFFICER
NAVAL WEAPONS SUPPORT CENTER
CRANE, IN 47522
ATTN TECHNICAL LIBRARY
ATTN CODE 70242, JOSEPH A. MUNARIN
ATTN CODE 7024, JAMES RAMSEY

COMMANDING OFFICER
NAVY ASTRONAUTICS GROUP
POINT MUGU, CA 93042
ATTN TECH LIB

DIRECTOR
STRATEGIC SYSTEMS PROJECT OFFICE
NAVY DEPARTMENT
WASHINGTON, DC 20376
ATTN NSP-2431, GERALD W. HOSKINS
ATTN SP2701, JOHN W. PITSENBERGER
ATTN NSP-2342, RICHARD L. COLEMAN
ATTN NSP-43, TECH LIB
ATTN NSP-230, DAVID GOLD

COMMANDER
US NAVAL COASTAL SYSTEMS LABORATORY
PANAMA CITY, FL 32401
ATTN TECH LIB

COMMANDER-IN-CHIEF
US PACIFIC FLEET
FPO SAN FRANCISCO 96610
ATTN DOCUMENT CONTROL

COMMANDER
ADC/DE
ENT AFB, CO 80912
ATTN DEEDS, JOSEPH C. BRANNAN
ATTN DDEEN

COMMANDER
ADC/XP
ENT AFB, CO 80912
ATTN XPQDQ, MAJ G. KUCH
ATTN XPDQ

AF GEOPHYSICS LABORATORY, AFSC
HANSCOM AFB, MA 01731
ATTN CHARLES PIKE
ATTN LQR EDWARD A. BURKE

AF INSTITUTE OF TECHNOLOGY, AU
WRIGHT-PATTERSON AFB, OH 45433
ATTN LIBRARY AFIT, BLDG 640, AREA B
ATTN ENP, CHARLES J. BRIDGMAN

AF MATERIALS LABORATORY, AFSC
WRIGHT-PATTERSON AFB, OH 45433
ATTN LIBRARY

AF WEAPONS LABORATORY, AFSC
KIRTLAND AFB, NM 87117
ATTN EL, MR. JOHN DARRAH
ATTN DYX, DONALD C. WUNSCH
ATTN SAT
ATTN ELA
ATTN ELC
ATTN ELP, CARL E. BAUM
ATTN EL
ATTN SAS
ATTN SAB
ATTN SUL
ATTN ELA, J. P. CASTILLO
ATTN EL (LIBRARY)

AFTAC
PATRICK AFB, FL 32925
ATTN TECH LIB

HEADQUARTERS
AIR FORCE SYSTEMS COMMAND
ANDREWS AFB
WASHINGTON, DC 20331
ATTN TECHNICAL LIBRARY

COMMANDER
AIR UNIVERSITY
MAXWELL AFB, AL 36112
ATTN AUL/LSE-70-250

COMMANDER
ASD
WRIGHT-PATTERSON AFB, OH 45433
ATTN ENFTV
ATTN ASD-YH-EX, LTC ROBERT LEVERETTE
ATTN 4950, TEST W/TZMH, PETER T. MARTH

HEADQUARTERS
ELECTRONIC SYSTEMS DIVISION, (AFSC)
L. G. HANSCOM FIELD
BEDFORD, MA 01730
ATTN YSEV, LTC DAVID C. SPARKS
ATTN TECHNICAL LIBRARY
ATTN XRRT
ATTN DCD/SATIN IV

COMMANDER
FOREIGN TECHNOLOGY DIVISION, AFSC
WRIGHT-PATTERSON AFB, OH 45433
ATTN TD-BTA, LIBRARY
ATTN ETET, CAPT RICHARD C. HUSEMANN

HQ USAF/RD
WASHINGTON, DC 20330
ATTN RDQPN

COMMANDER
OGDEN AIR LOGISTICS CENTER
HILL AFB, UT 84401
ATTN TECH LIB

COMMANDER
ROME AIR DEVELOPMENT CENTER, AFSC
GRIFFISS AFB, NY 13440
ATTN EMTLD, DOC LIBRARY
ATTN P. GIANINO

COMMANDER
SACRAMENTO AIR LOGISTICS CENTER
MCCLELLAN AFB, CA 95652
ATTN TECHNICAL LIBRARY

SAMSO/DY
POST OFFICE BOX 92960
WORLDWAY POSTAL CENTER
LOS ANGELES, CA 90009
ATTN DYS, MAJ LARRY A. DARDA
ATTN DYS, CAPT WAYNE SCHOBER

SAMSO/IN
POST OFFICE BOX 92960
WORLDWAY POSTAL CENTER
LOS ANGELES, CA 90009
ATTN IND, I. J. JUDY
ATTN IND, MAJ DARRYL S. MUSKIN

SAMSO/MN
NORTON AFB, CA 92409
ATTN MNNG, CAPT DAVID J. STROBEL
ATTN MNNH, CAPT WILLIAM M. CARRA
ATTN MNNH, CAPT B. STEWART
ATTN MNNG
ATTN MNNH, CAPT MICHAEL V. BELL

SAMSO/RS
POST OFFICE BOX 92960
WORLDWAY POSTAL CENTER
LOS ANGELES, CA 90009
ATTN RSSE, LTC KENNETH L. GILBERT
ATTN RSE

SAMSO/SK
POST OFFICE BOX 92960
WORLDWAY POSTAL CENTER
LOS ANGELES, CA 90009
ATTN SKF, PETER H. STADLER

SAMSO/XR
POST OFFICE BOX 92960
WORLDWAY POSTAL CENTER
LOS ANGELES, CA 90009
ATTN XRS

SAMSO/YD
POST OFFICE BOX 92960
WORLDWAY POSTAL CENTER
LOS ANGELES, CA 90009
ATTN YDD, MAJ M. F. SCHNEIDER

COMMANDER IN CHIEF
STRATEGIC AIR COMMAND
OFFUTT AFB, NB 68113
ATTN NRI-STINFO LIBRARY
ATTN DEF, FRANK N. BOUSHA
ATTN XPFS, CAPT DERAAD

DIVISION OF MILITARY APPLICATION
US ENERGY RSCH & DEV ADMIN
WASHINGTON, DC 20545
ATTN TECHNICAL LIBRARY

LOS ALAMOS SCIENTIFIC LABORATORY
P.O. BOX 1663
LOS ALAMOS, NM 87544
ATTN ARTHUR FREED
ATTN RICHARD L. WAKEFIELD
ATTN DONALD R. WESTERVELT
ATTN BRUCE W. NOEL
ATTN MARVIN M. HOFFMAN
ATTN P. W. KEATON
ATTN REPORTS LIBRARY
ATTN JOHN S. MALIK

SANDIA LABORATORIES
LIVERMORE LABORATORY
PO BOX 969
LIVERMORE, CA 94550
ATTN TECHNICAL LIBRARY
ATTN THEODORE A. DELLIN

SANDIA LABORATORIES
PO BOX 5800
ALBUQUERQUE, NM 87115
ATTN ORD 9353, R. L. PARKER
ATTN ORG 2315, JAMES E. GOVER
ATTN DIV 5231, JAMES H. RENKEN
ATTN ORG 2110, J. A. HOOD
ATTN GERALD W. BARR, 1114
ATTN 3141 SANDIA RPT COLL
ATTN ELMER F. HARTMAN
ATTN 5240, GERALD YONAS

US ENERGY RSCH & DEV ADMIN
ALBUQUERQUE OPERATIONS OFFICE
PO BOX 5400
ALBUQUERQUE, NM 87115
ATTN TECH LIBRARY

UNION CARBIDE CORPORATION
HOLIFIELD NATIONAL LABORATORY
P.O. BOX X
OAK RIDGE, TN 37830
ATTN TECH LIBRARY

UNIVERSITY OF CALIFORNIA
LAWRENCE LIVERMORE LABORATORY
PO BOX 808
LIVERMORE, CA 94550
ATTN HANS KRUGER, L-96
ATTN WILLIAM J. HOGAN, L-531
ATTN DONALD J. MEEKER, L-545
ATTN L-153, ROBERT A. ANDERSON
ATTN TECH INFO DEPT, L-3
ATTN LOUIS F. WOUTERS, L-48
ATTN FREDERICK R. KOVAR, L-31
ATTN DONALD W. VOLLMER, L-154
ATTN WALTER W. HOFER, L-24
ATTN JOSEPH E. KELLER, JR., L-125

CENTRAL INTELLIGENCE AGENCY
ATTN: RD/SI RM 5G48, HQ BLDG
WASHINGTON, DC 20505
ATTN WILLIAM A. DECKER
ATTN TECHNICAL LIBRARY

ADMINISTRATOR
DEFENSE ELECTRIC POWER ADMIN
DEPARTMENT OF THE INTERIOR
INTERIOR SOUTH BLDG, 312
WASHINGTON, DC 20240
ATTN DOCUMENT CONTROL

DEPARTMENT OF COMMERCE
NATIONAL BUREAU OF STANDARDS
WASHINGTON, DC 20234
ATTN JUDSON C. FRENCH

DEPARTMENT OF COMMERCE
NATIONAL OCEANIC AND ATMOSPHERIC
ADMINISTRATION
ENVIRONMENTAL RESEARCH LABORATORIES
BOULDER, CO 80302
ATTN DOCUMENT LIBRARY

DEPARTMENT OF TRANSPORTATION
FEDERAL AVIATION ADMINISTRATION
ASE-300, HEADQUARTERS SEC
800 INDEPENDENCE AVENUE, S.W.
WASHINGTON, DC 20591
ATTN FREDRICK S. SAKATE, ARD-350
ATTN ARD-350

NASA
600 INDEPENDENCE AVENUE, SW
WASHINGTON, DC 20546
ATTN TECHNICAL LIBRARY
ATTN CODE RFS GUID CON & INFO SYS

NASA
LEWIS RESEARCH CENTER
21000 BROOKPARK ROAD
CLEVELAND, OH 44135
ATTN LIBRARY
ATTN ROBERT R. LOVELL, MS 54-3

AEROJET ELECTRO-SYSTEMS CO. DIV.
AEROJET-GENERAL CORPORATION
P.O. BOX 296
AZUSA, CA 91702
ATTN TECH LIBRARY
ATTN THOMAS D. HANSCOME, B170/D6711

AERONUTRONIC FORD CORPORATION
AEROSPACE & COMMUNICATIONS OPS
AERONUTRONIC DIVISION
FORD & JAMBOREE ROADS
NEWPORT BEACH, CA 92663
ATTN E. R. PONCELET, JR.
ATTN KEN C. ATTINGER
ATTN TECH INFO SECTION

AERONUTRONIC FORD CORPORATION
WESTERN DEVELOPMENT LABORATORIES DIV
3939 FABIAN WAY
PALO ALTO, CA 94303
ATTN J. T. MATTINGLEY, MS X22
ATTN SAMUEL R. CRAWFORD, MS 531
ATTN DONALD R. MCMORROW, MS G30
ATTN LIBRARY

AEROSPACE CORPORATION
PO BOX 92957
LOS ANGELES, CA 90009
ATTN IRVING M. GARFUNKEL
ATTN JULIAN REINHEIMER
ATTN LIBRARY
ATTN NORMAN D. STOCKWELL
ATTN BAL KRISHAN
ATTN FRANK HAI
ATTN WILLIAM W. WILLIS
ATTN V. JOSEPHSON
ATTN C. B. PEARLSTON
ATTN J. BENVENISTE

AVCO RESEARCH & SYSTEMS GROUP
201 LOWELL STREET
WILMINGTON, MA 01887
ATTN RESEARCH LIBRARY, A830, RM 7201

BATTELLE MEMORIAL INSTITUTE
505 KING AVENUE
COLUMBUS, OH 43201
ATTN TECHNICAL LIBRARY
ATTN ROBERT H. BLAZEK

BDM CORPORATION, THE
1920 ALINE AVE
VIENNA, VA 22180
ATTN TECHNICAL LIBRARY

BDM CORPORATION, THE
PO BOX 9274
ALBUQUERQUE INTERNATIONAL
ALBUQUERQUE, NM 87119
ATTN B. GAGE
ATTN T. H. NEIGHBORS
ATTN TECH LIB

BENDIX CORPORATION, THE
COMMUNICATION DIVISION
EAST JOPPA ROAD - TOWSON
BALTIMORE, MD 21204
ATTN DOCUMENT CONTROL

BENDIX CORPORATION, THE
RESEARCH LABORATORIES DIV
BENDIX CENTER
SOUTHFIELD, MI 48075
ATTN TECH LIB
ATTN MGR PROGM DEV,
DONALD J. NIEHAUS

BENDIX CORPORATION, THE
NAVIGATION AND CONTROL DIVISION
TETERBORO, NJ 07608
ATTN TECH LIB
ATTN GEORGE GARTNER

BOEING COMPANY, THE
PO BOX 3707
SEATTLE, WA 98124
ATTN HOWARD W. WICKLEIN, MS 17-11
ATTN KENNETH D. FRIDDELL, MS 2R-00
ATTN D. E. ISBELL
ATTN ROBERT S. CALDWELL, 2R-00
ATTN DAVID DYE, MS 87-75
ATTN DONALD W. EGELKROUT, MS 2R-00
ATTN DAVID KEMLE
ATTN AEROSPACE LIBRARY

BOOZ-ALLEN AND HAMILTON, INC.
106 APPLE STREET
NEW SHREWSBURY, NJ 07724
ATTN TECH LIB
ATTN R. J. CHRISNER

BROWN ENGINEERING COMPANY, INC.
CUMMINGS RESEARCH PARK
HUNTSVILLE, AL 35807
ATTN JOHN M, MCSWAIN, MS 18
ATTN TECH LIB, MS12, P. SHELTON

BURROUGHS CORPORATION
FEDERAL AND SPECIAL SYSTEMS GROUP
CENTRAL AVE AND ROUTE 252
PO BOX 517
PAOLI, PA 29301
ATTN ANGELO J. MAURIELLO
ATTN TECH LIB

CALIFORNIA AT SAN DIEGO, UNIVERSITY OF
IPAPS, B-019
LA JOLLA, CA 92093
ATTN SHERMAN DE FOREST

CALIFORNIA INSTITUTE OF TECHNOLOGY
JET PROPULSION LABORATORY
4800 OAK PARK GROVE
PASADENA, CA 91103
ATTN A. G. STANLEY
ATTN J. BRYDEN

CALSPAN CORPORATION
PO BOX 235
BUFFALO, NY 14221
ATTN TECH LIBRARY

CHARLES STARK DRAPER LABORATORY INC.
68 ALBANY STREET
CAMBRIDGE, MA 02139
ATTN TECH LIB
ATTN RICHARD G. HALTMAIER
ATTN KENNETH FERTIG
ATTN PAUL R. KELLY

CINCINNATI ELECTRONICS CORPORATION
2630 GLENDALE - MILFORD ROAD
CINCINNATI, OH 45241
ATTN TECH LIB

COMPUTER SCIENCES CORPORATION
P.O. BOX 530
6565 ARLINGTON BLVD
FALLS CHURCH, VA 22046
ATTN TECH LIB
ATTN BARBARA F. ADAMS

COMPUTER SCIENCES CORPORATION
201 LA VETA DRIVE, NE
ALBUQUERQUE, NM 87108
ATTN RICHARD H. DICKHAUT
ATTN ALVIN SCHIFF

CUTLER-HAMMER, INC.
AIL DIVISION
COMAC ROAD
DEER PARK, NY 11729
ATTN CENTRAL TECH FILES,
ANN ANTHONY

DENVER, UNIVERSITY OF
COLORADO SEMINARY
DENVER RESEARCH INSTITUTE
PO BOX 10127
DENVER, CO 80210
ATTN TECH LIB

DEPLOMB, DR. EUGENE P.
2422 DEER PARK DRIVE
SAN DIEGO, CA 92110
ATTN EUGENE P. DEPLOMB

DIKEWOOD CORPORATION, THE
1009 BRADBURY DRIVE, SE
UNIVERSITY RESEARCH PARK
ALBUQUERQUE, NM 87106
ATTN TECH LIB
ATTN K. LEE
ATTN L. WAYNE DAVIS

E-SYSTEMS, INC.
GREENVILLE DIVISION
PO BOX 1056
GREENVILLE, TX 75401
ATTN LIBRARY 8-50100

EFFECTS TECHNOLOGY, INC.
5383 HOLLISTER AVENUE
SANTA BARBARA, CA 93105
ATTN EDWARD JOHN STEELE
ATTN TECH LIB

EG&G, INC.
ALBUQUERQUE DIVISION
PO BOX 10218
ALBUQUERQUE, NM 87114
ATTN TECHNICAL LIBRARY
ATTN HILDA H. HOFFMAN

ESL, INC.
495 JAVA DRIVE
SUNNYVALE, CA 94086
ATTN TECHNICAL LIBRARY

EXP AND MATH PHYSICS CONSULTANTS
P. O. BOX 66331
LOS ANGELES, CA 90066
ATTN THOMAS M. JORDAN

FAIRCHILD CAMERA AND INSTRUMENT
CORPORATION
464 ELLIS STREET
MOUNTAIN VIEW, CA 94040
ATTN 2-233, MR. DAVID K. MYERS
ATTN TECH LIB

FAIRCHILD INDUSTRIES, INC.
SHERMAN FAIRCHILD TECHNOLOGY CENTER
20301 CENTURY BOULEVARD
GERMANTOWN, MD 20767
ATTN LEONARD J. SCHREIBER
ATTN MGR CONFIG DATA & STANDARDS
ATTN TECH LIB

FRANKLIN INSTITUTE, THE
20TH STREET AND PARKWAY
PHILADELPHIA, PA 19103
ATTN RAMIE H. THOMPSON
ATTN TECH LIB

GARRETT CORPORATION
PO BOX 92248
LOS ANGELES, CA 90009
ATTN TECH LIB

GENERAL DYNAMICS CORP.
POMONA OPERATION
ELECTRO-DYNAMIC DIVISION
PO BOX 2507
POMONA, CA 91766
ATTN TECH LIB

GENERAL DYNAMICS CORP.
ELECTRONICS DIVISION
P.O. BOX 81127
SAN DIEGO, CA 92138
ATTN TECH LIB

GENERAL DYNAMICS CORP
ELECTRONICS DIV ORLANDO OPERATIONS
PO BOX 2566
ORLANDO, FL 32802
ATTN D. W. COLEMAN

GENERAL ELECTRIC COMPANY
SPACE DIVISION
VALLEY FORGE SPACE CENTER
P.O. BOX 8555
PHILADELPHIA, PA 19101
ATTN JAMES P. SPRATT
ATTN JOHN L. ANDREWS
ATTN DANIEL EDELMAN
ATTN DANTE M. TASCA
ATTN LARRY I. CHASEN
ATTN JOSEPH C. PEDEN, CCF 8301
ATTN TECH INFO CENTER

GENERAL ELECTRIC COMPANY
RE-ENTRY & ENVIRONMENTAL SYSTEMS DIV
PO BOX 7722
3198 CHESTNUT STREET
PHILADELPHIA, PA 19101
ATTN TECH LIB
ATTN ROBERT V. BENEDICT
ATTN JOHN W. PALCHEFSKY, JR.

GENERAL ELECTRIC COMPANY
ORDNANCE SYSTEMS
100 PLASTICS AVENUE
PITTSFIELD, MA 01201
ATTN JOSEPH J. REIDL

GENERAL ELECTRIC COMPANY
TEMPO-CENTER FOR ADVANCED STUDIES
816 STATE STREET (PO DRAWER QQ)
SANTA BARBARA, CA 93102
ATTN DASIAC
ATTN ROYDEN R. RUTHERFORD
ATTN JOHN D. ILLGEN
ATTN WILLIAM MCNAMARA

GENERAL ELECTRIC COMPANY
PO BOX 1122
SYRACUSE, NY 13201
ATTN TECH LIB

GENERAL ELECTRIC COMPANY
AIRCRAFT ENGINE GROUP
EVENDALE PLANT
CINCINNATI, OH 45215
ATTN TECH LIB
ATTN JOHN A. ELLERHORST, E2

GENERAL ELECTRIC COMPANY
AEROSPACE ELECTRONICS SYSTEMS
FRENCH ROAD
UTICA, NY 13503
ATTN TECH LIB
ATTN CHARLES M. HEWISON, DROP 624
ATTN W. J. PATTERSON, DROP 233

GENERAL ELECTRIC COMPANY
PO BOX 5000
BINGHAMTON, NY 13902
ATTN TECH LIB

GENERAL ELECTRIC COMPANY
HMES
COURT STREET PLANT NO. 5
SYRACUSE, NY 13201
ATTN U. COCCA

GENERAL ELECTRIC COMPANY-TEMPO
ATTN: DASIAC
C/O DEFENSE NUCLEAR AGENCY
WASHINGTON, DC 20305
ATTN WILLIAM ALFONTE

GENERAL RESEARCH CORPORATION
P.O. BOX 3587
SANTA BARBARA, CA 93105
ATTN TECH INFO OFFICE
ATTN JOHN ISE, JR.

GENERAL RESEARCH CORPORATION
WASHINGTON OPERATIONS
WESTGATE RESEARCH PARK
7655 OLD SPRINGHOUSE ROAD, SUITE 700
MCLEAN, VA 22101
ATTN DAVID K. OSIAS

GEORGIA INSTITUTE OF TECHNOLOGY
GEORGIA TECH RESEARCH INSTITUTE
ATLANTA, GA 30332
ATTN R. CURRY

GOODYEAR AEROSPACE CORPORATION
ARIZONA DIVISION
LITCHFIELD PARK, AZ 85340
ATTN B. MANNING

GRUMMAN AEROSPACE CORPORATION
SOUTH OYSTER BAY ROAD
BETHPAGE, NY 11714
ATTN JERRY ROGERS, DEPT 533
ATTN TECHNICAL LIBRARY

GTE SYLVANIA, INC.
ELECTRONICS SYSTEMS GRP-EASTERN DIV
77 A STREET
NEEDHAM, MA 02194
ATTN CHARLES A. THORNHILL, LIBRARIAN
ATTN LEONARD L. BLAISDELL
ATTN JAMES A. WALDON

GTE SYLVANIA, INC.
189 B STREET
NEEDHAM HEIGHTS, MA 02194
ATTN A S M DEPT, S. E. PERLMAN
ATTN DAVID P. FLOOD
ATTN COMM SYST DIV, EMIL P. MOTCHOK
ATTN HERBERT A. ULLMAN
ATTN H & V GROUP, MARIO A. NUREFORA

HARRIS CORPORATION
HARRIS SEMICONDUCTOR DIVISION
P.O. BOX 883
MELBOURNE, FL 32901
ATTN C. F. DAVIS, MS 17-220
ATTN WAYNE E. ABARE, MS 16-111
ATTN T. CLARK, MS 4040
ATTN TECH LIB

HAZELTINE CORPORATION
PULASKI ROAD
GREEN LAWN, NY 11740
ATTN TECH INFO CTR, M. WAITE

HERCULES, INC.
BACCHUS PLANT
P.O. BOX 98
MAGNA, UT 84044
ATTN 100K-26, W. R. WOODRUFF
ATTN TECH LIB

HONEYWELL INCORPORATED
GOVERNMENT AND AERONAUTICAL
PRODUCTS DIVISION
2600 RIDGEWAY PARKWAY
MINNEAPOLIS, MN 55413
ATTN TECH LIB
ATTN RONALD R. JOHNSON, A1622

HONEYWELL INCORPORATED
AEROSPACE DIVISION
13350 US HIGHWAY 19
ST. PETERSBURG, FL 33733
ATTN TECHNICAL LIBRARY
ATTN HARRISON H. NOBLE, MS 725-5A
ATTN RICHARD B. REINECKE, MS 725-5

HONEYWELL INCORPORATED
RADIATION CENTER
2 FORBES ROAD
LEXINGTON, MA 02173
ATTN TECHNICAL LIBRARY

HUGHES AIRCRAFT COMPANY
CENTINELLA & TEALE
CULVER CITY, CA 90230
ATTN M.S. D157, KEN WALKER
ATTN TECHNICAL LIB
ATTN B. W. CAMPBELL, M.S. 6-E110
ATTN JOHN B. SINGLETARY, MS 6-D133

HUGHES AIRCRAFT COMPANY
SPACE SYSTEMS DIVISION
P.O. BOX 92919
LOS ANGELES, CA 90009
ATTN TECHNICAL LIB
ATTN WILLIAM W. SCOTT, MS A1080
ATTN EDWARD C. SMITH, MS A620

IBM CORPORATION
ROUTE 17C
OWEGO, NY 13827
ATTN TECHNICAL LIBRARY
ATTN FRANK FRANKOVSKY

IIT RESEARCH INSTITUTE
ELECTROMAGNETIC COMPATABILITY ANAL CTR
NORTH SEVERN
ANNAPOLIS, MD 21402
ATTN TECH LIB

IIT RESEARCH INSTITUTE
10 WEST 35TH STREET
CHICAGO, IL 60616
ATTN TECHNICAL LIBRARY
ATTN JACK E. BRIDGES
ATTN IRVING N. MINDEL

INSTITUTE FOR DEFENSE ANALYSES
400 ARMY-NAVY DRIVE
ARLINGTON, VA 22202
ATTN IDA LIBRARIAN, RUTH S. SMITH

INTERNATIONAL TELEPHONE AND
TELEGRAPH CORPORATION
500 WASHINGTON AVENUE
NUTLEY, NJ 07110
ATTN TECHNICAL LIBRARY
ATTN DEF SP GROUP, J. GULACK
ATTN ALEXANDER I. RICHARDSON

ION PHYSICS CORPORATION
SOUTH BEDFORD STREET
BURLINGTON, MA 01803
ATTN TECH LIB
ATTN ROBERT D. EVANS

IRT CORPORATION
PO BOX 81087
SAN DIEGO, CA 92138
ATTN TERRY FLANAGAN
ATTN JAMES A. NABER
ATTN TECHNICAL LIBRARY
ATTN DENNIS SWIFT
ATTN RALPH H. STAHL
ATTN MDC
ATTN R. L. MERTZ

JAYCOR, INCORPORATED
1401 CAMINO DEL MAR
DEL MAR, CA 92014
ATTN ERIC P. WENAAS
ATTN ANDREW WOODS

JOHNS HOPKINS UNIVERSITY
APPLIED PHYSICS LABORATORY
JOHNS HOPKINS ROAD
LAUREL, MD 20810
ATTN PETER E. PARTRIDGE
ATTN TECH LIB

KAMAN SCIENCES CORPORATION
P.O. BOX 7463
COLORADO SPRINGS, CO 80933
ATTN LIBRARY
ATTN J. R. CURRY
ATTN DONALD H. BRYCE
ATTN JOHN R. HOFFMAN
ATTN ALBERT P. BRIDGES
ATTN W. FOSTER RICH
ATTN WALTER E. WARE

LITTON SYSTEMS, INC.
DATA SYSTEMS DIVISION
8000 WOODLEY AVENUE
VAN NUYS, CA 91406
ATTN TECH LIB

LITTON SYSTEMS, INC.
GUIDANCE & CONTROL SYSTEMS DIVISION
5500 CANOGA AVENUE
WOODLAND HILLS, CA 91364
ATTN R. W. MAUGHMER
ATTN VAL J. ASHBY, MS 67
ATTN TECHNICAL LIBRARY
ATTN JOHN P. RETZLER

LITTON SYSTEMS, INC.
AMECOM DIVISION
5115 CALVERT ROAD
COLLEGE PARK, MD 20740
ATTN TECH LIB

LOCKHEED MISSILES AND SPACE COMPANY
3251 HANOVER STREET
PALO ALTO, CA 94304
ATTN TECH INFO CTR D/COLL
ATTN CLARENCE F. KOOI, DEPT 52-11

LOCKHEED MISSILES AND SPACE
COMPANY, INC.
P.O. BOX 504
SUNNYVALE, CA 94088
ATTN DEPT 85-85, SAMUEL I. TAIMUTY
ATTN G. F. HEATH, D/81-14
ATTN BENJAMIN T. KIMURA,
DEPT 81-14, BLDG 154
ATTN EDWIN A. SMITH, DEPT 85-85
ATTN TECHNICAL LIBRARY
ATTN L-365 DEPT 81-20
ATTN PHILIP J. HART, DEPT 81-14
ATTN DEPT 81-01, G. H. MORRIS
ATTN L. ROSSI, DEPT 81-64

LTV AEROSPACE CORPORATION
VOUGHT SYSTEMS DIVISION
P.O. BOX 6267
DALLAS, TX 75222
ATTN TECHNICAL DATA CENTER
ATTN CHARLES H. COLEMAN

LTV AEROSPACE CORPORATION
MICHIGAN DIVISION
P.O. BOX 909
WARREN, MI 48090
ATTN JAMES F. SANSON, B-2
ATTN TECH LIB

M.I.T. LINCOLN LABORATORY
P.O. BOX 73
LEXINGTON, MA 02173
ATTN LEONA LOUGHLIN, LIBRARIAN
ATTN JEAN L. RYAN

MARTIN MARIETTA AEROSPACE
ORLANDO DIVISION
P.O. BOX 5837
ORLANDO, FL 32805
ATTN MONA C. GRIFFITH, LIB MP-30
ATTN WILLIAM W. MRAS, MP-413
ATTN JACK M. ASHFORD, MP-537

MARTIN MARIETTA CORPORATION
DENVER DIVISION
PO BOX 179
DENVER, CO 80201
ATTN RESEARCH LIB, 6617, J. R. MCKEE
ATTN PAUL G. KASE, MAIL 8203
ATTN BEN T. GRAHAM, MS PO-454
ATTN J. E. GOODWIN, MAIL 0452

MAXWELL LABORATORIES, INC.
9244 BALBOA AVENUE
SAN DIEGO, CA 92123
ATTN TECH LIB
ATTN VICTOR FARGO

MCDONNELL DOUGLAS CORPORATION
POST OFFICE BOX 516
ST. LOUIS, MO 63166
ATTN TECHNICAL LIBRARY

MCDONNELL DOUGLAS CORPORATION
5301 BOLSA AVENUE
HUNTINGTON BEACH, CA 92647
ATTN W. R. SPARK, MS 13-3
ATTN PAUL H. DUNCAN, JR.
ATTN STANLEY SCHNEIDER
ATTN A. P. VENDITT, MS 11-1
ATTN TECH LIBRARY SERVICES

MCDONNELL DOUGLAS CORPORATION
3855 LAKEWOOD BOULEVARD
LONG BEACH, CA 90846
ATTN TECHNICAL LIBRARY, C1-290/36-84

MISSION RESEARCH CORPORATION
735 STATE STREET
SANTA BARBARA, CA 93101
ATTN TECH LIB
ATTN CONRAD L. LONGMIRE
ATTN ROGER STETTNER
ATTN WILLIAM C. HART
ATTN DANIEL F. HIGGINS

MISSION RESEARCH CORPORATION
P.O. BOX 8693, STATION C
ALBUQUERQUE, NM 87108
ATTN LARRY D. SCOTT
ATTN TECH LIB
ATTN DAVID E. MEREWETHER

MISSION RESEARCH CORPORATION-SAN DIEGO
7650 CONVOY COURT
SAN DIEGO, CA 92111
ATTN V. A. J. VAN LINT

MITRE CORPORATION, THE
P.O. BOX 208
BEDFORD, MA 01730
ATTN LIBRARY
ATTN THEODORE JARVIS
ATTN M. F. FITZGERALD

MOTOROLA, INC
GOVERNMENT ELECTRONICS DIVISION
PO BOX 1417
SCOTTSDALE, AZ 85255
ATTN TECH INFO CTR,
A. J. KORDALEWSKI
ATTN JAMES R. BLACK, MS A112

NATIONAL ACADEMY OF SCIENCES
ATTN: NATIONAL MATERIALS ADVISORY BOARD
2101 CONSTITUTION AVE, NW
WASHINGTON,DC 20418
ATTN DR. R. S. SHANE,
NAT MATERIALS ADVSY

NORTHROP CORPORATION
ELECTRONIC DIVISION
1 RESEARCH PARK
PALOS VERDES PENINSULA, CA 90274
ATTN BOYCE T. AHLPORT
ATTN TECH LIB
ATTN JOHN M. REYNOLDS
ATTN VINCENT R. DEMARTINO

NORTHROP CORPORATION
NORTHROP RESEARCH AND TECHNOLOGY CENTER
3401 WEST BROADWAY
HAWTHORNE, CA 90250
ATTN ORLIE L. CURTIS, JR.
ATTN LIBRARY
ATTN DAVID N. POCOCK

NORTHROP CORPORATION
ELECTRONIC DIVISION
2301 WEST 120TH STREET
HAWTHORNE, CA 90250
ATTN TECH LIB
ATTN JOSEPH D. RUSSO

PALISADES INST FOR RSCH SERVICES INC.
201 VARICK STREET
NEW YORK, NY 10014
ATTN RECORDS SUPERVISOR

PHYSICS INTERNATIONAL COMPANY
2700 MERCED STREET
SAN LEANDRO, CA 94577
ATTN TECH LIB
ATTN JOHN H. HUNTINGTON
ATTN IAN D. SMITH
ATTN PHILIP W. SPENCE
ATTN CHARLES H. STALLINGS

PROCEDYNE CORPORATION
221 SOMERSET STREET
NEW BRUNSWICK, NJ 08903
ATTN TECH LIB

PULSAR ASSOCIATES, INC.
7911 HERSCHEL AVENUE
LA JOLLA, CA 92037
ATTN CARLETON H. JONES

R & D ASSOCIATES
PO BOX 9695
MARINA DEL REY, CA 90291
ATTN TECHNICAL LIBRARY
ATTN LEONARD SCHLESSINGER
ATTN RICHARD R. SCHAEFER
ATTN S. CLAY ROGERS
ATTN WILLIAM R. GRAHAM, JR.
ATTN CHARLES MO
ATTN WILLIAM J. KARZAS
ATTN GERARD K. SCHLEGEL

RAND CORPORATION, THE
1700 MAIN STREET
SANTA MONICA, CA 90406
ATTN TECHNICAL LIBRARY
ATTN DR. CULLEN CRAIN

RAYTHEON COMPANY
HARTWELL ROAD
BEDFORD, MA 01730
ATTN LIBRARY
ATTN GAJANAN H. JOSHI, RADAR SYS LAB

RAYTHEON COMPANY
528 BOSTON POST ROAD
SUDBURY, MA 01776
ATTN HAROLD L. FLESCHER

RCA CORPORATION
GOVERNMENT & COMMERCIAL SYSTEMS
ASTRO ELECTRONICS DIVISION
PO BOX 800, LOCUST CORNER
PRINCETON, NJ 08540
ATTN TECH LIB
ATTN GEORGE J. BRUCKER

RCA CORPORATION
DAVID SARNOFF RESEARCH CENTER
W. WINDSOR TWP
201 WASHINGTON ROAD, PO BOX 432
PRINCETON, NJ 08540
ATTN K. H. ZAININGER

RCA CORPORATION
GOVERNMENT & COMMERCIAL SYSTEMS
MISSILE & SURFACE RADAR DIVISION
MARNE HIGHWAY & BORTON LANDING RD
MOORESTOWN, NJ 08057
ATTN TECHNICAL LIBRARY
ATTN ELEANOR K. DALY
ATTN ANDREW L. WARREN

RCA CORPORATION
CAMDEN COMPLEX
FRONT & COOPER STREETS
CAMDEN, NJ 08012
ATTN TECH LIB
ATTN E. VAN KEUREN, 13-5-2

RESEARCH TRIANGLE INSTITUTE
PO BOX 12194
RESEARCH TRIANGLE PARK, NC 27709
ATTN ENG DIV, MAYRANT SIMONS, JR.

ROCKWELL INTERNATIONAL CORPORATION
3370 MIROLOMA AVENUE
ANAHEIM, CA 92803
ATTN N. J. RUDIE, FA53
ATTN J. SPETZ
ATTN L. H. PINSON, FB41
ATTN J. L. MONROE, DEPT 243-027, DIV 031
ATTN GEORGE C. MESSENGER, FB61
ATTN K. F. HULL
ATTN TECHNICAL LIBRARY
ATTN JAMES E. BELL, HA10
ATTN DONALD J. STEVENS, FA70

ROCKWELL INTERNATIONAL CORPORATION
SPACE DIVISION
12214 SOUTH LAKEWOOD BOULEVARD
DOWNEY, CA 90241
ATTN TIC D/41-092 AJ01

ROCKWELL INTERNATIONAL CORPORATION
4300 EAST FIFTH AVENUE
COLUMBUS, OH 43216
ATTN JOHN F. ROBERTS

ROCKWELL INTERNATIONAL CORPORATION
5701 WEST IMPERIAL HIGHWAY
LOS ANGELES, CA 90009
ATTN T. B. YATES

SANDERS ASSOCIATES, INC.
95 CANAL STREET
NASHUA, NH 03060
ATTN TECH LIB
ATTN 1-6270, R. G. DESPATHY, SR P E
ATTN JAMES L. BURROWS
ATTN M. L. AITEL NCA 1-3236

SCIENCE APPLICATIONS, INC.
PO BOX 2351
LA JOLLA, CA 92038
ATTN TECHNICAL LIBRARY
ATTN J. ROBERT BEYSTER
ATTN LARRY SCOTT

SCIENCE APPLICATIONS, INC.
HUNTSVILLE DIVISION
2109 W. CLINTON AVENUE
SUITE 700
HUNTSVILLE, AL 35805
ATTN NOEL R. BYRN
ATTN TECH LIB

SCIENCE APPLICATIONS, INC.
PO BOX 3507
ALBUQUERQUE, NM 87110
ATTN JAMES R. HILL

SCIENCE APPLICATIONS, INC.
2680 HANOVER STREET
PALO ALTO, CA 94303
ATTN CHARLES STEVENS

SCIENCE APPLICATONS, INC.
8400 WEST PARK DRIVE
MCLEAN, VA 22101
ATTN WILLIAM L. CHADSEY

SIMULATION PHYSICS, INC.
41 "B" STREET
BURLINGTON, MA 01803
ATTN ROGER G. LITTLE

SINGER COMPANY, THE
1150 MCBRIDE AVENUE
LITTLE FALLS, NJ 07424
ATTN IRWIN GOLDMAN, ENG MANAGEMENT
ATTN TECH LIB

SINGER COMPANY (DATA SYSTEMS), THE
150 TOTOWA ROAD
WAYNE, NJ 07470
ATTN TECH INFO CENTER

SPERRY RAND CORPORATION
UNIVAC DIVISION
DEFENSE SYSTEMS DIVISION
P.O. BOX 3525 MAIL STATION 1931
ST. PAUL, MN 55101
ATTN JAMES A. INDA, MS 41T25
ATTN TECH LIB

SPERRY MICROWAVE ELECTRONICS DIV
SPERRY RAND CORPORATION
PO BOX 4648
CLEARWATER, FL 33518
ATTN TECH LIB

SPERRY RAND CORPORATION
SPERRY DIVISION
SPERRY GYROSCOPE DIVISION
SPERRY MANAGEMENT DIVISION
MARCUS AVENUE
GREAT NECK, NY 11020
ATTN PAUL MARRAFFINO
ATTN CHARLES L. CRAIG EV
ATTN TECH LIB

SPERRY RAND CORPORATION
SPERRY FLIGHT SYSTEMS DIVISION
P.O. BOX 21111
PHOENIX, AZ 85036
ATTN TECH LIB
ATTN D. A. SCHOW, ROOM 104C
ATTN D. J. KEATING

STANFORD RESEARCH INSTITUTE
333 RAVENSWOOD AVENUE
MENLO PARK, CA 94025
ATTN MR. PHILIP DOLAN
ATTN ARTHUR LEE WHITSON
ATTN SETSUO DDAIRIKI
ATTN MEL BERNSTEIN
ATTN ROBERT A. ARMISTEAD

STANFORD RESEARCH INSTITUTE
306 WYNN DRIVE, N. W.
HUNTSVILLE, AL 35805
ATTN TECH LIB
ATTN MACPHERSON MORGAN

SUNDSTRAND CORPORATION
4751 HARRISON AVENUE
ROCKFORD, IL 61101
ATTN CURTIS B. WHITE

SYSTEMS, SCIENCE AND SOFTWARE
P.O. BOX 4803
HAYWARD, CA 94540
ATTN TECH LIB
ATTN DAVID A. MESKAN

SYSTEMS, SCIENCE AND SOFTWARE, INC.
PO BOX 1620
LA JOLLA, CA 92038
ATTN TECHNICAL LIBRARY
ATTN IRA KATZ
ATTN ANDREW R. WILSON

SYSTRON-DONNER CORPORATION
1090 SAN MIGUEL ROAD
CONCORD, CA 94518
ATTN HAROLD D. MORRIS
ATTN TECH LIB

TEXAS INSTRUMENTS, INC.
P.O. BOX 5474
DALLAS, TX 75222
ATTN TECH LIB
ATTN DONALD J. MANUS, MS 72

TEXAS TECH UNIVERSITY
PO BOX 5404
NORTH COLLEGE STATION
LUBBOCK, TX 79417
ATTN TRAVIS L. SIMPSON

TRW SEMICONDUCTORS
DIVISION OF TRW, INC.
14520 AVIATION BLVD
LAWNDALE, CA 90260
ATTN TECH LIB

TRW SYSTEMS GROUP
ONE SAPCE PARK
REDONDO BEACH, CA 90278
ATTN JERRY I. LUBELL
ATTN ROBERT M. WEBB, RL-2410
ATTN AARON H. NAREVSKY, R1-214
ATTN R. K. PLEBUCH, R1-2078
ATTN H. H. HOLLOWAY, R1-2036
ATTN O. E. ADAMS, R1-1144
ATTN TECH INFO CENTER/S-1930

TRW SYSTEMS GROUP
SAN BERNARDINO OPERATIONS
PO BOX 1310
SAN BERNARDINO, CA 92402
ATTN F. B. FAY, 527/710
ATTN EARL W. ALLEN
ATTN J. M. GORMAN, 520/114

DISTRIBUTION (Cont'd)

TRW SYSTEMS GROUP
PO BOX 368
CLEARFIELD, UT 84015
  ATTN TECH LIB
  ATTN DONALD W. PUGSLEY

UNITED TECHNOLOGIES CORP
NORDEN DIVISION
HELEN STREET
NORWALK, CT 06851
  ATTN TECH LIB
  ATTN CONRAD CORDA

UNITED TECHNOLOGIES CORPORATION
HAMILTON STANDARD DIVISION
BRADLEY INTERNATIONAL AIRPORT
WINDSOR LOCKS, CT 06069
  ATTN TECH LIB

VARIAN ASSOCIATES
611 HANSEN WAY
PALO ALTO, CA 94303
  ATTN TECH LIB

VECTOR RESEARCH ASSOCIATES
735 STATE STREET, RM 314
SANTA BARBARA, CA 93101
  ATTN W. A. RADASKY

WESTINGHOUSE ELECTRIC CORPORATION
ADVANCED ENERGY SYSTEMS DIV
PO BOX 10864
LARGE, PA 15025
  ATTN TECH LIB

WESTINGHOUSE ELECTRIC CORPORATION
DEFENSE AND ELECTRONIC SYSTEMS CENTER
P.O. BOX 1693
FRIENDSHIP INTERNATIONAL AIRPORT
BALTIMORE, MD 21203
  ATTN HENRY P. KALAPACA, MS 3525
  ATTN TECH LIB

WESTINGHOUSE ELECTRIC CORPORATION
RESEARCH AND DEVELOPMENT CENTER
1310 BEULAH ROAD, CHURCHILL BOROUGH
PITTSBURGH, PA 15235
  ATTN TECH LIB

HARRY DIAMOND LABORATORIES
  ATTN MCGREGOR, THOMAS, COL, COMMANDING
    OFFICER/FLYER, I.N./LANDIS, P.E./
    SOMMER, H./CONRAD, E.E.
  ATTN CARTER, W.W., DR., ACTING TECHNICAL
    DIRECTOR/MARCUS, S.M.
  ATTN KIMMEL, S., IO
  ATTN CHIEF, 0021
  ATTN CHIEF, 0022
  ATTN CHIEF, LAB 100
  ATTN CHIEF, LAB 200
  ATTN CHIEF, LAB 300
  ATTN CHIEF, LAB 400
  ATTN CHIEF, LAB 500
  ATTN CHIEF, LAB 600
  ATTN CHIEF, DIV 700
  ATTN CHIEF, DIV 800
  ATTN CHIEF, LAB 900
  ATTN CHIEF, LAB 1000
  ATTN RECORD COPY, BR 041
  ATTN HDL LIBRARY (3 COPIES)
  ATTN CHAIRMAN, EDITORIAL COMMITTEE
  ATTN CHIEF, 047
  ATTN TECH REPORTS, 013
  ATTN PATENT LAW BR, 071
  ATTN MCLAUGHLIN, P. W., 741
  ATTN ROSADO, J. A., LAB 200 (3 COPIES)
  ATTN MERKEL, G., 1000
  ATTN GILBERT, R., 230 (5 COPIES)
  ATTN DANDO, J., 240
  ATTN WIMENITZ, F. N., 0024
  ATTN GORNAK, G., 1020
  ATTN GRAYBILL, S. S., 290
  ATTN MILETTA, J. R., 240
  ATTN AGEE, F. J., 1040
  ATTN LOWERY, A., 1000
  ATTN PFEFFER, R. 1030
  ATTN SWETON, J. F., 1000
  ATTN BOMBARDT, J., 1000
  ATTN TOMPKINS, J. E. 230, (3 COPIES)

DEPARTMENT OF THE ARMY
HARRY DIAMOND LABORATORIES
2800 POWDER MILL RD
ADELPHI. MD 20783

OFFICIAL BUSINESS
PENALTY FOR PRIVATE USE $300

AN EQUAL OPPORTUNITY EMPLOYER

POSTAGE AND FEES PAID
DEPARTMENT OF THE ARMY
DOD 314

THIRD CLASS

VANGUARD OF FREEDOM
BICENTENNIAL 1775 1975
UNITED STATES ARMY